

**Aus der Medizinischen Klinik der Universität Heidelberg**

(Zentrumssprecher: Prof. Dr. med. Hugo A. Katus)

**Abteilung für Innere I und Klinische Chemie**

(Ärztlicher Direktor: Prof. Dr. med. Dr. h.c. Peter P. Nawroth)

**Metabolic switch from glycolysis towards fatty acid  
oxidation in Schwann cells in response to high glucose**

**Inauguraldissertation zur Erlangung**

**des Doctor scientiarum humanarum**

**an der Medizinischen Fakultät Heidelberg**

**der Ruprecht-Karls-Universität**

vorgelegt von

**Tamara Tjitske Antje Smit**

geboren in Achtkarspelen, die Niederlande

**Heidelberg, 2018**

**Dekan: Prof. Dr. med. Andreas Draguhn**

**Doktorvater: Prof. Dr. med. Dr. h. c. Peter P. Nawroth**

**Betreuer: Dr. sc. hum. Thomas H. Fleming**

## Table of contents

## Table of contents

<b>1 List of essential abbreviations .....</b>	<b>1</b>
<b>2 Introduction .....</b>	<b>3</b>
2.1 Diabetes Melitus .....	3
2.2 Diabetic Neuropathy .....	4
2.3 Molecular mechanism of diabetic complications: Unifying theory .....	6
2.4 Mitochondrial reactive oxygen species and diabetes .....	8
2.5 Mitochondrial dysfunction in diabetic neuropathy .....	11
2.6 Reactive nitrogen species and mitochondrial function .....	12
2.7 Aim study .....	16
<b>3 Materials and methods .....</b>	<b>17</b>
3.1 Mouse model .....	17
3.2 Cell culture .....	17
3.3 Patient study .....	18
3.3.1 Participants .....	18
3.3.2 Isolation PBMCs .....	18
3.4 Unifying theory .....	19
3.4.1 Glucose uptake .....	19
3.4.2 Polyol Pathway; Sorbitol .....	19
3.4.3 Hexosamine pathway; Glycosylation .....	20
3.4.4 Protein kinase C pathway; PKC activity .....	20
3.4.5 AGE pathway; Methyl Glyoxal .....	21
3.5 Mitochondrial properties and reactive metabolites.....	21
3.6 Mitochondrial bioenergetics .....	22
3.6.1 Optimization cell density and reagents for XF96 Seahorse Bionalyzer .....	22

## Table of contents

3.6.2 Glycolysis .....	22
3.6.3 Mitochondrial Respiration .....	23
3.7 Quantitative real-time PCR.....	24
3.7.1 RNA extraction and cDNA synthesis .....	24
3.7.2 Quantitative real-time PCR .....	24
3.8 Immunoblot .....	26
3.8.1 Protein isolation cells .....	26
3.8.2 Cell lysis and protein isolation for Glut 1 .....	27
3.8.3 Immunoblot .....	27
3.9 Fatty acid oxidation .....	29
3.9.1 BODIPY fatty acid uptake .....	29
3.9.2. Octanoate fatty acid oxidation .....	29
3.9.3 Acyl carnitines .....	30
3.10 Nitric oxide .....	30
3.10.1 eNOS, nNOS and iNOS .....	30
3.10.2 Nitric oxide synthase .....	30
3.10.3 S-nitrosylation .....	31
3.10.3.1 Isolation mitochondria.....	31
3.10.3.2 S-nitrosylation assay.....	31
3.10.4 Nitric oxide and ROS production .....	32
3.11 Mitochondrial bioenergetics PBMCs .....	32
3.11.1 Glycolysis and mitochondrial respiration .....	32
3.11.2 Staining PBMCs for flow cytometry .....	33
3.11.2.1 Glucose uptake .....	33
3.11.2.2 Mitochondrial mass and ROS .....	34
3.11.2.3. Specific CD-antibodies .....	34
3.12 Statistical analysis .....	35

## Table of contents

<b>4 Results</b> .....	<b>36</b>
4.1 Cell specific changes in response to glucose .....	36
4.1.1 Increased glucose uptake .....	36
4.1.2 Altered mitochondrial properties and reactive metabolites .....	37
4.2 Increased glucose uptake and glucose transporter expression in Schwann cells and fibroblasts .....	40
4.3 High glucose does not affect the pathways of the unifying theory .....	41
4.4 Decreased glycolysis and mitochondrial respiration .....	43
4.5 Decreased expression of glycolysis related genes and altered fatty acid metabolism in Schwann cells .....	47
4.6 No activation of the integrated stress response, the coupled protein response and the AMPK pathway .....	52
4.7 High glucose induces NOS activation in Schwann cells .....	53
4.8 Increased glycolytic capacity, mitochondrial respiration and superoxide formation in PBMCs of T2DM .....	56
<b>5 Discussion</b> .....	<b>60</b>
5.1 Hyperglycemia induced alterations are cell type specific .....	60
5.2 Unifying theory not applicable in Schwann cells and fibroblasts cell culture model of hyperglycemia .....	61
5.3 High glucose induced metabolic switch towards fatty acid oxidation in Schwann cells .....	63
5.4 The metabolic switch depends on the nitric oxide pathway .....	67
5.5 Increased mitochondrial bioenergetics in PBMCs of T2DM .....	70
5.6 Conclusion and future directions .....	71
<b>6 Summary</b> .....	<b>72</b>
<b>7 Zusammenfassung</b> .....	<b>74</b>
<b>8 References</b> .....	<b>76</b>

**Table of contents**

**9 Appendix .....89**

**10 Publications .....90**

**11 Curriculum Vitae .....91**

**12 Acknowledgement .....93**

**13 Eidestatlliche versicherung .....95**

## Abbreviations

### 1 List of essential abbreviations

Acaca	Acetyl-Coenzyme A carboxylase alpha
ACC	Acetyl-CoA carboxylase
AceCS1	Cytoplasmic acetyl-CoA synthetase
ACL (Acly)	ATP citrate lyase
ACSL	Long-chain acyl-CoA synthetase
ActB	$\beta$ -actin
AGE	Advanced glycation endproduct
Aldoa	Aldolase A (fructose-biphosphate)
AML12	Hepatocytes, mouse
AMPK	5' adenosine monophosphate-activated protein kinase
AmpB	Amphotericin B
ASNS	Asparagine synthetase
ATF4	Activating transcription factor 4
ATF6	Activating transcription factor 6
ATP	Adenosine triphosphate
B2m	Beta-2 microglobulin
BSA	Bovine serum albumin
CHOP	DNA-damage inducible factor 3 (Ddit3)
CoQ	Coenzyme Q
CO <sub>2</sub>	Carbon dioxide
Cpt1b	Carnitine palmitoyltransferase 1B
DM	Diabetes mellitus
DN	Diabetic neuropathy
Echs	Enoyl coenzyme A hydratase (mitochondrial)
eNOS	Endothelial nitric oxide synthase
eIF2 $\alpha$	Eukaryotic initiation factor 2
Eno1	Enolase 1 (alpha)
ETC	Electron transport chain
FAD(H <sub>2</sub> )	Flavin adenine dinucleotide
FAO	Fatty acid oxidation
FAS(N)	Fatty acid synthase
FCS	Fetal calf serum
FMN	Flavin mononucleotide
GAP(DH)	Glyceraldehyde 3-phosphate (dehydrogenase)
Glut 1	Glucose transporter 1
Glut 3	Glucose transporter 3
Gpx	Glutathione peroxidase
HbA1c	Hemoglobin A1c
HG	High glucose
HK2	Hexokinase 2
H <sub>2</sub> O <sub>2</sub>	Hydrogen peroxide
HO•	Hydroxyl radical

## Abbreviations

Hprt	Hypoxanthine guanine phosphoribosyl transferase
IENFD	Intraepidermal nerve fiber density
iNOS	Inducible nitric oxide synthase
IRE1 $\alpha$	Inositol-requiring enzyme 1 alpha
LG	Low glucose
Lipe	Lipase
LKB1	Liver kinase B1
M1	Kidney epithelial (tubular) cells, mouse
MEF	Mouse embryonal fibroblasts
MES13	Mesangial cells, mouse
MG	Methyl glyoxal
MHP	mitochondrial hyperpolarization
NAC	N-Acetylcystein
nNOS	Neuronal nitric oxide synthase
NO	Nitric oxide
NOS	Nitric oxide synthase
NOX	NAD(P)H oxidases
NSC	Nerve conduction study
Mdhfd2	Methylenetetrahydrofolate dehydrogenase 2
mtNOS	Mitochondrial nitric oxide synthase
mtO <sub>2</sub>	Mitochondrial oxygen consumption
NAD(H)	Nicotinamide adenine dinucleotide
NADP(H)	Nicotinamide adenine dinucleotide phosphate
O <sub>2</sub>	Oxygen
O <sub>2</sub> <sup>•-</sup>	Superoxide
O-GlcNAc	O-Linked $\beta$ -N-acetylglucosamine
PARP	Poly(ADP-ribose) polymerase
Pck2	Phosphoenolpyruvate carboxykinase 2
PBMC	Peripheral blood mononuclear cells
PKC	Protein kinase C
P/S	Penicillin streptomycin
ROS	Reactive oxygen species
RNS	Reactive nitrogen species
RnS18	18S ribosomal RNA
RT	Room temperature
SOD	Superoxide dismutase
Srebp1	Sterol regulatory element binding protein 1
SW10	Schwann cells, mouse
STZ	Streptozotocin
T1DM	Type 1 diabetes
T2DM	Type 2 diabetes
TCA	Tricarboxylic acid
Trib3	Tribbles pseudokinase 3



## Introduction

## 2 Introduction

### 2.1 Diabetes Mellitus

The prevalence of Diabetes mellitus (DM) has increased dramatically over the last decade. According to the International Diabetes Federation (IDF) Diabetes Atlas, 415 million people worldwide were diagnosed with diabetes in 2015. The prevalence of diabetes in adults was estimated to be 8.8%, mainly due to the increasing prevalence of type 2 diabetes mellitus (T2DM) which is closely linked to the epidemic of obesity, and is expected to increase about 5% per year (Ogustova et al., 2017; Ziegler et al., 2008; Zimmet et al., 2001). Moreover, the IDF reported that 318 million adults are estimated to have impaired glucose tolerance or prediabetes, giving them a higher risk of developing the disease.

DM is characterized by hyperglycemia resulting from insulin resistance, inadequate insulin secretion, excessive glucagon secretion or a combination of these factors. DM is primarily diagnosed by fasting blood glucose levels or by glycated haemoglobin (HbA1c). Prediabetes is diagnosed by a fasting blood glucose >100 mg/dL or HbA1C 5.7-6.4%. A diagnose of DM is given when fasting blood glucose is >126 mg/dL or HbA1c>6.5%. Type 1 diabetes mellitus (T1DM) characterized by insulin deficiency due to pancreatic  $\beta$ -cell loss, resulting into many changes in the organism including hyperglycaemia (Alberti and Zimmet, 1998). The aetiology of T1DM is not completely understood, however, it is suggested the pathogenesis of the disease involves T cell-mediated  $\beta$ -cells destruction (Davies et al., 1994). On the other hand, T2DM is associated with the dysfunction of the pancreatic  $\beta$ -cells, disruption of secretory function of adipocytes and impaired insulin action in liver and defect in insulin-mediated glucose uptake in the muscle (Cai et al., 2005; Spranger et al., 2003). The defects are evident early in the course of the disease, and emerging evidence suggests that mitochondria play an important role in these processes. Both T1DM and T2DM are associated with similar long-term diabetic complications, such as cardiomyopathy, nephropathy, neuropathy, retinopathy and atherosclerosis, which to some extent appear to result from pathogenic processes at mitochondrial level (Sivitz and Yorek, 2010).

## **Introduction**

### **2.2 Diabetic neuropathy**

Diabetic neuropathy (DN) is a common micro-vascular complication of long term diabetes and its prevalence is 30-50%, depending on the method used for diagnosis (Tesfaye et al., 2010). DN is characterized by distal-to-proximal loss of peripheral nerve axons. However, there is also evidence for vascular-independent development of neuropathy (Bierhaus et al., 2012; Eberhardt et al., 2012). DN is a debilitating, complex disorder and associated with a wide range of clinical manifestations, including hypersensitivity (hyperalgesia and allodynia), hyposensitivity, diabetic foot ulcers and neuropathic osteoarthropathy (Yagihashi et al., 2011), together with structural changes in peripheral nerve including endoneurial microangiopathy, abnormal Schwann cell pathology and axonal degeneration (Malik et al., 2005). The reason why axons are very sensitive to hyperglycemia and metabolic changes is due to the close interaction with the nerve blood supply and the large population of mitochondria (Edwards et al., 2010; Vincent et al., 2004; Vincent et al., 2010). When the mitochondria are damaged, axons undergo metabolic changes leading to energy failure and neurodegeneration.

Nerve biopsies of patients with diabetes have shown nerve fiber degeneration and clusters of regenerating axons (Engelstad et al., 1997). Reduced nerve conduction velocity due to demyelination and the loss of small and large myelinated fibers, and reduced nerve action potentials as result of axon loss have been observed in symptomatic neuropathy (Stewart et al., 1996). Alterations in nerve conduction velocity can be detected in patients with asymptomatic neuropathy, however, its presence does not predict the onset of the disease. Moreover, alterations in myelination of small nerve fibers and small fiber loss, present in the early stage of DN do not affect the sensory action potential detected by routine nerve conduction study (NCS) (Dyck et al., 2010; Vinik et al., 2006). Skin biopsies have been taken to determine intraepidermal nerve fiber density (IENFD) when small-fiber neuropathy is suspected and is a reliable tool for the diagnosis of distal symmetric polyneuropathy in patients with DM (Timar et al., 2016). A non-invasive quantitative method for the diagnosis of DN is corneal confocal microscopy, which is more sensitive than NCS or IENFD (Shtein and Callaghan, 2013).

The main treatment of DN is tight glycemic control. To control the pain, medication such as corticosteroids, carbamazepine, clonazepam, phenytoin, or paracetamol in combination with

## Introduction

codeine phosphate can be used (Said et al., 2007; Yagihashi et al., 2011). However, such medication is not uniformly effective in all DN patients. Many patients are resistant to one or more analgesics. Furthermore, such drugs have adverse side effects such as nausea, vomiting and depression of the central nerve system (Nawroth et al., 2010, Javed et al., 2015). Although a combination of certain medication might be effective to relieve the pain in DN, the secondary effects can still reduce the quality of life.

The lack of treatment options for DN reflects the incomplete understanding of its pathophysiology. Although chronic hyperglycemia is mainly accepted as the primary cause of DN in both T1DM and T2DM patients, other emerging factors such as impaired insulin signaling, hypertension, and dyslipidemia (mainly in T2DM) might precede hyperglycemia. Preclinical and some clinical studies indicate that DN is induced by microvascular disease, mainly focused on axonal degeneration secondary to ischemia and hypoxia (Callaghan et al., 2012a). However, this is likely to be one aspect in the complex pathophysiology of DN.

Clinical studies have indicated that normalizing blood glucose only partially prevents the manifestation of DN in T1DM patients (Albers et al., 2010) and does not prevent neuropathic symptoms in T2DM (Boussageon et al., 2011, Callaghan et al., 2012b). Moreover, lowering of blood glucose does not diminish the symptoms of DN in either T1DM or T2DM. Data from pancreatic transplantations in T1DM patients with DN showed normal blood glucose after transplantation and stability of DN, but no improvement in symptoms (Navarro et al 1997). In a study of 427 patients with mild to moderate DN, elevated triglyceride correlated with impaired sural myelinated fiber density, a direct measurement of neuropathy, but no association between glycemic control and neuropathy was found in this cohort (Wiggin et al., 2009). Bongaerts et al. showed that the prevalence of peripheral neuropathy was increased to the same extent in non-diabetic individuals with combined impaired fasting blood glucose and impaired glucose tolerance as compared to diabetic patients (Bongaerts et al., 2012). Furthermore, a major adverse side effect of intensive glycemic control is increased occurrence of hypoglycaemic episodes with a risk of brain injury and death. Therefore, to avoid hypoglycemic crisis, the acceptable target blood glucose level in controlled individuals is usually set to values above normal (6.7 to 10 mmol/L in Diabetes Control and Complications Trial and 6

## Introduction

mmol/L in U.K. trial in T2DM patients) (Nathan et al., 1993; Skyler, 1993). In prediabetic patients, it has been shown that glucose control does not target the pathogenesis of DN and hence is an ineffective treatment by itself (Smith et al., 2006). In addition, Gaede et al showed that a multifactorial treatment against hypertension, dyslipidemia and micro albuminuria along with aspirin and antioxidants was only effective against diabetes related cardiovascular disease, including nephropathy and retinopathy, while the prevalence of DN remained unaffected (Gaede et al., 1999).

The majority of clinical and basic research has focused primarily on the effects of hyperglycemia on neurons. However, in the earliest descriptions of DN pathology in 1979 it was described that axonal degeneration is accompanied by Schwannopathy, which is characterized by degenerative changes in myelin sheaths, basement membrane hyperplasia, crystalloid inclusion bodies and aggregates of glycogen particles in the cytoplasm of Schwann cells (Yagihashi et al., 1979). There is now increasing evidence that Schwann cells are equal indispensable component in the maintenance of neuronal structure and function, providing nourishment to axons, and promote survival and growth upon neuronal injury (Mizisin et al., 2014). Moreover, alterations in Schwann cells have been reported in experimental models of DN. Studies in rodents have shown that Schwann cells regulate many aspects of axonal function and that the disruption of Schwann cell metabolism induced by diabetes leads to diminished neuronal support factors and the accumulation of neurotoxic intermediates, including acyl carnitine species, palmitoylcarnitines and linoleylcarnitine, contributing to neuronal degeneration, endothelial dysfunction and subsequently to DN (Freeman et al., 2016; Viader et al., 2013).

### **2.3 Molecular mechanism of diabetic complications: Unifying theory**

The unifying theory is based on studies which showed increased reactive oxygen species (ROS) production under hyperglycemic conditions (Brownlee et al., 2005; Nishikawa et al., 2000). During periods of hyperglycemia, cells which take up glucose independently of blood insulin levels such as mesangial cell in kidney, capillary endothelial cells, neurons and Schwann cells will incorporate large amount of glucose leading to extreme high intracellular glucose concentrations (Brownlee et al., 2001). The increase metabolic flux through glycolysis due to

## Introduction

elevated glucose levels results in increased levels of substrates for the tricarboxylic acid (TCA) cycle and oxidative phosphorylation, causing elevated electron flux in complex III of the electron transport chain and subsequently the overproduction of ROS in the mitochondria (Figure 1). It has been shown that elevated ROS formation induces DNA damage resulting in the activation of poly(ADP-ribose) polymerase (PARP), which induces poly(ADP- ribosyl)ation of nuclear proteins and NAD<sup>+</sup> depletion (Atorino et al., 2001; Du et al., 2003; Du et al., 2000; Kanwar and Kowluru, 2009). The acceptor of PARP is glyceraldehyde-3-phosphate dehydrogenase (GAPDH), which is translocated to the nucleus where it is inhibited. The poly(ADP- ribosyl)ation of GAPDH together with NAD<sup>+</sup> depletion leads to the accumulation of glycolytic intermediates upstream of GAPDH, such as fructose-6-biphosphate, glyceraldehyde-3-phosphate and dihydroxy acetone phosphate, which are major precursors of advanced glycation endproducts (AGEs) (Ahmed, 2005; Brownlee et al., 2005; Bierhaus et al., 2005). Moreover, the inhibition of GAPDH by PARP also activates the polyol pathway (Vincent et al., 2004), the hexosamine pathway (Brownlee 2001; Sayeski et al., 1996), as well as protein kinase C (and subsequently NF-κB) (Xia et al., 1994), all which are involved in hyperglycemia induced cellular dysfunction and the subsequent development of diabetic complications.

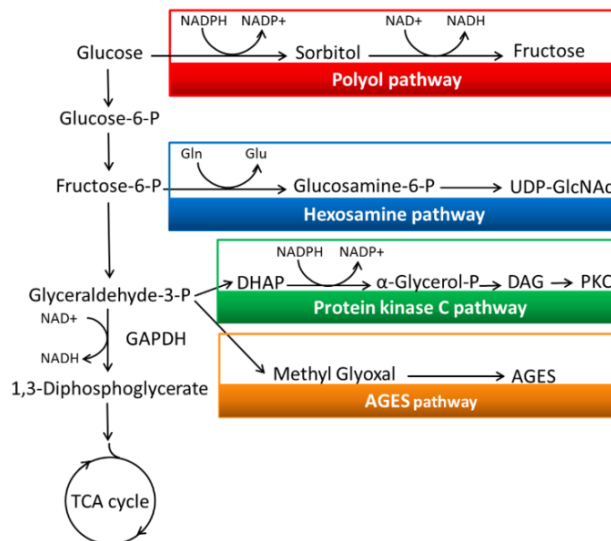


**Figure 1. Scheme of the Unifying theory, adapted figure of Brownlee (Brownlee, 2001).**

According to the unifying theory, diabetic complications can be explained due to hyperglycemia induced ROS production by one or more of the four pathways; polyol pathway, hexosamine pathway, protein kinase c (PKC) pathway and advanced glycation end products (AGEs).

## Introduction

### 2.4 Mitochondria, reactive oxygen species and diabetes

Mitochondria have a pivotal role within the unifying theory, as they are the source of the ROS which trigger the subsequent steps leading to cellular dysfunction under hyperglycemia. Under normal physiological conditions the mitochondria, through oxidative phosphorylation, is the primary metabolic pathway for ATP production from glucose. In the presence of molecular oxygen ( $O_2$ ), glucose is metabolized to Acetyl CoA that is then oxidized to carbon dioxide ( $CO_2$ ) once it enters the TCA cycle by the reduction of NAD to NADH. NADH is then utilized by the electron transport chain (ETC) as part of the oxidative phosphorylation (Chen and Zweier, 2014; Kowaltowski et al., 1999). A total of thirteen ATP molecules can be produced from one glucose molecule when all the reduced coenzymes are oxidized by the ETC and used for mitochondrial oxidative phosphorylation (Balaban 1990). In addition, to energy production, the mitochondria are also involved in the maintenance of the cellular calcium homeostasis, in addition to carrying out critical reactions involved in cell signaling and programmed cell death (Georgiou et al., 2015).

The mitochondrial ETC is an efficient system for ATP production, however, given the very nature of the alternating one-electron oxidation-reduction reactions, side-reactions with  $O_2$  can occur resulting in its reduction to the superoxide ( $O_2^{\bullet-}$ ). It is estimated from in vitro experiments using isolation mitochondria that 0.12-2% of respiration goes to  $O_2^{\bullet-}$  production (Murphy, 2009). The addition of a second electron and two protons generates hydrogen peroxide ( $H_2O_2$ ), whilst the addition of a third electron produces the hydroxyl radical ( $HO^{\bullet}$ ). These three oxygen containing compounds are collectively referred to as ROS, and they represent a major class of endogenous reactive metabolites. Under normal conditions, ROS function as second messenger and has health beneficial effects (Ray et al., 2012; Ristow and Schmeisser, 2014). However, when produced in an excess, ROS can lead to the disruption of cellular signaling leading to a state referred to as oxidative stress. ROS, despite the their short half-life (1 - 4  $\mu s$ ) and subsequent limited sphere of influence, can target several cellular molecules such as lipids, proteins, and DNA, thereby inducing peroxidation, conformational changes, DNA crosslinks, as well as DNA strand breaks (Birben et al., 2012; Brand et al., 2004; Jena, 2012).

## Introduction

Within the mitochondria, the major sources of ROS are complex I (NADH dehydrogenase) and complex III (coenzyme Q (CoQ)) (Figure 2), however, the  $O_2^{\bullet-}$  production depends on the local concentrations of  $O_2$  and electron donors such as NADH and flavin adenine dinucleotide (FADH<sub>2</sub>). Complex I couples the transfer of two electrons from NADH in two one-electron steps to the freely diffusible electron carrier coenzyme Q (CoQ). One molecule of flavin mononucleotide (FMN) and several iron-sulphur clusters participate in the reaction as redox groups (Weiss et al., 1991). It remains unclear which component of the complex is the major source of  $O_2^{\bullet-}$ , however, it has been suggested that either flavin mononucleotide (FMN) or the iron-sulfur cluster could be responsible (Kushnareva et al., 2002; Kussmaul and Hirst, 2006; Vinogradov and Grivennikova, 2005).

Complex III oxidizes ubiquinol to ubiquinone and passes the electrons by asymmetric absorption onto two electron acceptor cytochrome c oxidase and then to one electron acceptor cytochrome c. (Mitchell et al., 1975; Zhang et al., 1998). During this asymmetric absorption  $O_2^{\bullet-}$  can be produced. However, the exact mechanism of  $O_2^{\bullet-}$  production at the  $Q_o$  site still remains a matter of debate, whether the formation of  $O_2^{\bullet-}$  is induced by a semi forward reaction by the oxidation of ubiquinone radical or by the semi-reverse reaction transmitted by the oxidation of cytochrome c (Bleier et al., 2016).

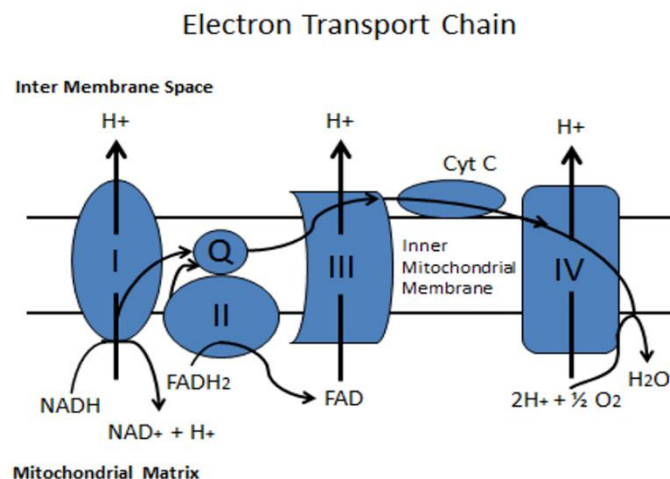


**Figure 2. The electron transport chain.**

The electron transport chain is a series of electron transporters embedded in the inner mitochondrial membrane that shuttles electrons from NADH and FADH<sub>2</sub> to oxygen. In this process, protons are pumped from the mitochondrial matrix to the inter membrane space, and oxygen is reduced to form water.

## Introduction

Under normal conditions mitochondria are rarely in the state of excessive ROS formation since the body has evolved an endogenous anti-oxidant defense system that counterbalance toxic ROS levels, consisting of low-molecule scavengers, such as vitamins, glutathione, vitamin and enzymatic oxidants. Common enzymatic antioxidants include superoxide dismutase (SOD) to detoxify  $O_2^{\bullet-}$ , catalase (CAT) to detoxify  $H_2O_2$ , glutathione peroxidase (GPx) to detoxify lipid peroxidases, and glutathione reductase (GRx) to detoxify  $HO^{\bullet}$  (Chelikani et al., 2004; Johansen et al., 2005; Farachi and Didion, 2004; Okado-Matsumoto et al., 2001).

Despite the prevailing view that overproduction of mitochondrial ROS is a central mechanism in the development of diabetic complications, there are only a few clinical and experimental studies which have reported increased indicators of oxidative stress and altered mitochondrial function. It has been shown in peripheral blood mononuclear cells (PBMCs) that mitochondrial oxygen consumption ( $mtO_2$ ) was increased in diabetic patients (Hartman et al., 2014). Widlansky et al., found that PBMCs of patients with type 2 diabetes have decreased mitochondrial mass, increased mitochondrial hyperpolarization (MHP), as well as increased  $H_2O_2$ , and  $O_2^{\bullet-}$  production (Widlansky et al., 2010). VanderJagt et al., however, has shown in patients with T1DM that with respect to complications, plasma and intracellular markers of oxidative stress remain unchanged (VanderJagt et al., 2001). It has also been shown in lymphocytes ( $CD4+CD8+$ ) from patients with T1DM that whilst MHP was increased,  $mtO_2$  remained unchanged and glycolysis was increased (Chen et al., 2017). In murine models of diabetes, it has been shown that with respect to mitochondrial dysfunctions, the result can vary considerably depending upon the models, the type of diabetes, as well as the organs and methods used for analysis. For example, it was shown in  $Ins2^{\pm}$  Akita mice that mitochondrial ATP production was unchanged in the heart, liver and kidney. However,  $mtO_2$ , was decreased in the heart, increased in the kidney and remained unchanged in the liver (Bugger et al., 2008; Bugger et al., 2009). De Cavanagh et al. showed that mitochondrial  $H_2O_2$  production was increased in the kidneys of STZ-diabetic rats (De Cavanagh et al., 2008). However, the renal  $O_2^{\bullet-}$  production has been shown to be decreased in STZ-diabetic mice. Impaired respiration was observed in mitochondria isolated from heart and brain, whereas it was increased in the kidney (Dugan et al., 2013). Studies to mitochondrial properties revealed increased mitochondrial size



## Introduction

in endothelial cells of patients with T1DM (Cester et al., 1996) whereas the mitochondrial size in skeletal muscle of patients with T2DM was found to be decreased (Kelley et al., 2002). In STZ-diabetic rats no change in matrix volumes of gastrocnemius, heart and liver mitochondria was observed as compared to the control. Moreover, superoxide production of gastrocnemius and heart mitochondria was unchanged, whilst the respiratory coupling was increased (Herlein et al., 2009). Boudina *et al.* showed that heart mitochondria of leptin receptor-deficient *db/db* mice generated excess of ROS and are, in fact, mildly uncoupled (Boudina et al., 2007). Based upon such studies it can be concluded that whilst increased oxidative stress maybe a general feature of diabetes, it may not necessary be directly associated with alterations to the mitochondria.

### 2.5 Mitochondrial dysfunction in diabetic neuropathy

Within the context of DN, there is increasing evidence to suggest that mitochondrial dysfunction is a key pathological contributor to the complication. Accumulation of mitochondria together with vesicles, neurofilaments and mildly enlarged mitochondria has been reported in intraepidermal axons in both clinical and experimental diabetes (Ebenezer et al., 2007; Fernyhough et al., 2010). Interestingly, mitochondrial abnormalities in neurons of patients with peripheral neuropathy are often localized in Schwann cells (Kalichman et al., 1998; Schroder et al., 1993, Viader et al., 2013). Degenerative alterations in nerve fibers are accompanied by the presence of enlarged mitochondria and effaced cristae and numerous vacuoles in Schwann cells, whereas axonal mitochondria appeared to be relatively normal in human peripheral neuropathy (Kalichman et al., 1998). Moreover, studies of human sensory neurons and experimental models of DN have shown impaired mitochondrial activity and bioenergetics (Freeman et al., 2016; Schroder et al., 1993), which was not associated with ROS production, suggesting that within the context of DN, there are mitochondrial-independent sources of ROS. The mitochondrial dysfunction that has been reported in Schwann cells has been shown to impact on axonal function and this association has been suggested to play an important role in DN (Freeman et al., 2016, Viader et al., 2013).

## Introduction

In vitro studies have shown that Schwann cell exposed to high glucose causes oxidative stress, accompanied by increased activation of apoptosis regulators such as BAX and caspase 9, and decreased levels of anti-apoptotic protein Bcl-12, indicating internal mitochondrial stress (Han et al., 2014). The study of a transgenic mouse model of tissue-specific deletion of the mitochondrial transcription factor A gene (*Tfam*) with impaired mitochondrial metabolism exclusively in Schwann cells (*Tfam*-SCKOs) revealed peripheral neuropathy secondary to targeted mitochondrial defects in Schwann cells and showed a neuropathy phenotype closely resembling DN (Viader et al., 2011). The disruption of the mitochondria within Schwann cells activates the integrated stress response, inducing a shift away from fatty acid synthesis towards lipid oxidation, leading to the accumulation of acyl-carnitines; an important intermediated of the  $\beta$ -oxidation pathway (Viader et al., 2013). Once released from the Schwann cells, acyl carnitines can induce neurodegeneration, highlighting the importance of Schwann cell metabolism in axon- glia interactions and neuronal function. Studies looking at the effect of hyperglycemia on Schwann cell metabolism have also revealed alterations in the mitochondrial proteasome and decreased efficiency of coupled respiration, which was shown to be independent of superoxide production (Zhang et al., 2010).

### 2.6 Reactive nitrogen species and mitochondrial function

There is emerging evidence of the importance of RNS in DN and neuropathy pain. Nitric oxide (NO) is free radical and is a major RNS generated within the body. It is synthesized from L-arginine by the enzyme nitric oxide synthase (NOS). Three isoforms of NOS has been characterized; endothelial (eNOS), neuronal (nNOS) and inducible NOS (iNOS). Increased glucose levels have been associated with elevated serum NO levels in T2DM patients (Adela et al 2015; Assmann et al., 2016) together with increased plasma levels asymmetric dimethylarginine and altered arginine methylation in both T1DM and T2DM (Lee et al., 2011; Tarnow et al., 2004).

Besides inflammatory cells found in the nerve roots, where demyelination is predominately found, Schwann cells themselves can also release NO when activated by inflammatory stimuli and hyperglycemia (Gadua, 2012). In vitro studies in human Schwann cells exposed to high glucose have been reported to have elevated levels of nitrosylated proteins together with

## Introduction

increased iNOS expression, both markers of nitrosative stress (Obrosova et al., 2005). The importance of NO in DN is supported by the effect of iNOS and nNOS deletion in STZ-diabetic mice which showed improved nerve conductivity and reduced hypoalgesia (Vareniuk et al., 2008, Vareniuk et al. 2009). Moreover, in an in vitro neuron-Schwann cells co-culture model, high concentrations of NO induced robust demyelination of the neurons, whereas the Schwann cell viability remained unchanged, indicating that the loss of myelin is selective damage to neuron rather than to the Schwann cells (Lehmann et al., 2007). These findings indicate that NO is involved in the pathological changes observed in inflamed nervous system, characterized by axonal injury and subsequently myelin degeneration, also described as the Wallerian effect.

To understand the effect of NO in Schwann cells and its effect on demyelination and neurodegeneration in DN it is important to focus on the relationship between NO and mitochondrial metabolism. The first report of the presence of a mitochondrial isoform of NOS (mtNOS) was first described by Bates et al., which showed immunocytochemical localization of NOS in rat brain and liver mitochondria (Bates et al., 1995). mtNOS is described as a protein of the inner mitochondrial membrane that generates NO in  $Ca^{2+}$ -dependent manner (Ghafourifar and Richter 1997; Giulivi et al., 1998; Ghafourifar and Cadenas, 2005; Finocchietto et al., 2009) but this is debated by others (Lacza et al., 2006; Lacza, 2009; Tay et al., 2004; Venkatakrisnan et al., 2009). Another theory is that mitochondria might produce NO via another mechanism, specifically, the reduction of nitric to NO by ubiquinone in cytochrome  $bc_1$  complex (Kozlov et al., 1999). It is noteworthy that eNOS is located on the outer membrane of mitochondria in endothelial cells as well as in neurons, suggesting that mitochondria might regulate NO activity and, in return, eNOS might regulate mitochondrial function (Goligorski, 2004; Gao et al., 2004; Henrich et al., 2002).

An effect of NO on mitochondrial respiration is supported by the finding that NO binds to the oxygen site of cytochrome c oxidase (complex IV) (Boelens et al., 1984; Blackmore 1991, Brunori et al., 2004, Horvat et al., 2006), indicating that NO is an inhibitor of cytochrome c oxidase in competition with oxygen (Figure 3). Brown et al. reported that NO addition to isolated cytochrome oxidase immediately inhibited oxygen consumption which was reversed when NO was broken down, confirming that NO is potent and fast inhibitor of cytochrome c oxidase

## Introduction

(Brown et al., 2002). Another study showed that non-toxic concentrations of NO had little effect on basal respiration but reversibly decreased the mitochondrial reserve capacity in endothelial cells (Dranka et al., 2010). These findings imply that NO has a high affinity for cytochrome c oxidase, thereby affecting mitochondrial maximal respiration and reserve capacity.

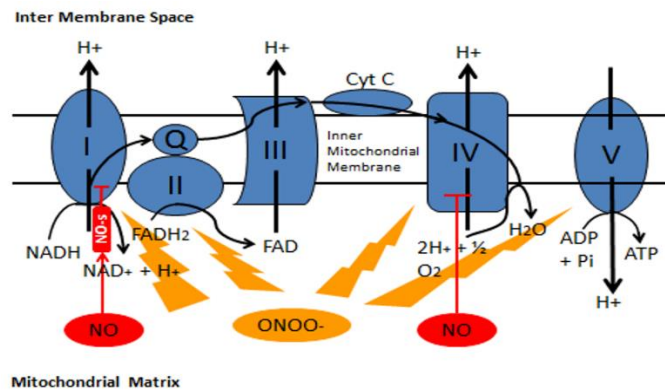


**Figure 3. Effect of nitric oxide and peroxynitrite on mitochondrial respiration.**

Nitrite oxide (NO) reversibly inhibits cytochrome c oxidase (complex IV) and NO induced S-nitrosylation can inhibit complex I (at the long term), whereas peroxynitrate (ONOO<sup>-</sup>) can inhibit complexes I, II, IV and V (ATP synthase). These alterations can lead to proton leak and the activation of the permeability transition pore and subsequently to NO-induced cell death.

NO can also react spontaneously with superoxide anion in the mitochondria to form peroxynitrite, which is a highly reactive radical, 1000 times more oxidizing than H<sub>2</sub>O<sub>2</sub> (Muijsers et al., 1997; Pacher et al., 2007). Peroxynitrite damage is stable and in some tissues, such as the retina, it is not reversed upon improvement of blood glucose levels (Kowluru et al., 2007; Pacher et al., 2005). Peroxynitrite can inhibit mitochondrial complex I, II, IV and V, thereby reducing mitochondrial respiration (Brown et al., 2001). Peroxynitrite has multiple cytotoxic effect including protein nitration and s-nitrosylation, breakage of single DNA strands and base modification, activation of PARP which alters the gene transcription and expression, leading to mitochondrial dysfunction and eventually apoptosis (Pacher et al., 2005; Szabo et al., 2007). Accumulation of 3-nitrotyrosine, a product of peroxynitrite-induced protein nitration has been reported in peripheral nerves and dorsal root ganglion of ob/ob mice (Drel et al., 2006), STZ-diabetic mice (Drel et al., 2007; Vareniuk et al., 2007) and rats (Obrosova et al., 2005). Moreover, elevated levels of NOS and 3-nitrotyrosine have been reported in diabetic patients,

## Introduction

particularly in the Schwann cells from patients with DN (Askwith et al., 2012; Gadau, 2012). These findings suggest that diabetes not only induces oxidative stress, but also induces oxidative-nitrosative stress in the peripheral nerve system in patients with DN. The association of Schwann cell dysfunction and DN is summarized in Figure 4.

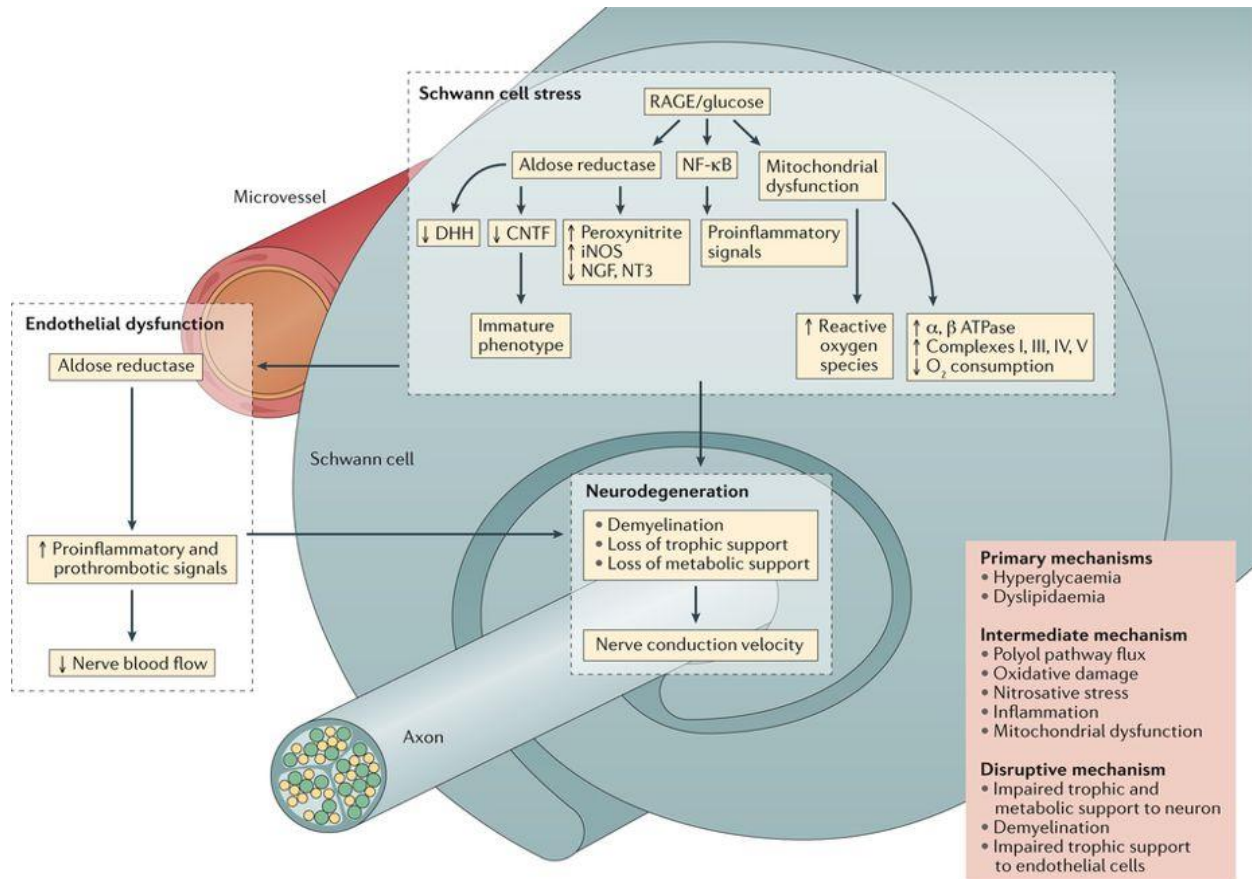


**Figure 4. Schwann cell dysfunction in diabetic neuropathy, adapted from Gonçalves et al., 2017.**

In diabetic patients hyperglycaemia ultimately leads to reduced neuronal support from Schwann cells. In Schwann cells, hyperglycemia and dyslipidaemia induces increased signaling through the receptor for advanced glycosylation end products (RAGE) and subsequently to increased flux through glycolysis by aldose reductase and the generation of reactive oxygen species, including peroxynitrite, and decreased expression of  $\beta$ -nerve growth factor (NGF) and neurotrophin 3 (NT3). This leads to local oxidative damage, inflammation and a switch to an immature Schwann cell phenotype. It also affects mitochondrial function by the increased expression of complex I, II, IV and V, and ATP production whereas the oxygen consumption is reduced. In addition, it reduces the production Schwann-cell-derived neurotrophic factors, including ciliary neurotrophic factor (CNTF) and desert hedgehog (DHH), which affects vascular endothelial cell function. Endothelial cells also express aldose reductase, and increased polyol pathway flux activates proinflammatory and prothrombotic pathways that reduce nerve blood flow. Disruption of neuronal support by Schwann cells and its effect on the vascular system contributes to development of DN.

## Introduction

### 2.7 Aim Study

The primary treatment for diabetes is tight control of a patient's blood glucose levels. However, recent studies showed that hyperglycemia alone is insufficient to account for the development and the progression of diabetic complications. Metabolomic and proteomic analysis has revealed that a failure of energy homeostasis, particularly within the Schwann cell-rich sciatic nerve may be a driving force in the pathogenesis of DN. The aim of this study was to investigate the effect of hyperglycemia on mitochondrial energy homeostasis in Schwann cells. Primary mouse immortalized Schwann cells (SW10) and mouse embryonal fibroblasts (MEF) were cultured for 6 days under high glucose conditions (25 mM) as an in vitro model for long term hyperglycemia, and compared to cells cultured under low glucose conditions (5 mM). To determine the mitochondrial bioenergetics of the cells, glucose uptake, mitochondrial properties, reactive metabolites, glycolysis and mitochondrial respiration were measured. The four activation pathways of ROS described by the unifying theory were assessed, together with pathways involved in mitochondrial metabolic dysfunction described by Viader et al., such as of fatty acid synthesis, fatty acid oxidation and the integrated stress response (Viader 2013). Since nitric oxide might also play an important role in hyperglycemia induced changes in mitochondrial function, the expression of the three different NOS isoforms, nitric oxide and S-nitrosylated protein concentration were determined.

## Materials and Methods

### 3 Material and Methods

#### 3.1 Mouse Model

The animal experiments are performed in accordance of EU and national regulations for animal experimentation and all animal work was approved by the local ethics committee Regierungspräsidium Karlsruhe, Germany (file number: 35-9185.81/G295/15). Wild type mice (C57BL/6N) were obtained from Charles River, Sulzfeld, Germany. Mice were housed in groups of maximal 3 animals/cage in temperature- and humidity- controlled rooms with a 12 h light/dark cycle, having free access to food and drinking water. Diabetes was induced by intra-peritoneal injection of Streptozotocin (STZ 50 mg/kg bodyweight, in 50 mM Sodium citrate, pH 4.5) for 3 or 5 successive days in eight weeks old mice (Like and Rossini, 1976). Wild-type age-matched littermates receiving sodium citrate served as controls. Blood glucose levels of blood samples taken from the tail vein were determined once a week, using a ACCU-CHEK sticks (Bierhaus et al., 2004; Bierhaus et al., 2012) and adjusted with insulin glargin (Lantus, Sanofi) to <350 mg/dl. After 3 or 6 months STZ-induced diabetes the animals were sacrificed using carbon dioxide and peritoneal cavity lavage was performed post-mortem. After reperfusion with ice-cold PBS, sciatic nerves were taken and washed in ice-cold PBS, excessive fat tissue was removed, and directly snap-frozen and stored at -80 °C or used directly for the acyl carnitines assay.

#### 3.2 Cell culture

Murine embryonic fibroblasts (MEF; ATCC®, CRL-2991™), murine hepatocytes (AML12; ATCC®, CRL-2254), murine renal tubular cells (M1; ATCC®, CRL-2038), murine mesangial cells (MES13; ATCC®, CRL-1927) and murine Schwann cells (SW10; ATCC®, CRL-2766™) were all primary immortalized cell lines obtained from ATCC®. MEF were cultured in DMEM medium (1 g/L glucose, Gibco™, 31885-023) supplemented with 10% Fetal Calf Serum (FCS; Sigma®, C8056), 1% penicillin streptomycin (P/S; Sigma®, P0781), Amphotericin B (AmpB; Sigma®, A2942), and 1% Non-Essential Amino Acids (NEAA, Sigma®, M7145). AML12 were cultured in DMEM-F12 medium (17.5 mM glucose, Gibco™, 11320-074), supplemented with 10% FCS, 1% P/S, 1% AmpB, 40 ng/ml dexamethasone (Sigma®, D1756), 10% Insulin-Transferrin-Selenium (Gibco™, 41400-045) and 50 µg/ml gentamycin (Sigma®, G1397). M1 were cultured in DMEM medium (1 g/L

## Materials and Methods

glucose, Gibco™, 31885-023) supplemented with 10% FCS, 1% P/S and 1% AmpB, 15 mM HEPES (Sigma®, TMS-003), 0.5 mM sodium pyruvate (Sigma®, S8636), 2.5 mM L-glutamine (Sigma®, G7513) and 1.2 g/L sodium bicarbonate (Sigma®, S8761). MES13 were cultured in DMEM (1 g/L glucose, Gibco™, 31885-023) supplemented with 10% FCS, 1% P/S, 1% AmpB and 14 mM HEPES. SW10 were cultured in DMEM medium (1 g/L glucose, Gibco™, 31885-023) supplemented with 10% FCS, 1% P/S and 1% AmpB. MEF, AML12, M1 and MES13 were incubated at 37°C, whereas SW10 were incubated at 33°C. To determine the effect of high glucose MEF, M1, MES13 and SW10 were cultured in high glucose DMEM (4.5 g/L glucose DMEM, Gibco™, 41965-039) and AML12 were cultured in high glucose DMEM-F12 (Gibco™, 11320-074, supplemented with glucose (Sigma®, G7021), 50 mM final concentration) supplemented with the appropriate supplements as described. MEF, M1, MES13 and SW10 cultured in DMEM (1 g/L glucose) and AML12 cultured in DMEM-F12 (17.5mM glucose) for equal amount of time served as control.

### 3.3 Patient study

#### 3.3.1 Participants

This study was performed in accordance with the ethical principles of the Declaration of Helsinki. The study protocol was approved by the local ethical committee of the Medical Faculty of the University of Heidelberg (HEIDIS-2: S-515/2012), and all participants signed an informed consent form. Fourteen patients with T2DM were included. Nine age-matched healthy volunteers with no recorded medical conditions and a body mass index <25 served as controls. The study design was prospective and uncontrolled.

#### 3.3.2 Isolation PBMCs

For this study, peripheral blood mononuclear cells (PBMCs) were isolated from 9 ml venous blood of overnight fasted non-diabetic control and T2DM patients. Erythrocyte lysis buffer (ECL; 150 mM NH<sub>4</sub>Cl, 10 mM NaHCO<sub>3</sub>, 2 mM EDTA, pH 7.3) was added to the blood and filled up to 50 ml in total, mixed thoroughly and incubated for 20 min on ice. The PBMCs are pelleted by centrifugation at 1300 rpm and 4°C for 10 min. The pellet was resuspended in 1 ml ECL Buffer, transferred into a new 1.5 ml tube and incubated on ice for 5 min. The PBMCs are pelleted by



## Materials and Methods

centrifugation at 1300 rpm and 4°C for 5 min. The pellet is resuspended in 1 ml PBS Buffer and cell number was determined using a coulter counter. PBMCs were kept on ice and used within 1 hour after isolation.

### 3.4 Unifying theory

#### 3.4.1 Glucose uptake

Glucose uptake was measured by flow cytometry analysis, using the fluorescent glucose analog 2-(N-(7-Nitrobenz-2-oxa-1,3,diazol-4-yl)Amino)-2-Deoxyglucose (2-NDBG; Invitrogen™, N1319). After 3, 6, 12 or 24 days of high glucose treatment the cells were washed with PBS and  $1.5 \times 10^5$  cells per well were seeded into a 12-well plate. After overnight attachment at 33°C for SW10 and 37°C for MEF, the cell monolayer was washed with PBS. To each well, 1 ml Kreb's Ringer - HEPES buffer (KRH buffer; 136 mM NaCl, 4.7 mM KCL, 1.25 mM CaCl<sub>2</sub>, 1.25 mM MgSO<sub>4</sub>, 10 mM HEPES and 0.1% fatty acid free bovine serum albumin (BSA), pH 7.4, 37°C) containing 1 drop/ml NucBlue Life Ready Probes Reagent (Hoechst 33342; Invitrogen™, R37605) was added to stain the living cells. The cells were incubated at 37°C, 5% CO<sub>2</sub> for 30 min, protected from light. Thereafter the KRH buffer was removed and the cell monolayer was washed once with KRH buffer (37°C). To each well 0.5 ml KRH buffer containing appropriated concentration of 2-NDBG (5 μM, 10 μM, 25 μM, 50 μM, 75 μM or 100 μM) was added to the cell monolayer and incubated for 1 h at 37°C, protected from light. The cells were harvested, centrifuged (1300 rpm, 5 min, 4°C) and resuspended in 0.5 ml ice-cold FACS buffer (10% FCS, 1mM EDTA in PBS). The cells were analyzed using Becton Dickinson LSR II flow cytometer (*Heidelberg, Germany*).

#### 3.4.2 Polyol pathway; Sorbitol

The amount of sorbitol in the samples was determined using a D-Sorbitol Colormetric Assay Kit (Biovision®, K631-100), according to the manufacturer's protocol. In the assay, sorbitol is oxidized to fructose with the proportional development of intense color with an absorbance maximum at 560 nm. Freshly isolated cells,  $1 \times 10^6$  per condition, were lysed using 100 μl RIPA buffer containing 50 mM Tris-HCl pH 7.5, 150 mM NaCl, 1% Triton X-100, 0.5% Na-deoxycholate, 0.1% SDS, 1 mM DTT, 1% protease inhibitor cocktail (Sigma®, P9599) and 40 U/ml benzonase

## Materials and Methods

(Millipore®, 71206). The cell lysates were diluted 1:10 in dH<sub>2</sub>O. To each well of a 96-well plate, 50 µl sample or sorbitol standard and 50 µL reaction mix was added. After 30 min incubation at 37°C the O.D. at 560 nm was measured using microplate reader. Sorbitol level was calculated from the standard curve and correct for the protein concentration measured by Bradford.

### 3.4.3 Hexosamine pathway; Glycosylation

Glycosylation was determined by immunoblotting using primary antibody against O-Linked β-N-acetylglucosamine (O-GlcNAc (CTD110.6); Cell Signaling Technology®, 9875) as described below.

### 3.4.4 Protein kinase C pathway; PKC activity

Protein Kinase C (PKC) activity was determined using PKC kinase activity assay kit (Enzo® Life Sciences, ADI-EKS-420A) according to manufacturer's protocol. Fresh isolated cells were lysed using Lysis Buffer (20 mM MOPS, 5 mM EGTA, 2 mM EDTA, 1% NP40, 1 mM DTT, 1% protease inhibitor cocktail (Sigma®, P9599) and 1% phosphatase inhibitor cocktail (HALT™; Thermo Fisher Scientific, 78420) for 10 min on ice. The sample lysates were sonicated (3 times 20 sec) and centrifuged (13000 rpm, 15 min). The supernatant was transferred in pre-chilled 1.5 ml tubes and kept on ice. To each well of the PKC Substrate Microtiter Plate 50µl kinase Assay Dilution Buffer is added and incubated for 10 min at RT. The liquid was aspirated and all samples were added to the wells. The reaction was initiated by adding 10 µL of diluted ATP solution, except the blank, and incubated for 90 min at 30°C on a shaker (rotate angle 60 rpm). All the wells were aspirated and 40 µl of Phosphospecific Substrate Antibody was added to each well, except the blank, and incubated at RT for 1 h. The wells were washed 4 times with Wash Buffer. 40 µL of the diluted Anti-Rabbit IgG:HRP Conjugate was added to each well, except the blank, and incubated at RT for 30 min. The wells were washed again 4 times with Wash Buffer. To each well 60µl of Tetramethylbenzidine Substrate Buffer was added and incubated for 30 min at RT. The reaction was stopped by adding 20 µl of Stop Solution to each well. The absorbance was measured at 450 nm and corrected for 570 nm using microplate reader.

## Materials and Methods

### 3.4.5 AGE pathway; Methylglyoxal

The concentration of MG in the samples was determined by liquid chromatography with tandem mass spectrometric detection (LC-MS/MS), as described previously (Rabbani and Thornalley, 2014). Briefly,  $1 \times 10^6$  cells/sample were deproteinized by adding 10  $\mu$ l of 20% trichloroacetic acid and the internal standard of 2 pmol of [13C2]-MG (prepared in-house) was added. For the derivatization of MG, the samples and standard (0-20 pmol MG) were incubated with 100  $\mu$ M 1,2-diaminobenzene, 100  $\mu$ M diethylenetriamine-penta-acetic acid, 5 mM sodium dithionite stabilizer and 0.3% (w/v) NaN<sub>3</sub> in the dark at RT for 4 hrs (Dobler et al., 2006; Thornalley and Rabbani, 2014). Samples were analysed by LC-MS/MS using an ACQUITY UPLC-I class with a Xevo TQ-S mass spectrometric detector (Waters Corporation). A BEH C18 column (ACQUITY, 1.7  $\mu$ m, 100 x 2.1 mm, Waters Corporation) fitted with a pre-column (ACQUITY, 1.7  $\mu$ m, 5 x 2.1 mm, Waters Corporation) was used to separate the samples. The mobile phase was 0.1% formic acid with a linear gradient of 0-100% of 0.1% formic acid in 50% (v/v) acetonitrile over 10 min at a flow rate of 0.2 ml/min. The column was washed with 100% of 0.1% formic acid in 50% (v/v) acetonitrile and re-equilibrated with 100% of 0.1% formic acid. LC-MS/MS settings were: capillary voltage 0.5 kV, desolvation gas flow 800 l/h and cone gas flow 150 l/h, source temperature 150°C, desolvation gas temperature 350°C. The analytes were measured by positive ionization with multiple reaction monitoring with a retention time of 5.9 min and the Mass transition (parent ion > fragment ion; collision energy; cone voltage) were: MG 145.01 > 77.10; 24 eV; 2 V and [13C2]-MG 148.06 > 77.16; 24 eV; 2 V. A calibration curve was established from 0-20 pmol of MG and the limited MG detection was a concentration of 0.520 pmol.

### 3.5 Mitochondrial properties and reactive metabolites

Mitochondrial mass, mitochondrial polarity, O<sub>2</sub>•<sup>-</sup>, ROS and NO were determined using MitoTracker™ Orange CMTM-Ros (Invitrogen™, M7510), JC-1 (Invitrogen™, T3168), MitoSOX™ Red (Invitrogen™, M36008), CM-H2DCFDA (Invitrogen™, C6827) and DAF-FM Diacetate (Invitrogen™, D23844) fluorescent dyes, respectively. The cells were harvested, counted and  $1.5 \times 10^5$  cells per well were seeded into a 12-well plate. After overnight attachment at 33°C for SW10 and 37°C for MEF, the cell monolayer was washed with PBS. The cell monolayer was washed with

## Materials and Methods

PBS, and 0.5 ml KRH buffer containing Hoechst (1 drop/ml), MitoTracker™ Orange CMTM-Ros (300nM) or JC-1 (2 $\mu$ M) was added to the respective wells, incubated at 37°C, 5% CO<sub>2</sub> for 30 min, protected from light. After incubation the cell monolayer was washed with PBS, 0.5 ml of KRH buffer was added and incubated at 37°C, 5% CO<sub>2</sub> for 1 h, protected from light. The cells were harvested, centrifuged (1300 rpm, 5min, 4°C) and resuspended in 0.5 ml ice-cold FACS buffer (10% FCS, 1mM EDTA in PBS). The cells were analyzed using Becton Dickinson LSR II flow cytometer (*Heidelberg, Germany*).

### 3.6 Mitochondrial bioenergetics

#### 3.6.1 Optimization cell density and reagents XF96 Seahorse Bioanalyzer

For optimization of the reagents 2 x 10<sup>4</sup> cells/well of XF96 cell culture plate (Agilent Seahorse XF, XF96 FluxPack) and attached overnight at 33°C for SW10 and 37°C for MEF. Optimization of the reagents was performed using the protocol and algorithm program in the XFe96 Seahorse Bioanalyzer. Briefly, 1 h before the assay the medium was changed to Agilent Seahorse XF Assay Medium (Agilent Seahorse, 102353-100) supplemented with Glucose (Sigma, D8375, 10mM), Glutamine (Sigma® 59202C, 2 mM) and sodium pyruvate (Sigma, S8636, 1 mM). The concentrations of oligomycin (Sigma®, 75351), Carbonyl cyanide 4-(trifluoromethoxy)-phenylhydrazone (FCCP; Sigma® C2920), Rotenone (Sigma®, R8875) and Antimycin A (Sigma®, A8674) were optimized over a concentration range using 2 x 10<sup>4</sup> cells/well for both cell types. The bioenergetics Mito stress assay was performed using the algorithm program in the XFe96 Seahorse Bioanalyzer.

#### 3.6.2 Glycolysis

Glycolysis was measured using the Seahorse Bioanalyzer (XF96 Bioanalyzer, Aligent) according to the manufacturer's protocol. SW10 and MEF cells were seeded 2 x 10<sup>4</sup> cells/well of XF96 cell culture plate (Agilent Seahorse XF, XF96 FluxPack) and attached overnight at 33°C for SW10 and 37°C for MEF. On the day of the assay, the media was changed to Agilent Seahorse XF Assay Medium (Agilent Seahorse, 102353-100) supplemented with 2 mM Glutamine (Sigma®, 59202C), and incubated for 1 h prior assay in a non-CO<sub>2</sub> incubator at 37°C. Injections of glucose

## Materials and Methods

(Sigma®, D8375, 10 mM final), oligomycin (Sigma® 75351, 1 µM final) and 2-deoxy-d-glucose (2-DG; Sigma® D8375, 0.1 M final) were diluted in the Agilent Seahorse XF Assay Medium and loaded onto ports A, B and C respectively. The machine was calibrated and the assay was performed using Glycolytic Stress Test protocol as suggested by the manufacturer (Agilent Seahorse Bioscience, Supplemental figure 19). The assay was run in one plate with 8-10 replicates. The assay was repeated at least 3 times, both LG and 6dHG cultured cells on one plate. The rate of glycolysis is calculated as the extracellular acidification rate (ECAR) after the addition of glucose. Glycolytic capacity is the rate of increase in ECAR after the injection of oligomycin following glucose. Oligomycin inhibits mitochondrial ATP production and therefore shifts the energy production to glycolysis with increase in ECAR revealing maximum glycolytic capacity of the cells. The glycolytic reserve is the difference between glycolytic capacity ECAR rate and glycolysis ECAR rate. The non-glycolic ECAR is calculated as the ECAR after the addition of 2-DG that competitively inhibits the formation of glucose-6-phosphate from glucose and thereby the glycolysis.

### 3.6.3 Mitochondrial respiration

Mitochondrial respiration was measured using the Seahorse Bioanalyzer (Agilent Seahorse, XF96 Bioanalyzer) as described before (Salabei et al., 2014). SW10 and MEF cells were seeded  $2 \times 10^4$  cells/well of XF96 cell culture plate (Agilent Seahorse XF, XF96 FluxPack) and attached overnight at 33°C for SW10 and 37°C for MEF. On the day of the assay, the media was changed to Agilent Seahorse XF Assay Medium (Agilent Seahorse, 102353-100) supplemented with glucose (10 mM), sodium pyruvate (1 mM) and Glutamine (2 mM), and incubated for 1 h prior assay in a non-CO<sub>2</sub> incubator at 37°C. Injections of oligomycin (1 µM final), FCCP (1 µM final), a combination of rotenone and antimycin-A (1 µM final each) were diluted in the Agilent Seahorse XF Assay Medium and loaded onto ports A, B and C respectively. The machine was calibrated and the and the assay was performed using Mito Stress Test protocol on one XF96 cell culture plate 8-10 replicates and the assay was repeated at least 3 times. The following indices of mitochondrial respiration were calculated as previously described before (Brand and Nicholls, 2011). Basal oxygen consumption rate (OCR) is the difference in OCR without any substrates and the OCR after addition of a combination of rotenone and antimycin-A, inhibiting

## Materials and Methods

complex I and III respectively. ATP production is the ATP turnover via oxidative phosphorylation and calculated as the difference in OCR after the addition of oligomycin (ATP synthase, complex V inhibitor) and basal OCR. Maximal respiration is induced by FCCP which uncouples ATP from ADP and calculated as the difference between OCR after addition of FCCP and OCR after the addition of the combination of rotenone and antimycin-A. The spare respiratory capacity is calculated as the difference in OCR with FCCP and basal OCR. From these data the bioenergetic health index (BHI) was calculated as described before (Chacko et al., 2014).

### 3.7 Quantitative real-time PCR

#### 3.7.1 RNA extraction and cDNA synthesis

Flash frozen cell pellets ( $1 \times 10^6$  cells/ sample) were homogenized in RTL lysis buffer. The subsequent extraction was performed according to the manufacturer's protocol (Qiagen RNeasy kit, spin column protocol, Quagen). Quantification of RNA was performed using a photometer (Eppendorf, GmbH). A total of 2  $\mu\text{g}$  of RNA were used for the cDNA synthesis reaction and performed according to the manufacturer's protocol (High-capacity cDNA Reverse Transcription Kit, Thermo Fisher Scientific).

#### 3.7.2 Quantitative real-time PCR

cDNA was diluted 1:10 with  $\text{dH}_2\text{O}$  and used for qPCR analysis performed in duplicates with QuantiNova™ SYBR® Green qPCR Kit (Qiagen, 1076717). Briefly, 2  $\mu\text{l}$  of cDNA was transferred into a 96-well qPCR microplate and 18  $\mu\text{l}$  of reaction mix containing 1 x SYBR Green Mastermix, 200 nM forward primer and 200 nM reverse primer (Eurofins Genomics, Germany) was added (Table 1). The plate was sealed with a film and centrifuged (1000 rpm, 4°C, 2 min). Quantitative real-time PCR analysis was performed using Roche LightCycler 480 applying the following protocol (Table 2). The cross-points ( $C_p$ ) were calculated and the relative ratio of the mRNA levels were determined applying the following formula  $2 \times (2^{C_p(\text{target}) - C_p(\text{reference})}) - 1$  and using the geometric mean of the  $C_p$  values of *B2m*, *Actb*, *Hprt*, and *Rn18s* as a reference (Hruz et al., 2011; Svingen et al., 2015).

## Materials and Methods

**Table 1. Primers**

Target Gene	Species	Gene ID		Sequence [5'→3']
Acaca	mouse	107476	for rev	ATGGGGCGGAATGGTCTCTTTTC TGGGGACCTTGTCTTCATCAT
Acly	mouse	104112	for rev	AGGAAGTGCCACCTCCAACAGT CGCTCATCACAGATGCTGGTCA
Actb	mouse	11461	for rev	GGCTGTATCCCCTCCATCG CCAGTTGGTAACAATGCCATGT
Aldob	mouse	230163	for rev	GAAACCGCTGCAAAGGATAA GAGGGTCTCGTGGAAAAGGAT
Asns	mouse	27053	for rev	GCCCAAGTTCAGTATCCTCTC TAAATACATGCCACAGATGCC
Atf4	mouse	11911	for rev	GGCTATGGATGATGGCTTGG AATTGGGTTCAGTGTCTGAGG
B2m	mouse	12012	for rev	TTCTGGTGCTTGTCTCACTGA CAGTATGTTCCGGCTTCCCATTCC
Chop (Ddit3)	mouse	13198	for rev	AAGTGCATCTTCATACACCACC TTGATTCTTCTTCTCGTTTCTGT
Cpt1b	mouse	12895	for rev	GCACACCAGGCAGTAGCTTT CAGGAGTTGATTCCAGACAGGTA
Eno1	mouse	13806	for rev	TGCGTCCACTGGCATCTAC CAGAGCAGGCGCAATAGTTTTA
Echs1	mouse	93747	for rev	TTGTGAACTTGCCATGATGTGT TGCTCGGGTGAGTCTCTGAG
Fasn	mouse	14104	for rev	GGGTGCTGACTACAACCTCTCC TGACAGACACCTTCCCCTC
Glut1	mouse	20512	for rev	ACCAAAAGCAACGGAGAAGAG GGCATTCCGAAACAGGTAACCTC
Glut3	mouse	20527	for rev	ATGGGGACAACGAAGGTGAC GTCTCAGGTGCATTGATTGACTC
Hadha	mouse	97212	for rev	TGCATTTGCCGCAGCTTTAC GTTGGCCCAGATTTTCGTTCA
Hk2	mouse	15277	for rev	TGATCGCCTGCTTATTCACGG AACCGCCTAGAAATCTCCAGA
Hmgcr	mouse	15357	for rev	TGGTGGACCAACCTTCTAC GCCATCACAGTGCCACATAC
Hprt	mouse	15452	for rev	TCAGTCAACGGGGGACATAAA GGGGCTGTACTGCTTAACCAG
Lipe	mouse	16890	for rev	CCAGCCTGAGGGCTTACTG CTCCATTGACTGTGACATCTCG
Pck1	mouse	18534	for rev	CTGCATAACGGTCTGGACTTC CAGCAACTGCCCGTACTCC
Pck2	mouse	74551	for rev	ATGGCTGCTATGTACTCTCC GCGCCACAAAGTCTCGAAC
Mthfd2	mouse	17768	for rev	AATTAAGCGAACAGGCATTCCA AGGATCGTGTGCTTCTTCAG
eNOS	mouse	18127	for rev	GGCTGGGTTTAGGGCTGTG CTGAGGGTGTCTAGGTGATG
iNOS	mouse	18126	for rev	GTTCTCAGCCCAACAATACAAGA GTGGACGGGTGATGTCAC

## Materials and Methods

Target Gene	Species	Gene ID		Sequence [5'→3']
nNOS	mouse	18125	for rev	CTGGTGAGGGAACGGGTGAC CCGATCATTGACGGCGAGAAT
Rn18s	mouse	19791	for rev	CGGCTACCACATCCAAGGAA GCTGGAATTACCGCGGCT
Srebp1	mouse	20787	for rev	CATGCCATGGGCAAGTACAC TGTTGCCATGGAGATAGCATCT
Trib3	mouse	228775	for rev	CACTTTAGCAGCGGAAGAGG GTGTAGCTCGCATCTTGTC

**Table 2. Thermocycler protocol for qPCR**

	Temperature, °C	Time	Ramp rate, °C/sec	Number of cycles
<b>Preincubation</b>	95	7 min	4.4	1
<b>Amplification</b>	95	10 sec	4.4	
	60	20 sec	2.2	45
	72	1 sec	4.4	
<b>Melting curve</b>	95	5 sec	4.4	
	65	1 sec	2.2	1
	97	5 acquisitions/°C	0.11	
<b>Cooling</b>	4	forever	4.4	1

### 3.8 Immunoblot

#### 3.8.1. Protein isolation cells

Cells,  $1 \times 10^6$  per condition in triplicates, were washed with PBS and isolated using trypsin and were centrifuged (1300 rpm, 4°C, 5 min). The samples were washed with PBS and centrifuged as described, for 2 times. Protein isolation was performed using RIPA buffer (50 mM Tris-HCl pH 7.5, 150 mM NaCl, 1% Triton X-100, 0.5% Na-deoxycholate, 0.1% SDS, 1 mM DTT, 1% PIC and 40 U/ml benzonase). Per sample 100  $\mu$ l RIPA was added, vortexed for 30 sec, incubated for 1 h on a 360° rotator in cold room (4°C) and centrifuged (14000 rpm, 4°C, 30 min). The protein concentration of the supernatant was determined using Bradford reagent and the samples were stored at -20°C until further analysis (Bradford, 1976).



## Materials and Methods

### 3.8.2 Cell lysis and protein isolation for GLUT 1

Glut 1 is highly hydrophobic and consists of 12 transmembrane segments, and can form aggregates upon cell lysis, resulting in a Glut 1 smear by immunoblot. Therefore a special cell lysis protocol is recommended to minimize Glut 1 aggregation as described by Zhao et al., 2008. Cells are lysed in Glut 1 lysis buffer (1% Triton X-100, 0.1% SDS, 1% protease inhibitor cocktail (Sigma®, P9599)) for 1 h on ice and centrifuged (13000 rpm, 10 min, 4°C). Protein concentration of the supernatant was determined by Bradford (Bradford, 1976). To fully collapse GLUT 1 bands, the GLUT 1 Glycosylation was removed using PNGase F kit (New England Biolabs®, P0704S) according to the manufacturer's protocol. To 10 µg protein in 9 µl dH<sub>2</sub>O, 1 µl of denaturing buffer was added and incubated for 30 min at RT. After incubation, 4 µl dH<sub>2</sub>O, 2 µl G7 reaction buffer, 2 µl NP-40 and 2 µl PNGaseF was added, vortexed for 20 sec and incubated for 1 h at 37°C. Glut sample buffer (5x sample buffer; 1.56 ml 2M Tris-HCL (pH 6.8), 1 g SDS, 5 ml glycerol, 2.5 ml 2-mercaptoethanol, 5mg bromophenol blue) is added at 1x to the samples, incubated for 30 min at RT before loading the gel.

### 3.8.3 Immunoblot

About 10-20 µg protein were denatured by incubation in Laemmli buffer, containing 0.8% SDS, 4% glycerol, 100 mM DTT, 25 mM Tris-HCl (pH 6.8), 0.005% bromophenol blue, at 98°C for 10 min (Laemmli, 1970), unless mentioned otherwise. Proteins were separated by SDS-PAGE (pre-casted 4-20% gels, Mini-PROTEAN® TGX™, Bio-Rad) applying 160 V for 50 min and transferred onto a nitrocellulose membrane applying 25 V for 30 min. Transfer was checked using Ponceau Red and membranes were blocked using 3% Bovine Serum Albumin (BSA; Sigma®, A8806) in TBS-T or in the case of O-GlcNAc, Phospho-Acetyl CoA-Carboxylase and Phospho-ATP citrate lyase in Pierce™ Protein-Free Blocking Buffer (Thermo Fischer Scientific, 37572). After 1 h blocking at RT, the primary antibody was added in the appropriate concentration (Table 3). After overnight incubation at 4°C the membranes were washed with PBS-T and incubated with the secondary antibody anti-Rabbit IgG coupled to horseradish peroxidase for 1 h at RT (Table 4). The proteins were detected using ECL™ reagent (GE Healthcare, RPN2106). For reprobing, membranes were stripped in an 80°C water bath for 20

## Materials and Methods

min using Stripping buffer (0.2 M glycine pH 2.5 and 0.05% Tween 20). Thereafter, the membranes were washed with TBS-T, blocked and processed as described above. Images were acquired and quantified using the GS-800<sup>®</sup> calibrated densitometer and Quantity One <sup>®</sup> 1-D analysis software, Bio-Rad.

**Table 3. Primary antibodies**

Antibody	Isotype	Company	Dilution
Acetyl-CoA Carboxylase (ACC)	Rabbit	Cell Signaling Technology, 3676	1/1000
Phospho-ACC (Ser79)	Rabbit	Cell Signaling Technology, 11818	1/1000
AceCS1	Rabbit	Cell Signaling Technology, 3658	1/1000
b-Actin	Rabbit	Cell Signaling Technology, 4970	1/1000
ACSL1	Rabbit	Cell Signaling Technology, 9189	1/1000
AMPKa	Rabbit	Cell Signaling Technology, 2535	1/1000
Phospho-AMPKa (Tyr172)	Rabbit	Cell Signaling Technology, 9957	1/1000
AMPKb1/2	Rabbit	Cell Signaling Technology, 4150	1/1000
Phospho-AMPKb1 (Ser182)	Rabbit	Cell Signaling Technology, 4186	1/1000
ASNS	Rabbit	Sigma, HPA029318	1/1000
ATF-4	Rabbit	Cell Signaling Technology, 11815	1/1000
ATF-6	Rabbit	Cell Signaling Technology, 65880	1/1000
ATP-Citrate Lyase (ACL)	Rabbit	Cell Signaling Technology, 4332	1/1000
Phospho-ACL (Ser445)	Rabbit	Cell Signaling Technology, 4332	1/1000
CaMKII	Rabbit	Cell Signaling Technology, 4436	1/1000
CHOP	Rabbit	Cell Signaling Technology, 5554	1/1000
eIF2a	Rabbit	Cell Signaling Technology, 5324	1/1000
Phospo-eIF2a (Ser 51)	Rabbit	Cell Signaling Technology, 3398	1/1000
iNOS	Rabbit	Novus Biologicals, NB300-605SS	1/500
FAS	Rabbit	Cell Signaling Technology, 3180	1/1000
Glut 1	Rabbit	Abcam, ab115730	1/10000
Glut 3	Rabbit	Abcam, ab41525	1/8000
IRE1a	Rabbit	Cell Signaling Technology, 3294	1/1000
LKB1	Rabbit	Cell Signaling Technology, 3047	1/1000
PhosPho-LKB1	Rabbit	Cell Signaling Technology, 3482	1/1000
O-GlcNAc	Mouse	Cell Signaling Technology, 9875	1/1000

**Table 4. Secondary antibodies**

Antibody	Company	Dilution
Rabbit IgG, HRP-linked	Cell Signaling Technology, 7074	2x dilution of
Mouse IgG, HRP-linked	Cell Signaling Technology, 7076	Primary antibody

## Materials and Methods

### 3.9 Fatty acid oxidation

#### 3.9.1 BODIPY fatty acid uptake

The fatty acid uptake of short chain and mid-chain fatty acid was determined using FL C<sub>5</sub> (4,4-Difluoro-5,7-Dimethyl-4-Bora-3a,4a-Diaza-s-Indacene-3-Pentanoic Acid) (BODIPY<sup>®</sup> FL C<sub>5</sub>, Invitrogen<sup>™</sup>, D3834) and C<sub>1</sub>, C<sub>12</sub> (4,4-Difluoro-5-Methyl-4-Bora-3a,4a-Diaza-s-Indacene-3-Dodecanoic Acid) (BODIPY<sup>®</sup> C<sub>1</sub>, C<sub>12</sub> 500/510, Invitrogen<sup>™</sup>, D3823) respectively, according to manufacturer's protocol. After 6 days of high glucose treatment the cells were washed with PBS and 1.5 x 10<sup>5</sup> cells per well were seeded into a 12-well plate. After overnight attachment at 33°C for SW10 and 37°C for MEF, the cell monolayer was washed with PBS. To each well, 1 ml KRH buffer containing 1 drop/ml NucBlue Life Ready Probes Reagent (Hoechst 33342; Invitrogen<sup>™</sup>, R37605) was added to stain the living cells. The cells were incubated at 37°C, 5% CO<sub>2</sub> for 30 min, protected from light. The media of the cell monolayer was removed and washed once with PBS. To each well 0.5 ml KRH buffer containing appropriate concentration (0.5 μM, 1 μM, 2.5 μM, 5 μM, 7.5 μM and 10 μM) of BODIPY<sup>®</sup> was added, and incubated at 37°C for 5 min, protected from light. The cells were harvested by trypsination, centrifuged (1300 rpm, 5min, 4°C) and resuspended in 0.5 ml ice-cold FACS buffer (10% FCS, 1mM EDTA in PBS). The cells were analyzed using Becton Dickinson LSR II flow cytometer (*Heidelberg, Germany*).

#### 3.9.2 Octanoate fatty acid oxidation

Measurement of fatty acid oxidation was performed using octanoate in combination with the Aligent Seahorse XF Cell Mito Stress test according to adapted manufacturer's XF Palmitate-BSA FAO Substrate protocol in permeabilized cells using saponin (Salabei et al., 2014). Cells were seeded into XF96 cell culture plate, 2 x 10<sup>4</sup> cells per well in substrate limited medium (1% FCS), allowed to attach overnight. The compounds were dissolved in Mannitol and Sucrose buffer (MAS buffer; 70 mM Sucrose, 220 mM Mannitol, 10 mM KH<sub>2</sub>PO<sub>4</sub>, 5 mM MgCl<sub>2</sub>, 2 mM HEPES, 1 mM EGTA and fatty acid free BSA, pH 7.2) . The compounds in were loaded into the ports of the assay cartridge, octanoate (1 mM final, co-injected with 25 mg/ml Saponin, 0.5 μM L-Carnitine, 0.5 mM malate and 1 mM ADP in MAS buffer), oligomycin (1 μM final), FCCP (0.5 μM final), and a combination of rotenone and antimycin-A (1 μM final each), in ports A, B, C and D

## **Materials and Methods**

respectively. The media of the cells was exchanged to MAS buffer 10 min prior start of the assay. The machine was calibrated and the assay was performed using Mito Stress Test protocol on one XF96 cell culture plate 8-10 replicates.

### **3.9.3 Acetylcarnitines**

Fresh isolated sciatic nerves were rinsed 2 times with wash media (4.5 g/L DMEM containing 10% FCS, 1% P/S and 1% AmpB). Single sciatic nerves were transferred into a well of 24-well plate containing 1 ml culture media (4.5 g/L DMEM containing 10% FCS, 1% P/S 1% AMPB, 2 mM L-glutamine, 100 ng/ml Nerve Growth Factor (Sigma®, N8773)). After 48 h media was collected and snap-frozen. The samples were sent to the Kinderklinik Stoffwechsellabor, Heidelberg and concentrations of acyl carnitines were assessed using liquid chromatography coupled fluorescence detection (Dr. J. G. Okun, Stoffwechsellabor, Kinderklinik Heidelberg).

### **3.10 Nitric Oxide**

#### **3.10.1 eNOS, nNOS and iNOS**

The gene expression of eNOS, nNOS and iNOS in whole protein lysates of both SW10 and MEF cultured for 6 days in either high glucose condition or control low glucose condition was determined by quantitative real-time PCR as previously described (see 3.7).

#### **3.10.2 Nitric oxide synthase**

Nitric oxide synthase (NOS) activity was determined using NOS Activity Colorimetric Assay kit (Biovision®, K205-110), according to the manufacturer's protocol. In this assay, NO generated by NOS undergoes series of reactions and reacts with Griess Reagent 1 and Griess Reagent 2 to generate a colored product with absorbance at 540 nm. The cells were lysed using ice-cold NOS assay buffer containing 0.1% PIC, homogenized by passing the cells 20 times through a 30 gauge needle and centrifuged (10,000 g, 10 min, 4°C). Protein concentrations were determined by Bradford (Bradford, 1979). To each well 60 µl sample (300 µg protein in 60 µL NOS assay buffer), Nitrite standard or positive control and 40 µl reaction mix was added. After 1h incubation at 37°C, 50 µL of Griess Reagent 1 and 50 µL of Griess Reagent 2 was added to the wells, incubated

## **Materials and Methods**

for 10 min at RT and O.D. at 540 nm was measured using microplate reader. NOS activity was calculated from the standard curve and correct for the amount of protein measured by Bradford (Bradford 1976).

### **3.10.3 S-Nitrosylation**

#### **3.10.3.1 Isolation mitochondria**

Mitochondria of Schwann cells ( $10 \times 10^6$  cells / condition) were isolated according to Cox and Emili with slight modifications (Cox and Emili, 2006). Briefly, the cells were homogenized in ice-cold isolation buffer I (250-STM DPS) containing 250 mM mannitol, 50 mM Tris (pH 7.4), 5 mM  $MgCl_2$  and 1 % protease inhibitor cocktail (Sigma®) using a 18 gauge syringe. The lysate was centrifuged (800 g, 4 °C, 15 min, 2x). The supernatant was the source for the mitochondria was transferred to a new tube and centrifuged (6000 g, 4°C, 15 min). The mitochondria were resuspended in isolation buffer II containing 280 mM mannitol, 10 mM  $MgCl_2$ , 5 mM  $K_2HPO_4$ , 10 mM MOPS, 1mM EGTA, pH 7.4 and centrifuged (6000 g, 4°C, 15 min, 3x). Isolated mitochondria were resuspended in respiration buffer containing 250 mM sucrose, 15 mM KCl, 1 mM EGTA, 5 mM  $MgCl_2$ , 30 mM  $K_2HPO_4$ , pH 7.4. Mitochondria were kept on ice and the S-nitrosylation assay was performed within 1 h after isolation.

#### **3.10.3.2 S-Nitrosylation assay**

The level of S-Nitrosylation in Schwann cells ( $10 \times 10^6$  cells/condition) and isolated mitochondria of Schwann cells was determined using the Pierce™ S-Nitrosylation Western Blot Kit (Thermo Fisher Scientific, 90105) according to the manufacturer's protocol with slight adaptations. Briefly, samples were washed 2 times with PBS and lysed in HENS Buffer, incubated on ice for 10 min, sonicated and centrifuged (10,000 g, 20 min, 4°C). Protein concentration was determined by Bradford (Bradford 1976). Protein concentrations were prepared to 1 mg/ml in 100 µL HENS Buffer. To each sample methyl methanethiosulfonate (MMTS, 20 mM final concentration) was added, vortex mixed and incubated for 30 min at RT. To precipitate the protein, 6 volumes of ice-cold acetone were added, incubated for 1 h at -80°C and centrifuged (10,000 g, 30 min, 4°C). To each pellet 1 ml acetone was added and centrifuged (10,000 g, 10 min, 4°C) to remove all

## Materials and Methods

MTTS. The acetone was removed and the pellet was dried using vacuum centrifuge concentrator (medium speed, 40°). 1 ul of labeling reagent (2 mM) and 2 uL of sodium ascorbate (1M) was added to the pellet and incubated for 90 min at RT. Thereafter, 6 volumes of ice-cold acetone was added, incubated overnight at -80°C for 1 h and centrifuged (10,000 g, 30 min, 4°C). The pellets were washed with 1 ml ice-cold acetone, centrifuged (10,000 g, 10 min, 4°C) and dried using vacuum centrifuge (medium speed, 40°) for 30 min. To each sample 50 ul of 1x reducing Laemmli sample buffer was added and heated for 10 min at 98°C. Immunoblotting was performed as previously described using anti-TMT antibody 1:1000 in 5% nonfat dry milk in 1x TBS-T as primary anti-body and anti-mouse IgG HRP linked antibody (Cell Signaling Technology, 7060s) 1:2000 in 5% nonfat dry milk in 1x TBS-T as secondary antibody.

### 3.10.4 Nitric oxide and ROS expression

Cells were incubated with 1mM DetaNONOate (Cayman Chemical, 146724-94-9) in low or high glucose medium for 30 min at 37°C, 5% CO<sub>2</sub> to measure the effect of direct NO on mitochondrial function and S-nitrosylation, as a positive control for NO. To determine the effect of NOS inhibition on mitochondrial function different concentrations of L-NG-monomethyl Arginine citrate (L-NMMA, Santa Cruz®, sc-364686), and N-[3-(Aminomethyl)benzylacetamide Dihydrochloride (1400W, Santa Cruz®, sc-3564) was added and incubated for 16hrs prior start of the assay. NO and ROS were determined using DAF-FM Diacetate (Invitrogen™, D23844) and CM-H<sub>2</sub>DCFDA (Invitrogen™, C6827) fluorescent dyes, respectively, as previously described. The cells were analyzed using Becton Dickinson LSR II flow cytometer (*Heidelberg, Germany*).

### 3.11 Mitochondrial bioenergetics PBMCs

#### 3.11.1 Glycolysis and mitochondrial respiration

Glycolysis and mitochondrial respiration was determined using the Seahorse Bioanalyzer (XF96 Bioanalyzer, Aligent) according to the manufacturer's protocol, with a few adaptations. Prior start of the assay, the XF96 cell culture microplate was coated with 50 µM poly-D lysine (Sigma®, A-003-E), 50 µl/well and incubated at 37°C for 1 h. The PBMCs of each subject were diluted to a concentration of 1.7 x 10<sup>6</sup> cells/ml using the appropriate assay medium; Glycolysis

## Materials and Methods

assay medium (XF Base Medium (Agilent Seahorse, 102353-100) + 1 mM sodium pyruvate) and MitoStress assay medium (XF Base Medium + 5 mM glucose + 1 mM sodium pyruvate). A total  $3 \times 10^5$  cells in 175  $\mu$ l per well were seeded, 16 wells/subject (8 wells for glycolysis assay and 8 wells for mitochondrial stress assay, Supplemental figure 20). To attach the PBMCs the plate was centrifuged at 600 rpm for 2 min with no brake. The plate was rotated 180° and centrifuged (600 rpm, 2 min, no brake) for equal distribution of the cells. The XF96 cell culture microplate was incubated in a non-carbon dioxide incubator at 37 °C for 30 min. The glycolysis and mitochondrial respiration of the PBMCs were determined simultaneously as described above (3.6.2 and 3.6.3). Glycolysis was measured by sequential injection of glucose (10 mM final concentration), oligomycin (1  $\mu$ M final concentration) and 2-DG (100 mM final concentration) in Glycolysis assay medium. Mitochondrial respiration was measured by sequential injection of oligomycin (1  $\mu$ M final concentration), FCCP (0.25 $\mu$ M final concentration) and a combination of rotenone and antimycin A (1 $\mu$ M final concentration each) in MitoStress assay medium.

### 3.11.2 Staining PBMCs for flow cytometry

#### 3.11.2.1 2-NDBG glucose uptake

PBMCs were diluted in KRH buffer to a concentration of  $5 \times 10^6$  cells/ml and 100  $\mu$ l ( $0.5 \times 10^6$  cells) are transferred into wells of a V-shaped, non-binding 96-well plate. The plate was centrifuged (1300 rpm, 3 min, RT). To each well 100  $\mu$ l of KRH buffer + 0.1% FCS are added and the plate was incubated at 37 °C for 30 min and centrifuged (1300 rpm, 3 min, RT). Glucose uptake was measured using the fluorescent glucose analog 2-NDBG as previously described. In short, 100  $\mu$ l of the different 2-NDBG solutions (5, 10, 25, 50 and 100  $\mu$ M in KRH buffer + 0.1% FCS) were added to the appropriate wells and incubated at 37 °C for 1 h, protected from light. The plate was centrifuged (1300 rpm, 3 min, RT). 150 $\mu$ l KRH buffer + 0.1% FCS was added to each well and centrifuged (1300 rpm, 3 min, RT). This step was repeated once more and the samples were stained with CD-antibodies as described below.

## Materials and Methods

### 3.11.2.2 Mitochondrial mass and ROS

To determine mitochondrial mass and ROS production the PBMCs were stained with Mitotracker® Green (Invitrogen™, M7514) and MitoSOX™ Red (Invitrogen™, M36008), respectively. To the respective wells 100 µL KRH buffer + 0.1% FCS containing Mitotracker® Green (300 nM) or MitoSOX™ Red (30 µM) was added and incubated for at 37°C for 30 min. The plate was centrifuged (1300 rpm, 3 min, RT). 150 µl KRH buffer + 0.1% FCS was added to each well and centrifuged (1300 rpm, 3 min, RT). This step was repeated once more and the samples were stained with CD-antibodies as described below.

### 3.11.2.3 Specific CD-antibodies

And cells were stained with 50 µL the CD-antibodies, diluted 1:250 in FACS buffer, to measure the glucose uptake in granulocytes, monocytes, T-cells and T-helper cells using Alexa Fluor® 647 anti-human CD66b antibody (clone: G10F5, Biolegend, cat. no. 305110 APC/Cy7) Brilliant Violet™ anti-human CD14 antibody (clone: HCD14, Biolegend, cat. no. 325628), anti-human CD3 antibody (clone: UCHT1, Biolegend, cat. no. 300426) and Alexa Fluor® 700 anti-human CD4 antibody (clone: OKT4, Biolegend, cat. no. 317426) respectively. The plate was incubated in ice protected from light for 15 min. The plate was centrifuged (1300 rpm, 3 min, RT) and the samples were dissolved in total 1 ml FACS buffer transferred into a FACS tubes and stored on ice until further analysis. The samples were analysed using Becton Dickinson LSR II flow cytometer (Heidelberg, Germany).

**Table 5. Fluorophores**

Fluorophore	Channel/Colour
2-NDBG	FITC
MitoSOX™	PE
MitoTracker® Green FM	FITC
CD3	AlexaFluor 700
CD4	APC/Cy7
CD14	Brilliant Violet 421
CD66b	APC



## Materials and Methods

### 3.12 Statistical analysis

Statistical analyses were performed using GraphPad Prism 7 and the level for statistical significance was defined as  $p < 0.05$ . Outlier elimination was performed applying Tukey's method of leveraging the interquartile range (Tukey, 1977). Differences between data groups were evaluated for significance using one-sample *t*-test.

## Results

### 4 Results

#### 4.1 Cells specific changes in response to glucose

##### 4.1.1 Increased glucose uptake

To determine the effect of high glucose on cellular glucose uptake, murine endothelial fibroblasts (MEF), kidney tubular epithelial cells (M1), mesangial cells (MES13) and Schwann cells (SW10) were cultured under normal glucose (LG, 5 mM) and under high glucose (HG, 25 mM), representative of hyperglycemia in patients, for 3 days. Murine hepatocytes (AML12) were found to grow better under 12.5 mM glucose, as such, this concentration of glucose was considered as normal condition (LG) and 50 mM glucose was considered as high glucose (HG) condition. The glucose uptake was measured by flow cytometry analysis using the glucose analog, 2-NDBG. The amount of intracellular 2-NDBG fluorescence was calculated per  $1 \times 10^6$  per minute and the slope of linear regression fit was calculated from the data points. Increased 2-NDBG uptake was observed in the MEF (slope  $3.128 \pm 0.1269$  versus  $3.833 \pm 0.3195$ ;  $p=0.0042$ ) (Figure 5.A), AML12 (slope  $3.352 \pm 0.08488$  vs  $3.908 \pm 0.05$ ;  $p=0.0079$ ) (Figure 5.B) MES13 (slope  $5.074 \pm 0.1799$  vs  $10.08 \pm 0.2302$ ;  $p<0.0001$ ) (Figure 5.D) and SW10 (slope  $6.866 \pm 0.3613$  vs  $8.134 \pm 0.3545$ ;  $p=0.0231$ ) (Figure 5.E) when cultured for 3 days under HG conditions compared LG cultured cells, but no changes was observed in M1 (Figure 5.C) cells. Focusing on the 100  $\mu$ M 2-NDBG uptake, the uptake was increased by 31% in MEF ( $334.8 \pm 10.89$  vs  $439.6 \pm 16.68$ ;  $p=0.0042$ ), 14% increase in both AML12 ( $365.9 \pm 18.09$  vs  $418.3 \pm 3.611$ ;  $p=0.0079$ ) and SW10 ( $732.2 \pm 41.46$  vs  $835.7 \pm 28.06$ ;  $p=0.0231$ ) a 83% increase in MES13 ( $557 \pm 8.389$  vs  $1021 \pm 10.73$ ;  $P<0.0001$ ).

To determine the long term effect of hyperglycemia, a time course study was performed. MEF, M1 and AML12 were selected representing one cell type for neurons, kidney and liver respectively. MEF, M1 and AML12 were cultured for 6, 12 and 24 days and glucose uptake measured, as described. After 6 days of HG treatment, maximal 2-NDBG uptake was observed in the MEF (Figure 6.A, D) and M1 (Figure 6.B, E); in MEF the uptake was increased by 65% ( $314.9 \pm 18.6$  vs  $519.6 \pm 97.95$ ;  $p<0.0001$ ) and in M1 the uptake was increased 128% ( $346 \pm 38.59$  vs  $787.2 \pm 110.4$ ;  $p<0.0001$ ). The 2-NDBG uptake of did not increase any further after 6 days in

## Results

either cell type. In contrast, maximal 2-NDBG uptake in the AML-12 cells was observed after 12 days of HG (Figure 6.C, F); uptake was increased 73% ( $332.2 \pm 47.91$  vs  $575.8 \pm 52.33$ ;  $p < 0.0001$ ) and increased further after 24 days by 92% ( $332.2 \pm 47.91$  vs  $639.2 \pm 174.8$ ;  $p = 0.0036$ ), as compared to LG cultured cells.

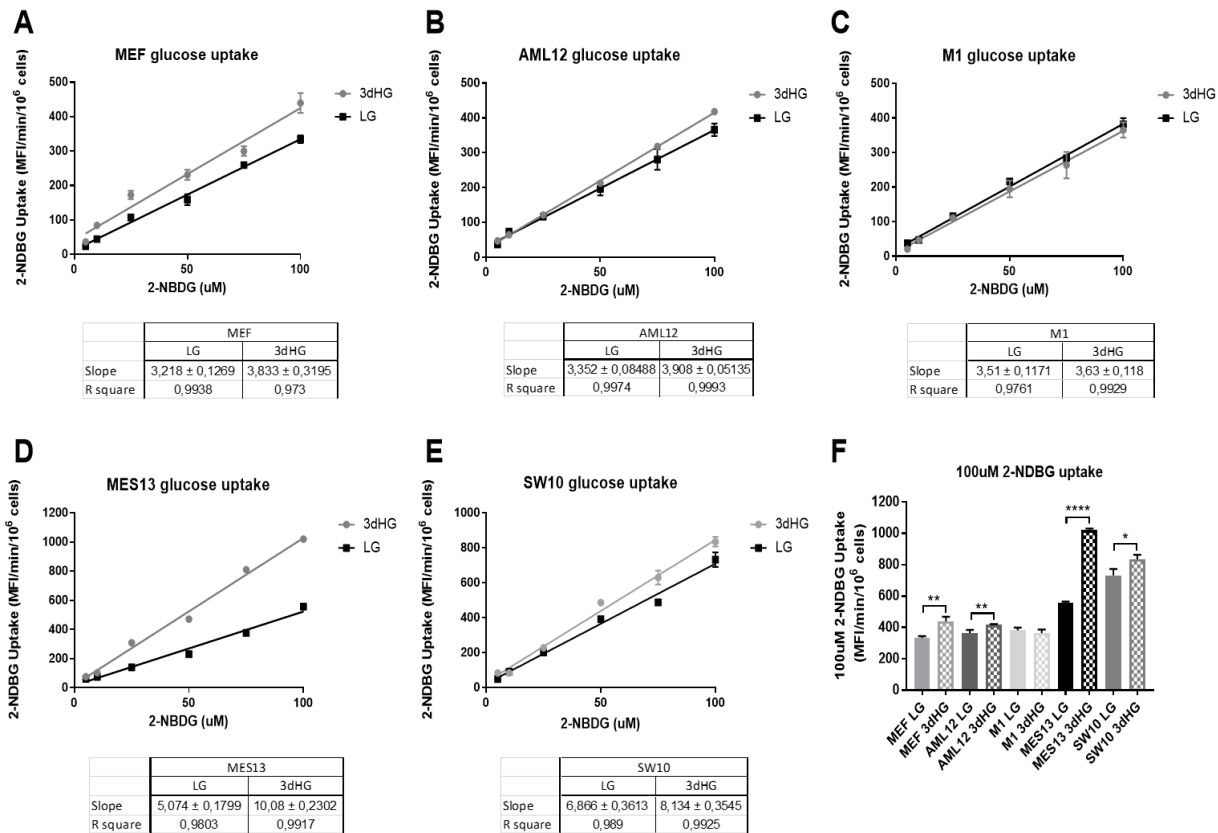


**Figure 5. 2-NDBG glucose uptake in short term hyperglycemia.**

Using 2-NDBG, glucose uptake was analyzed in fibroblasts (MEF) (A), hepatocytes AML12 (B) and renal tubular cells (M1) (C), mesangial cells (MES13) (D) and Schwann cells (SW10) (E) cultured for 3 days in high glucose media (3dHG) versus low glucose media (LG). Mean fluorescence intensity (MFI) was plotted against the concentration of 2-NDBG used and the slope was calculated. The maximal 100uM 2-NDBG uptake was calculated for all the cell type (F). Data is represented as mean +/- SD, n=3. For statistical analysis two sided t-test was applied \* $p < 0.05$ , \*\* $p < 0.01$ , \*\*\*\* $p < 0.0001$ .

### 4.1.2 Altered mitochondrial properties and reactive metabolites

To determine the effect of high glucose on mitochondrial properties and reactive metabolites in MEF, AML12, M1, MES13 and SW10 were cultured for 3 days in high glucose (HG) media or low

## Results

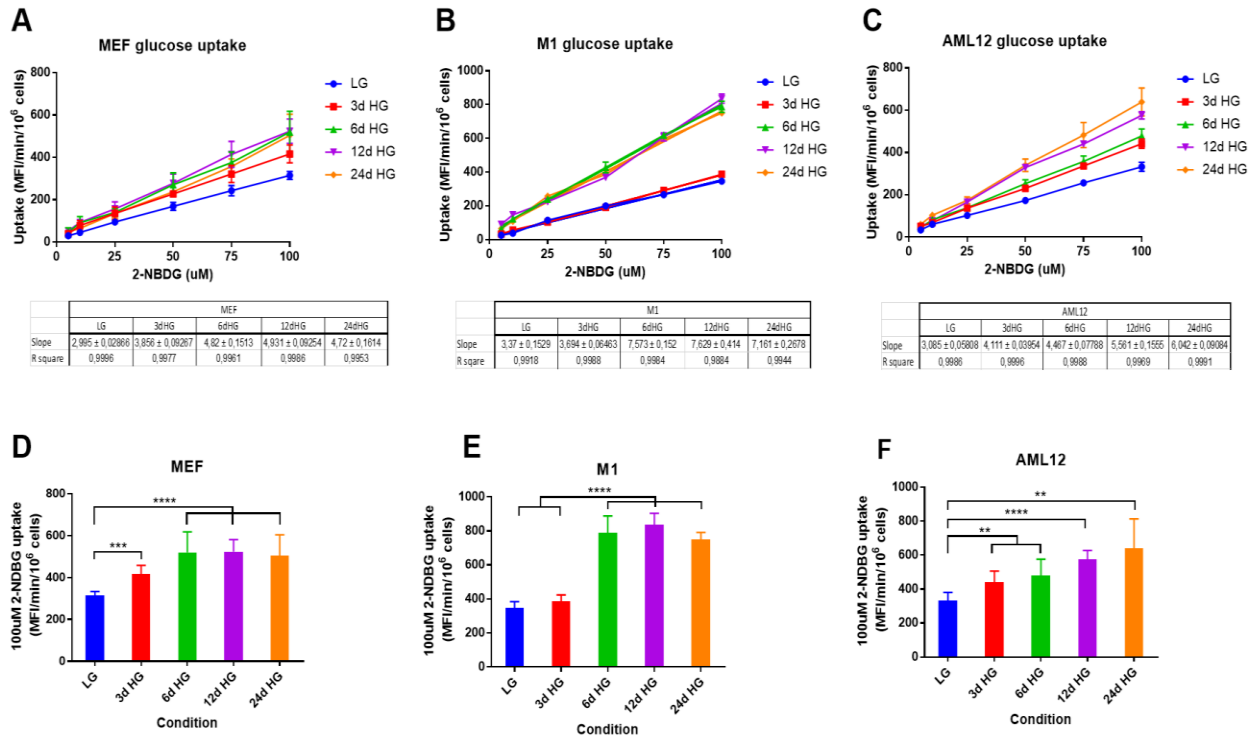


**Figure 6. 2-NDBG glucose uptake in long term hyperglycemia.**

Using 2-NDBG, glucose uptake was analyzed in fibroblasts (MEF) (A), hepatocytes AML12 (B) and renal tubular cells (M1) (C) cultured for 3, 6, 12 and 24 days in high glucose media (HG) versus low glucose media (LG). Mean fluorescence intensity (MFI) was plotted against the concentration of 2-NDBG used and the slope was calculated. The maximal 100uM 2-NDBG uptake was calculated for MEF (D), M1 (E) and AML12 (F). Data is represented as mean +/- SD, n=3. For statistical analysis two sided *t*-test was applied \*\**p*<0.01, \*\*\**p*<0.001, \*\*\*\**p*<0.0001.

glucose media (LG) by flow cytometry. ROS was increased by 11% in MEF ( $92.73 \pm 1.102$  vs  $103.3 \pm 2.028$ ; *p*=0.00042), 86% in AML12 ( $55.33 \pm 0.5774$  vs  $103.3 \pm 5.132$ ; *p*=0.0034), 108% in M1 ( $103.3 \pm 2.028$  vs  $215 \pm 5$ ; *p*=0.001), whereas 203% increase was observed in MES13 ( $620.6 \pm 424.2$  vs  $1878 \pm 407.7$ ; *p*=0.0208) and 159% SW10 ( $2930 \pm 969.3$  vs  $7599 \pm 2369$ ; *p*=0.0117) (Figure 7.A). O<sub>2</sub>•<sup>-</sup> was increased by 27% in MEF ( $135.7 \pm 3.055$  vs  $173 \pm 3$ ; *p*=0.0001), indicating that not all superoxide production was used to form ROS. In AML12 O<sub>2</sub>•<sup>-</sup> was increase by 46% ( $53.67 \pm 4.726$  vs  $78.33 \pm 4.726$ ; *P*=0.0017), whereas the ROS production was elevated by 1.8-fold indicating that the ROS formation was also derived from another source next to O<sub>2</sub>•<sup>-</sup> (Figure 7.C). O<sub>2</sub>•<sup>-</sup> was increased by 217% in MES13 ( $1990 \pm 532.9$  vs  $6318 \pm 718.2$ ; *p*=0.0011) and by 214% in SW10 ( $1259 \pm 575.1$  vs  $3955 \pm 272.3$ ; *p*=0.0018), which is in accordance with the increase in ROS production. In contrast, in M1 O<sub>2</sub>•<sup>-</sup> was reduced with 10% ( $161.3 \pm$

## Results

2.517 vs  $151 \pm 3.464 \pm 2$ ;  $p=0.0139$ ) observed, indicating another source for ROS. Another source for ROS might be NO (Figure 7.B). NO was increased by 119% in MEF ( $61.67 \pm 0.5774$  vs  $135.3 \pm 7.572$ ;  $P=0.0033$ ), 108% in AML12 ( $91 \pm 26$  vs  $189.7 \pm 10.6$ ;  $p=0.0127$ ), 32% in M1 ( $684.7 \pm 12.42$  vs  $904.3 \pm 12.22$ ;  $p=0.0001$ ), and trend towards increased NO in SW10 ( $3714 \pm 9065 \pm 4857$ ;  $p=0.116$ ). However, no change in NO was observed in MES13 (Figure 7.B).

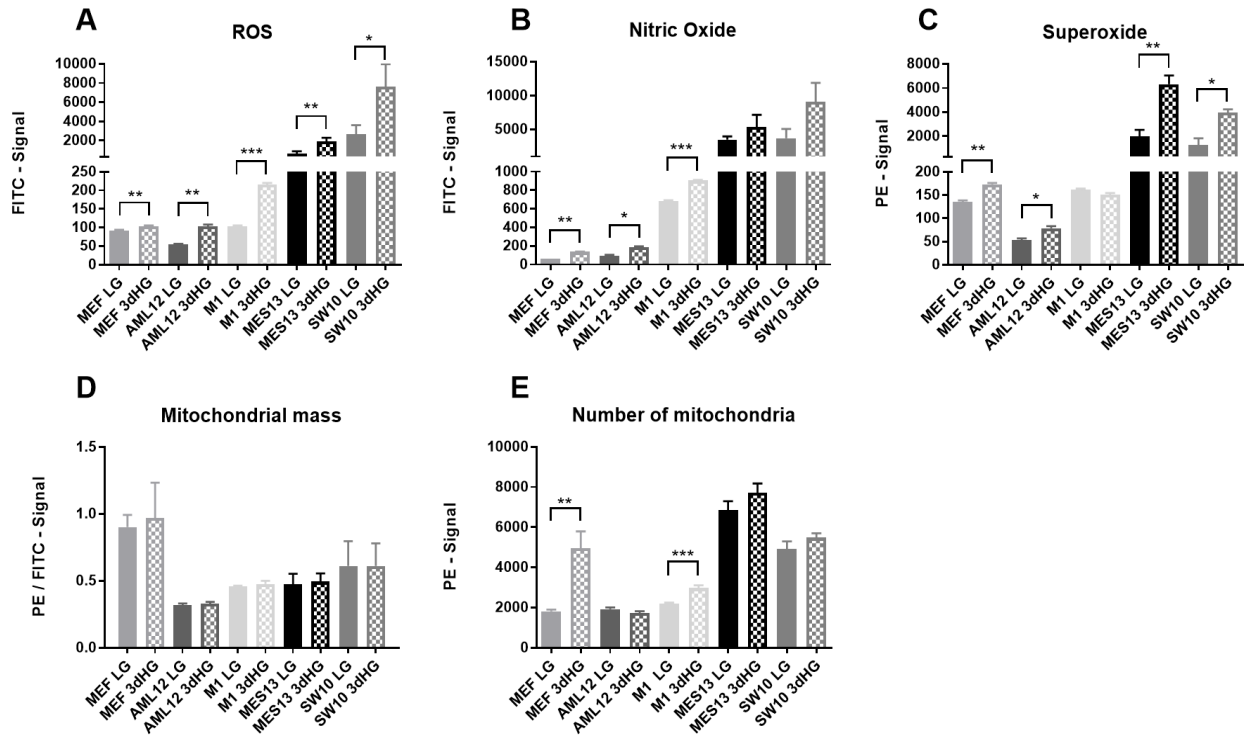


**Figure 7. Mitochondrial properties and reactive metabolites.**

The different murine primary cell lines, fibroblast (MEF), hepatocytes (AML12), renal tubular cells (M1), mesangial cells (MES13) and Schwann cells (SW10) were cultured for 3 days in high glucose media (3dHG) as compared to low glucose (LG) cultured cells. ROS, NO, Superoxide, mitochondrial membrane potential and mitochondrial mass were measured by flow cytometry using DCF (2',7'-dichloro-dihydro-fluorescein) (A), DAF-FM (4-Amino-5-methylamino-2'7'-Difluorescein Diacetate) (B) and MitoSOXred™ (C), JC-1 (D) and MitoTracker® Orange FM (E) respectively. Mean fluorescence intensity (MFI) was detected by flow cytometry. Data is represented as mean +/- SD, n=3. For statistical analysis two sided t-test was applied \* $p<0.05$ , \*\* $p<0.01$  and \*\*\* $p<0.001$ .

An indirect indication for mitochondrial stress is changes in mitochondrial properties such as mitochondrial mass and mitochondrial density. No changes in mitochondrial polarity by JC-1, a marker for mitochondrial density, were observed in any of the cell types (Figure 7.D). However,

## Results

mitochondrial mass was increased in MEF ( $1817 \pm 89.63$  vs  $4961 \pm 833.2$ ;  $p=0.0029$ ) and M1 ( $2213 \pm 43.65$  vs  $2969 \pm 154.4$ ;  $p=0.001$ ) (Figure 7.E). The changes in mitochondrial reactive metabolites are not in line with the changes in mitochondrial properties, suggesting a disconnection between the two.

### 4.2 Increased glucose uptake and glucose transporters expression in Schwann cells and fibroblasts

Due to the importance of Schwann cells in pathophysiology of DN, it was decided to focus specifically on this cell type. Moreover, the isolation of Schwann cells from sciatic nerves often results in a co-culture of Schwann cells and fibroblasts. Therefore, SW10 and MEF were taken to investigate whether the hyperglycemia induced changes are cell type specific or occur in both cell types. The study of these two cell types is relevant to diabetic neuropathy as the firstly represent the major cell type found within the sciatic nerve and secondly, it has been suggest that metabolic dysfunction within the sciatic nerves play an important role in the pathophysiology of diabetic neuropathy. Previous data had shown that maximal glucose uptake was reached at 6 days of high glucose for most cell lines therefore all subsequent experiments were continued with 6 days of high glucose treatment.

Increased glucose uptake was associated with increased expression in glucose transporter expression. A tendency towards increased Glut 1 gene expression in MEF ( $0.07551 \pm 0.02032$  vs  $0.1008 \pm 0.01640$ ;  $p=0.1668$ ) (Figure 8.A) and, despite its low expression, a trend towards increased Glut 3 gene expression was observed in SW10 ( $0.00132 \pm 0.00005$  vs  $0.00156 \pm 0.000156$ ;  $p=0.0676$ ) (Figure 8.B). A 107% increase in Glut 1 protein expression was observed in MEF ( $440.211 \pm 139.474$  vs,  $909.066 \pm 139.853$   $p=0.0147$ ) (Figure 8.C, D), whereas Glut 3 which more neuronal specific glucose transporter, was increased by 75% in SW10 ( $0.75 \pm 0.06$  vs  $1.31 \pm 0.28$ ;  $p=0.0267$ ) (Figure 8.C and E), as compared to LG cultured cells. However, Glut 3 protein expression was reduced by 28.3 % in MEF ( $1.77 \pm 0.19$ ,  $1.27 \pm 0.16$ ;  $p=0.0246$ ) (Figure 8.C and E). The expression of glucose transporter 2 (Glut 2) and glucose transporter 4 (Glut 4) remained unaffected (data not shown). These findings together with the glucose uptake data indicate that

## Results

increased glucose uptake in response to high glucose is due increased expression of Glut 3 in SW10 and Glut1 in MEF.

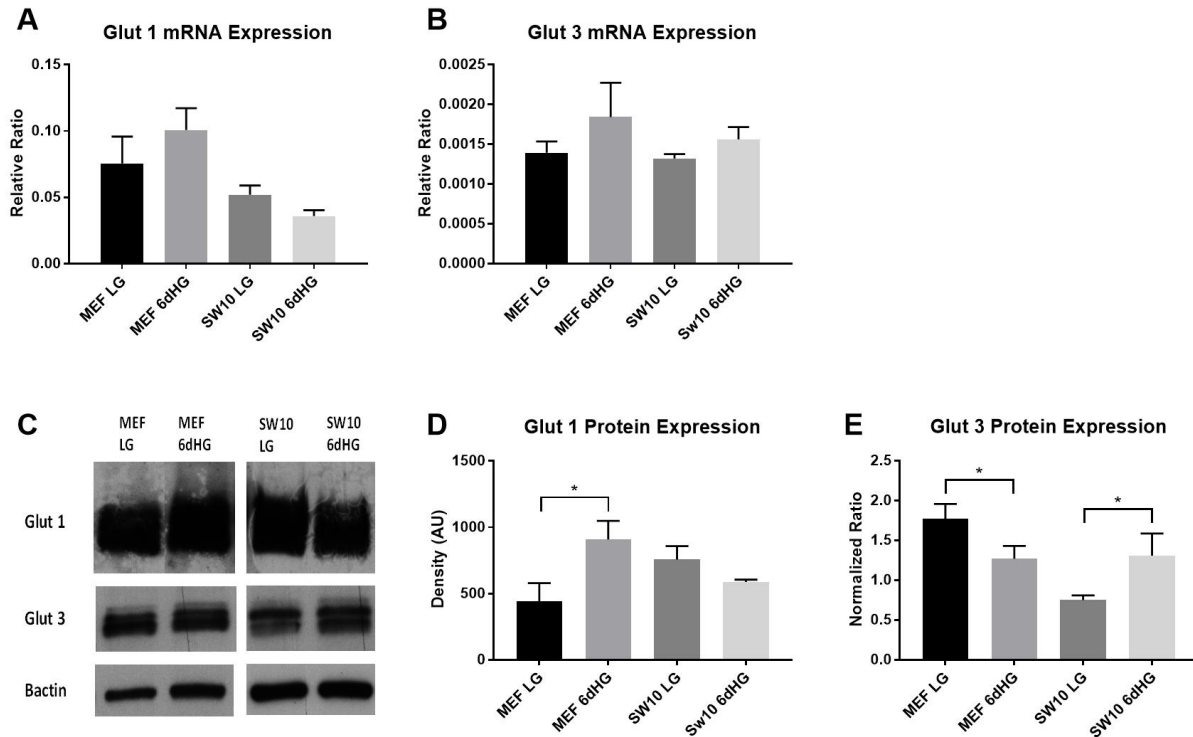


**Figure 8. Glucose uptake and glucose transporter expression.**

MEF and SW10 were cultured under high glucose condition for 6 days (6dHG) as compared to low glucose condition (LG). The mRNA expression of glucose transporter 1 (Glut 1) (A) and glucose transporter 3 (Glut 3) (B) were determined by RT-qPCR. Immunoblotting (C) was performed to analyze the protein expression of Glut 1 (D) and Glut 3 (E). Data is represented as mean  $\pm$  SD,  $n=3$ . For statistical analysis two sided  $t$ -test was applied  $*p<0.05$ .

### 4.3 High glucose does not affect the pathways of the unifying theory

The effect of high glucose on the polyol pathway was determined by measuring levels of sorbitol in the samples of SW10 and MEF cultured for 6 days in high glucose or low glucose. Sorbitol levels were increased by 13% in MEF ( $702.733 \pm 40.02$  vs  $797.08$ ,  $p=0.0203$ ) in response to 6 days high glucose treatment, whereas no differences in the sorbitol levels were observed in SW10 (Figure 9.A), suggesting that this cell culture model of long term high glucose does upregulate the polyol pathway in MEF but not in SW10.

## Results

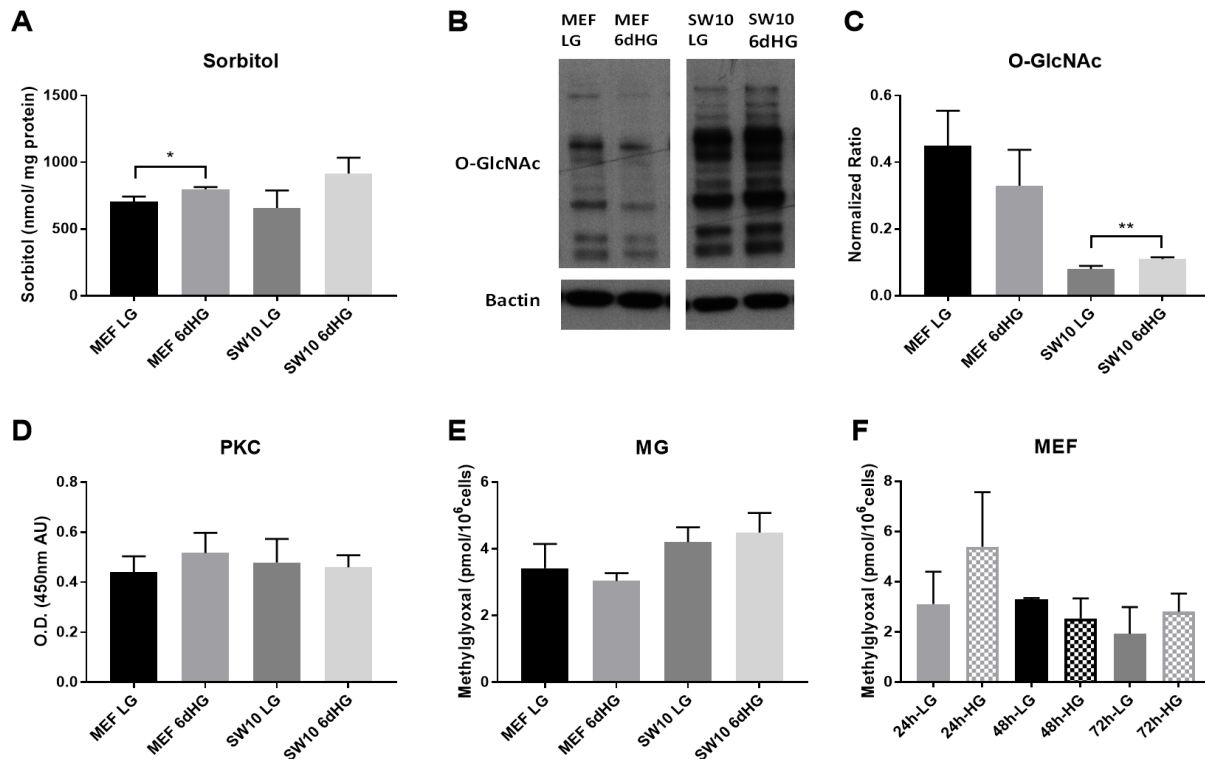


**Figure 9. Effect of high glucose on pathways of the unifying theory.**

MEF and SW10 were cultured under high glucose condition for 6 days (6dHG) as compared to low glucose condition (LG). Sorbitol was determined by D-Sorbitol Colorimetric Assay (A). Glycosylation was determined by immunoblotting (C) using primary antibody against O-Linked  $\beta$ -N-acetylglucosamine (B). The effect of high glucose on PKC pathway was determined by PKC activity assay (D). Methyl glyoxal concentration were determined by LC-MS/MS as a marker for AGE formation (E). MG levels in MEF cells (E) and the media (F) was determined, after being cultured for 24h, 48h and 72 h in high glucose (HG) versus low glucose media (LG). Data is represented as mean  $\pm$  SD, n=3. For statistical analysis two sided *t*-test was applied \* $p$ <0.05, \*\* $p$ <0.01.

The hexosamine pathway was investigated by measuring the post-translational modification, O-linked N-acetylglucosamine (O-GlcNAc) (Figure 9.B, C). No differences in O-GlcNAc protein expression was observed in MEF. However, O-GlcNAc protein concentration was increased by 38% in SW10 ( $0.08 \pm 0.01$  vs  $0.11 \pm 0.01$ ,  $P = 0.0086$ ) as compared to LG cultured cells (Figure 9.C), indicating a 6 days of high glucose treatment did upregulate hexosamine pathway only in SW10. Protein kinase C activity was measured by ELISA. No differences in PKC activity was observed in both SW10 and MEF in response to the high glucose treatment (Figure 9.D), suggesting that high glucose condition did not affect the PKC pathway in this cell culture model.



## Results

To determine the effect of high glucose on AGEs pathway in SW10 and MEF the MG levels, the precursor of AGEs, were measured by LC-MS/MS. No differences in the intracellular MG levels were observed in both cell types (Figure 9.E). To investigate the effect of short term high glucose also intracellular (cells) and extracellular (media) MG levels in MEF cultured for 24h, 48h and 72h in high glucose media was measured. No changes in MG levels were observed in 24h, 48h and 72h of high glucose versus normal glucose cultured MEF cells (Figure 9.F). These findings indicate that both short and long term high glucose does not affect MG levels, and thereby the AGEs pathway.

### 4.4 Decreased glycolysis and mitochondrial respiration

Previous data has shown that there are differences in reactive metabolites and mitochondria properties under high glucose condition, whilst the pathways of unifying theory are not active (Figure 3), therefore mitochondrial function was determined. The Seahorse XF96 Bioanalyzer instrument can measure glycolysis and oxidative phosphorylation simultaneously in the same cells. Glycolysis is determined through measurements of the extracellular acidification rate (ECAR) of the surrounding media of the cells, which is predominately from the excretion of lactic acid per unit time after its conversion from pyruvate (Wu et al., 2007) Glucose is supplied to feed glycolysis, and the difference between ECAR before and after addition of glucose is a measure of the glycolytic rate, which is called glycolysis in our results. Oligomycin inhibits ATP synthase in the ETC, thereby reducing the ATP/ADP ratio which drives glycolysis and subsequently to maximum conversion of glucose to pyruvate or lactate also called glycolytic capacity. The difference between ECAR before and after the addition of oligomycin is equal to the glycolytic reserve capacity of cells. 2-DG inhibits the first step in glycolysis. Therefore, the ECAR measured after 2-DG addition accounts for the non-glycolytic ECAR of cells (TeSlaa and Teitell, 2014).

In response to 6 days of high glucose treatment, the glycolysis was decreased by 72% ( $23.7 \pm 4.4$  vs  $6.6 \pm 3.4$ ;  $p=0.006$ ) (Figure 10.A, C) together with a 67% decrease in glycolytic capacity ( $70 \pm 11$ , vs  $23.0 \pm 12.0$   $p= 0.0168$ ) (Figure 10.D) and a 45% decrease in glycolytic reserve ( $46.3 \pm 11$  vs

## Results

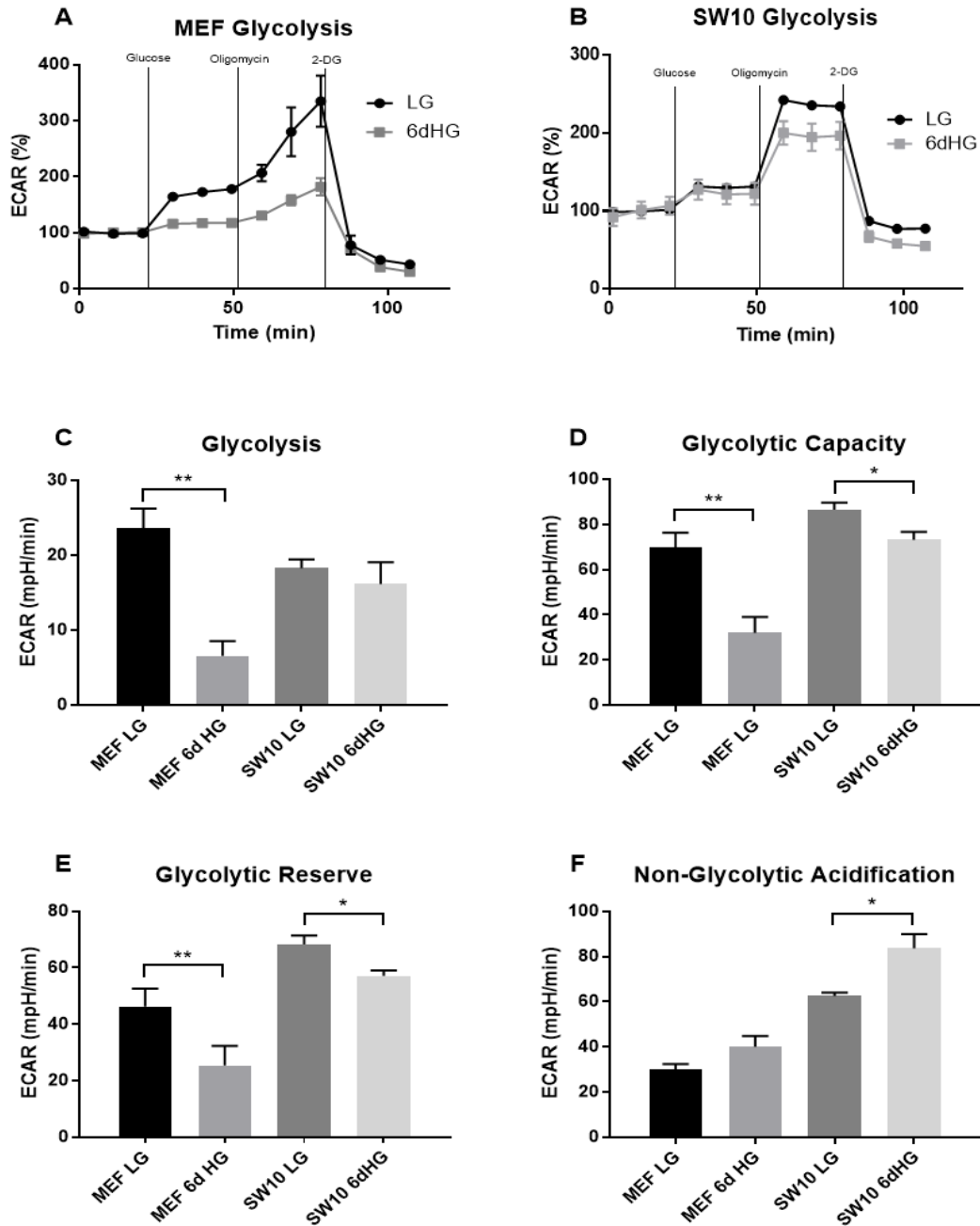


**Figure 10. Effect high glucose on glycolysis.**

MEF and SW10 were cultured under high glucose condition for 6 days (6dHG) as compared to low glucose condition (LG). The glycolysis was in MEF (A) and Sw10 (B) determined by measuring the extracellular acidification rate (ECAR) of the surrounding media using the XF96 Seahorse Bioanalyzer. Glycolysis (C), glycolytic capacity (D) and glycolytic reserve (E) were measured by sequential injection of 10mM glucose, 1mM oligomycin and 100mM 2-Deoxy-D-glucose (2-DG). Non-glycolytic acidification (F) is calculated as the difference between basal ECAR and ECAR after the injection of 2-DG. Data is represented as mean +/- SEM (n=9). For statistical analysis two sided *t*-test was applied \**p*<0.05, \*\**p*<0.01.

## Results

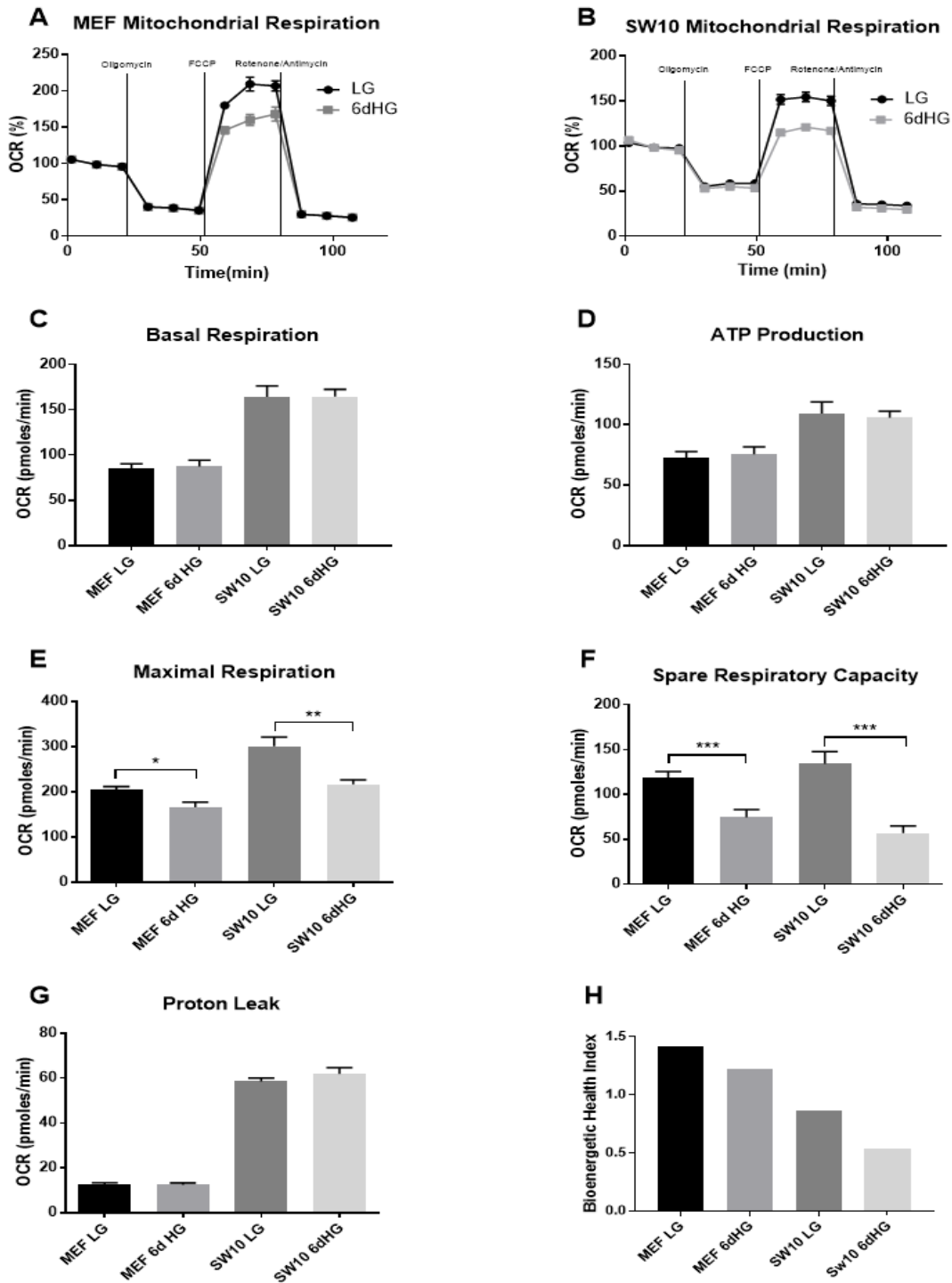


**Figure 11. Effect high glucose on in mitochondrial respiration.**

MEF and SW10 were cultured under high glucose condition for 6 days (6dHG) as compared to low glucose condition (LG). The mitochondrial respiration in MEF (**A**) and SW10 (**B**) determined by measuring the oxygen consumption rate (OCR) of the surrounding media using the XF96 Seahorse Bioanalyzer. First the basal OCR (**C**) was measured. The ATP production (**D**) the maximal respiration (**E**) and non-mitochondrial respiration (**F**) were measured after sequential injection of 1mM oligomycin, 0.5mM FCCP and a combination of 1mM rotenone and

## Results

1mM antimycin-A, respectively. Spare respiratory capacity (**G**) is calculated as the difference in OCR of maximal respiration and OCR of basal respiration. Proton leak is calculated as the difference in OCR related to ATP production and non-mitochondrial respiration (**H**). From these OCR values the bioenergetic health index (BHI) (**I**) was calculated. Data is represented as mean +/- SEM, n=9. For statistical analysis two sided *t*-test was applied \**p*<0.05, \*\**p*<0.01, \*\*\**p*<0.001.

25.4 ± 11.9; *P*=0.0018) in MEF (Figure 10.A, E). In the SW10 cells, the glycolytic capacity was decreased by 15% (86.53 ± 5.4 vs 73.6 ± 6 *P*=0.0325) (Figure 10.D) and the glycolytic reserve was also decreased by 15% (67.87 ± 5.3 vs 57.43 ± 3.3; *p*=0.0419), (Figure 10.E), whereas the glycolytic rate (Figure 10.B, C) remained unaffected in response to 6 days of high glucose treatment. Interestingly, the non-glycolytic acidification in SW10 was increased by 34% (62.5 ± 2.7 vs 83.63 ± 10.9; *P*=0.0297) (Figure 10. F), in response to hyperglycemia, as compared to cells cultured in LG media. Although elevated glucose uptake and glucose transport protein were observed previously, these findings suggest downregulation of the glycolysis pathway in response to hyperglycemia. Interestingly, the non-glycolytic acidification was increased in SW10, indicating another source for extracellular acidification rather than glycolysis itself.

Another source of acidification might come from mitochondrial oxidative phosphorylation. Oxidative phosphorylation was determined by measuring the oxygen consumption rate (OCR) using the Seahorse XF Bioanalyzer. First the basal OCR, also called basal respiration of the surrounding media of the cells is measured followed by serial injection of the compounds oligomycin, carbonyl cyanide 4-(trifluoromethoxy)phenylhydrazone (FCCP), and a combination of rotenone and antimycin A. Oligomycin, which inhibits ATP synthase (complex V of the ETC), was added to calculate the amount of OCR is used for ATP production. FCCP is an uncoupling agent disrupting the ETC leading to maximum electron flow and subsequently maximal respiration. The spare respiratory capacity can be calculated as the difference in OCR of basal respiration and maximal respiration. The higher the reserve capacity the more effective the mitochondria are to meet their need for ATP and energetic demand in response to stress.

In response to 6 days of high glucose, the maximal respiration decreased by 19% in MEF (205.5 ± 19.36 vs 165.8 ± 33.86; *p*=0.0076) (Figure 11.A, E), together with a reduction in spare respiratory capacity of 37% (118.7 ± 19.85 vs 74.66 ± 25.08), as compared to LG cultured cells. In

## Results

SW10 the maximal respiration was decreased by 28% ( $301.3 \pm 59.11$  vs  $216.8 \pm 28.82$ ;  $P=0.0014$ ,  $n=9$ ) (Figure 11.B, E) and the spare respiratory capacity reduced by 58% ( $134.4 \pm 40.5$  vs  $56.93 \pm 24.6$ ;  $p=0.0001$ ,  $n=9$ ) (Figure 11.F). The other functional markers of mitochondrial respiration remained unaffected.

Chronic metabolic stress causes defects in the mitochondrial respiratory machinery as characterized by reduced ATP-linked respiration, reduced reserve capacity and increased non-mitochondrial respiration (e.g. ROS formation). These bioenergetically inefficient damaged mitochondria also show increased proton leak and require higher levels of ATP to meet their energy demand in order to maintain organelle integrity, leading to increased basal mitochondrial respiration. Each of these different parameters is susceptible to different forms of oxidative stress. Chacko et al. proposed that due to the close interactive nature of these different parameters, they can be integrated into a single value known as the Bioenergetic Health Index (BHI) (Chacko et al., 2014). The BHI can be calculated as follows:

$$\text{BHI} = \log \frac{(\text{reserve capacity})^a \times (\text{ATP linked})^b}{(\text{non mitochondrial})^c \times (\text{proton leak})^d}$$

In general, defects in the ETC lead to reduced BHI due to decrease in reserve capacity, ATP-linked respiration or increased uncoupling. It is important to note that cells which show a decrease reserve capacity, but an increase in proton leak and non-mitochondrial respiration can still potentially provide sufficient ATP to meet the energetic demands of the cell, but is less efficient. Calculation of BHI of our data showed a decrease in bioenergetic health in response to hyperglycemia in both cell types (Figure 11.H), mainly due to the decrease in mitochondrial reserve capacity, implying that in the response to high glucose both SW10 and MEF are less efficient to meet the energetic demand of the cell.

### 4.5 Decreased expression of glycolysis related genes and altered fatty acid metabolism in Schwann cells

Based upon the finding that glycolysis is reduced in response to high glucose in our cell culture model, the expression of several genes in the glycolysis pathways was determined by qPCR. mRNA expression of Hk2 ( $0.0541 \pm 0.0051$  vs  $0.0307 \pm 0.0062$ ;  $p=0.0221$ ), PCK2 ( $0.1834 \pm 0.0211$

## Results

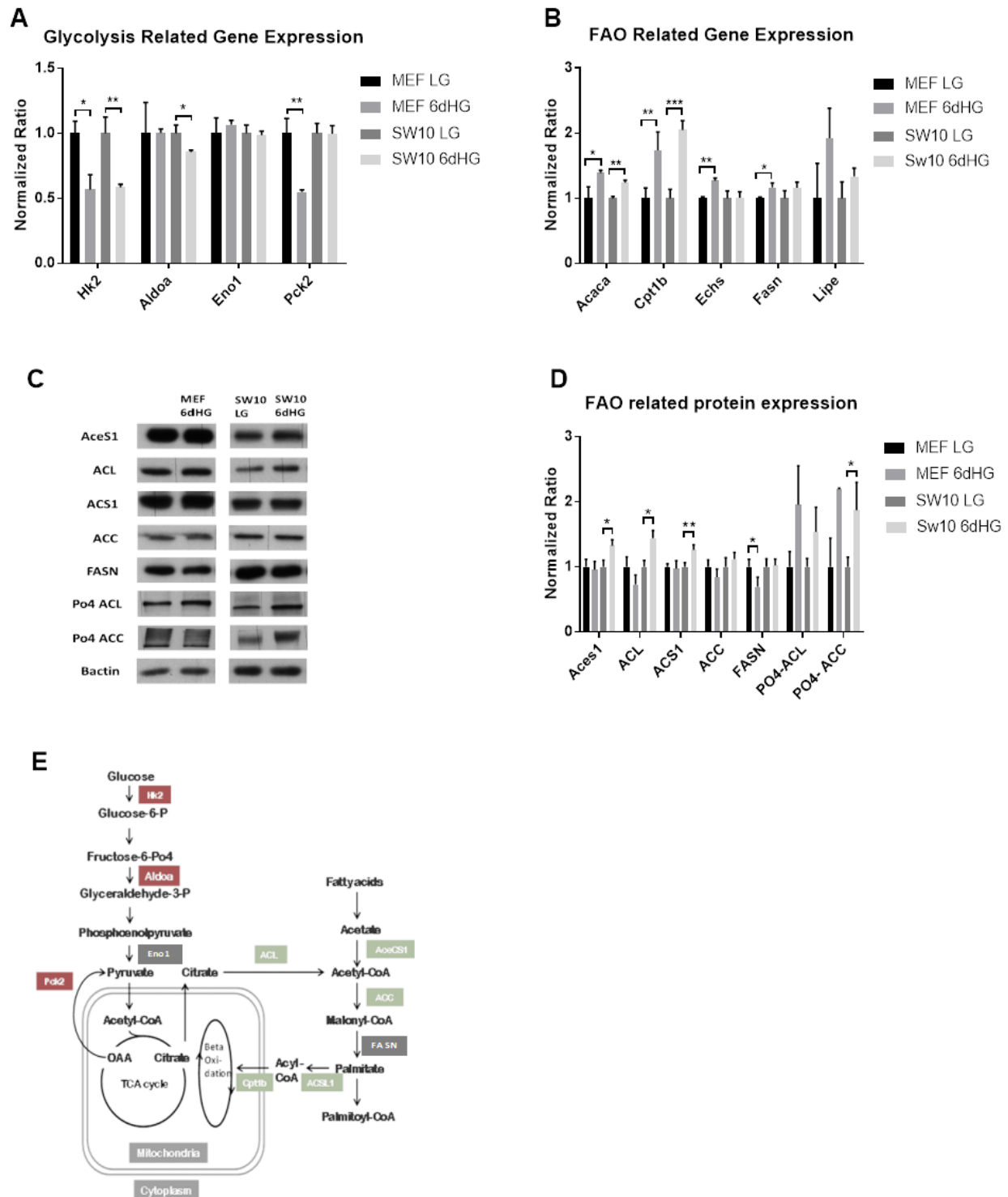


**Figure 12. Glycolysis and fatty acid oxidation (FAO) related gene and protein expression.**

The mRNA expression of genes related to the glycolysis pathway including hexkinase-2 (HK2), aldolase-alpha (Aldoa), enolase 1 (Eno1) and phosphosolpyruvate carboxykinase (PCK2) (**A**) and for the FAO pathway

## Results

including (Acaca) carnitine acyl transferase (Cpt1b), enoyl-CoA hydratase (Echs), fatty acid synthase (Fasn) and hormone sensitive lipase (Lipe) (**B**) was determined by RT-qPCR. Immunoblotting was performed to measure the FAO related protein expression (**C, D**) of the following proteins AceS1, ATP-citrate lyase (ACL), (ACS1), Acetyl-CoA carboxylase (ACC), fatty acid synthase (FASN), phosphorylated ACL (Po4-ACL) and phosphorylated ACC (Po4-ACC). The data is summarized in a figure (**E**). Data is represented as normalized ratio (LG cultured cells was set to 1) +/- SD, n=3. For statistical analysis two sided *t*-test was applied \**p*<0.05, \*\**p*<0.01, \*\*\**p*<0.001.

vs  $0.0277 \pm 0.0276$  *p*=0.005) was observed in MEF (Figure 12.A) and decreased mRNA expression of Hk2 ( $0.0182 \pm 0.0023$  vs  $0.0107 \pm 0.0004$ ; *P*=0.0049) and Aldoa ( $0.5820 \pm 0.0376$  vs  $0.4986 \pm 0.0080$ ; *P*=0.0198) was observed in SW10 thereby confirming the previous findings that glycolysis pathway in response to high glucose is reduced.

As the glycolysis pathway is reduced, the mitochondria must use another pathway to meet their energy demand, since previous data showed that the ATP production remained unaffected in both cell types (Figure 11.D). Another important mitochondrial energy fuel, next to glucose, is fatty acid oxidation (FAO). Therefore, in addition to the glycolysis related genes, genes related to FAO were also screened. Increased mRNA expression of Acaca was observed in both MEF ( $0.03797 \pm 0.00548$  vs  $0.05281 \pm 0.00336$ ; *p*=0.0161) and SW10 ( $0.03038 \pm 0.00092$  vs  $0.03776 \pm 0.00123$ ; *p*=0.0012) (Figure 12.B) in response to high glucose treatment. Moreover, Cpt1a, which transports long-fatty acid into the mitochondrial matrix and is the rate limited step on FAO, was increased in MEF ( $0.00086 \pm 0.00012$  vs  $0.0015 \pm 0.00012$ ; *p*=0.0102) and SW10 ( $0.000495 \pm 0.00007$  vs  $0.001016 \pm 0.000069$ ; *p*=0.0009). Increased mRNA of Echs ( $0.1101 \pm 0.0036$  vs  $0.1377 \pm 0.0052$ ; *p*=0.0017), Fasn ( $0.1695 \pm 0.0106$  vs  $0.1976 \pm 0.0111$ ; *p*=0.0337) and trend toward increased Lipe ( $0.0017 \pm 0.0008$  vs  $0.003281 \pm 0.0007$ ) *p*=0.0575) was observed in response to high glucose treatment in MEF, but not in SW10. The increase in FAO was confirmed on protein level by immunoblot in SW10 (Figure 12.C, D). In response to high glucose treatment AceCS1 ( $1 \pm 0.0294$  vs  $1.3267 \pm 0.0903$ ; *P*=0.0192), Acl ( $1 \pm 0.0978$  vs  $1.4390 \pm 0.1208$ ; *p*=0.0195), Po4-ACC ( $1 \pm 0.4996$  vs  $1.8735 \pm 0.4252$ ; *P*=0.0274) protein expression were elevated and a trend towards increased PO4-Acl ( $1 \pm 0.128$  vs  $1.5350 \pm 0.386$ ; *p*=0.0577) was observed in SW10 when cell were culture for 6 days in HG media as compared to cell cultured in LG media, but not in MEF. Fasn was reduced in MEF ( $1 \pm 0.1153$  vs  $0.6999 \pm 0.1168$  *p*=0.0262),

## Results

but not in SW10. These findings indicate that high glucose induces a metabolic switch from glycolysis towards FAO in SW10, summarized in figure (Figure 12. E).

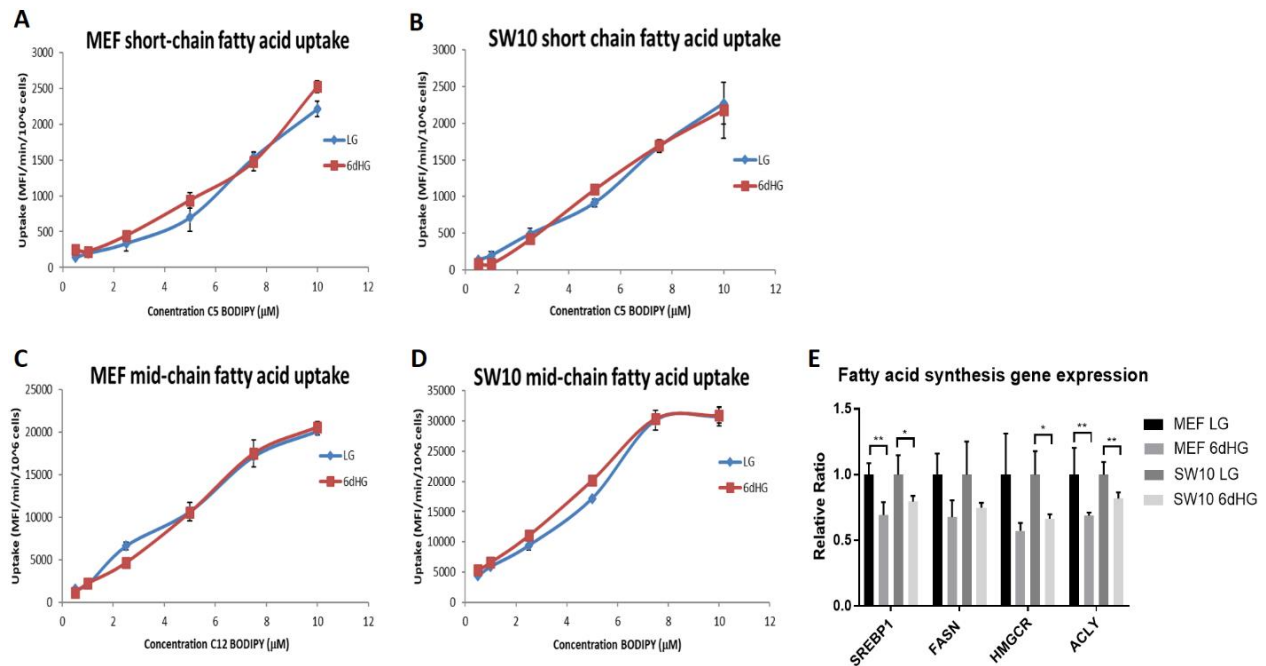


**Figure 13. Fatty acid uptake and fatty acid gene expression**

Fatty acid uptake was determined by flow cytometry using BODIPY 5 to measure short-chain fatty acid uptake in MEF (A) and SW10 (C), and BODIPY C12 to measure mid-chain fatty acid uptake in MEF (B) and SW10 (D) cultured for under high glucose conditions (6dHG) versus low glucose control conditions (LG). Real time qPCR was performed to determine the mRNA expression of genes related to fatty acid synthesis pathway (E). Data is represented as normalized ratio (LG cultured cells was set to 1) +/- SD, n=3. For statistical analysis two sided *t*-test was applied \**p*<0.05, \*\**p*<0.01.

To investigate the importance of fatty acids as an energy fuel the mid- and long- chain fatty acid uptake was determined by flow cytometry analysis using BODIPY-C5 and BODIPY-C12 respectively. No alterations in mid-chain fatty acid uptake in MEF (Figure 13.A) and in SW10 (Figure 13.B) was observed. In addition, no changes in long chain fatty acid uptake were observed in both cell types (Figure 13.C, D). However, the fatty acid synthesis was altered after 6 days of high glucose treatment. Decreased gene expression of Srebp1 ( $1 \pm 0.0899 \pm$  vs  $0.6928 \pm 0.1092$ ; *p*= 0.0198), Acly ( $1 \pm 0.2049$  vs  $0.6886 \pm 0.0236$  *p*= 0.028), and a trend in towards decreased Fasn was found in MEF ( $1 \pm 0.1603$  vs  $0.6771 \pm 0.2171$  *p*=0.0523). In SW10 the gene



## Results

expression of *Srebp1*, *Hmcgr* ( $1 \pm 1911$  vs  $0.6661 \pm 0.0342$ ;  $p=0.0408$ ) and *Acly* ( $1 \pm 0.0154$  vs  $0.8197 \pm 0.0497$ ;  $p=0.0078$ ) were significantly decreased (Figure 12.E). In contrast, when determining the effect of octanoate on mitochondrial respiration, increased mitochondrial respiration ( $0.1112 \pm 0.4502$  vs  $6.0899 \pm 0.1492$ ;  $p<0.0001$ ) was observed in MEF cultured under high glucose condition (Figure 14.A). However, the ATP production was decreased by 40% ( $2.3918 \pm 0.0565$  vs  $1.4282 \pm 0.1308$ ;  $p=0.0003$ ) in high glucose cultured MEF upon octanoate addition (Figure 14.B), suggesting that octanoate is not used as an energy fuel in high glucose cultured MEF. Interestingly, upon octanoate addition there is increased ATP production by 32% ( $4.4718 \pm 0.0836$  vs  $5.9053 \pm 0.1436$ ;  $p=0.0001$ ) in high glucose cultured SW10 (Figure 14.D), indicating that high glucose cultured SW10 use octanoate as an energy fuel. Taken together, these findings suggesting that high glucose induces remodeling of Schwann cell mitochondrial metabolism away from fatty acid synthesis towards fatty acid oxidation in order to generate ATP.

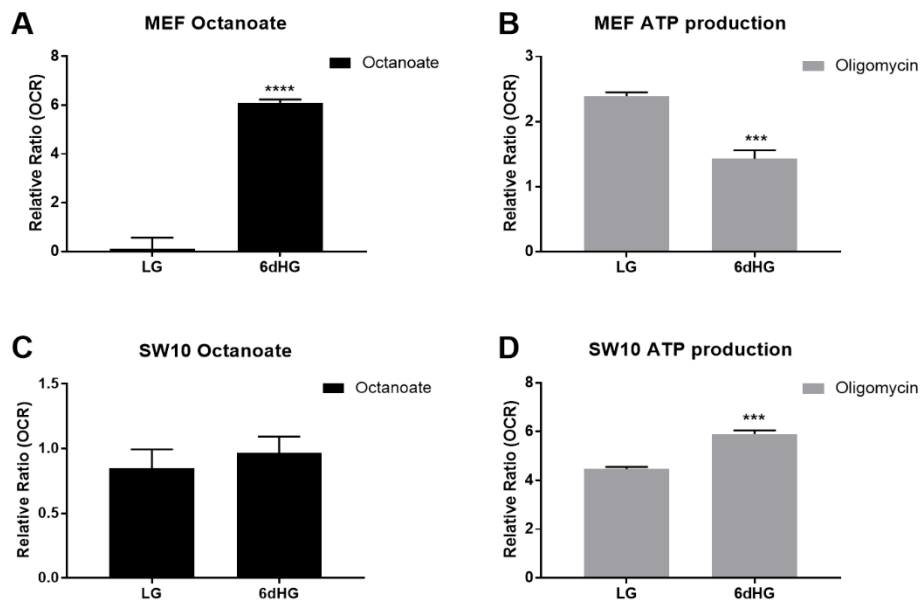


**Figure 14. Effect octanoate on mitochondrial respiration in permeabilized MEF and SW10.**

Effect of octanoate as an energy fuel for mitochondrial respiration was determined by sequential injection of both 25mg/ml saponin and 1mM octanoate, and 1mM oligomycin using the XF96 Seahorse Bioanalyzer to measure the effect of octanoate on basal respiration in MEF (A) and SW10 (C), and on ATP production in MEF (B) and SW10 (D), respectively. Data is represented as normalized ratio to the control without octanoate +/- SD, n=3. For statistical analysis two sided *t*-test was applied \*\*\* $p<0.001$ , \*\*\*\* $p<0.0001$ .

## Results

### 4.6 No activation of the integrated stress response, the uncoupled protein response and the AMPK pathway

Previous studies have shown that the activation of the integrated stress response (IRS), the uncoupled protein response (UPR) and or 5'AMP-activated protein kinase (AMPK) pathway can be a regulator of a metabolic switch towards FAO pathway (Viader et al., 2013; O'Neill et al., 2013). The effect of hyperglycemia on IRS was determined by qPCR and immunoblotting. In response to 6 days of high glucose treatment several genes of the fatty acid synthesis pathway were downregulated in both cell types as compared to LG cultured cells. In MEFs, the gene expression of ATF4 was reduced by 31% ( $1 \pm 0.0899$  vs  $0.6928 \pm 0.1092$ ;  $P=0.0198$ ), but not in SW10. ASNS gene expression in SW10 was reduced by 43% ( $1 \pm 0.3276$  vs  $0.5729 \pm 0.06138$ ;  $P=0.0083$ ), but not in MEF. In MEFs, the Mthfd2 gene expression was reduced by 85% in MEF ( $1 \pm 0.3012$  vs  $0.1527 \pm 0.0209$ ;  $p=0.0083$ ) and in SW10 it was reduced by 44% ( $1 \pm 0.1553$  vs  $0.5601 \pm 0.0185$ ;  $p=0.0079$ ). The gene expression of Trib3 was reduced by 73% in SW10 ( $1 \pm 0.2495$  vs  $0.2706 \pm 0.0084$ ;  $p=0.0068$ ), whereas it was almost completely gone in MEF ( $1 \pm 0.3847$  vs  $0.0397 \pm 0.0085$ ;  $p=0.0179$ ) (Figure 15.A).

However, the reduction in IRS gene expression was not completely reflected on the protein level. The protein expression of ATF4 was downregulated by 61% in MEF ( $1 \pm 0.3281$  vs  $0.3932 \pm 0.0534$ ;  $p=0.0341$ ), confirming the downregulation of ATF4 in MEF. In contrast, phosphorylated Elf2 $\alpha$  protein expression was increased by 70% in MEF ( $1 \pm 0.1432$  vs  $1.696 \pm 0.1830$ ;  $p=0.0168$ ). In SW10 the Elf2 $\alpha$  protein expression was decreased by 22% ( $1 \pm 0.0611$  vs  $0.7756 \pm 0.0150$ ;  $p=0.035$ ) (Figure 15.B, C). The protein levels of the other downstream markers of IRS were not altered in response to high glucose treatment in both cell types. Taken together, these findings indicate that the IRS is not associated with the metabolic switch to FAO.

The UPR and AMPK pathway were assessed by immunoblotting. No changes in IRE $\alpha$  and ATF6 protein expression, both markers of the UPR, were observed in response to high glucose in both SW10 and MEF. Concerning the AMPK pathway, in SW10 the phosphorylated-AMPK $\alpha$  protein expression was increased by 47% ( $0.3176 \pm 0.0728$  vs  $0.4666 \pm 0.0436$ ;  $p=0.0383$ ), however, when normalized to total expression of AMPK $\alpha$  effect was gone. No alterations in protein

## Results

expression of in AMPK $\beta$  and phosphorylated AMPK $\beta$  were observed in both cell types (Figure 15.D, E). Taken together, these findings indicate that the UPR or AMPK pathway is not associated with the metabolic switch to FAO.

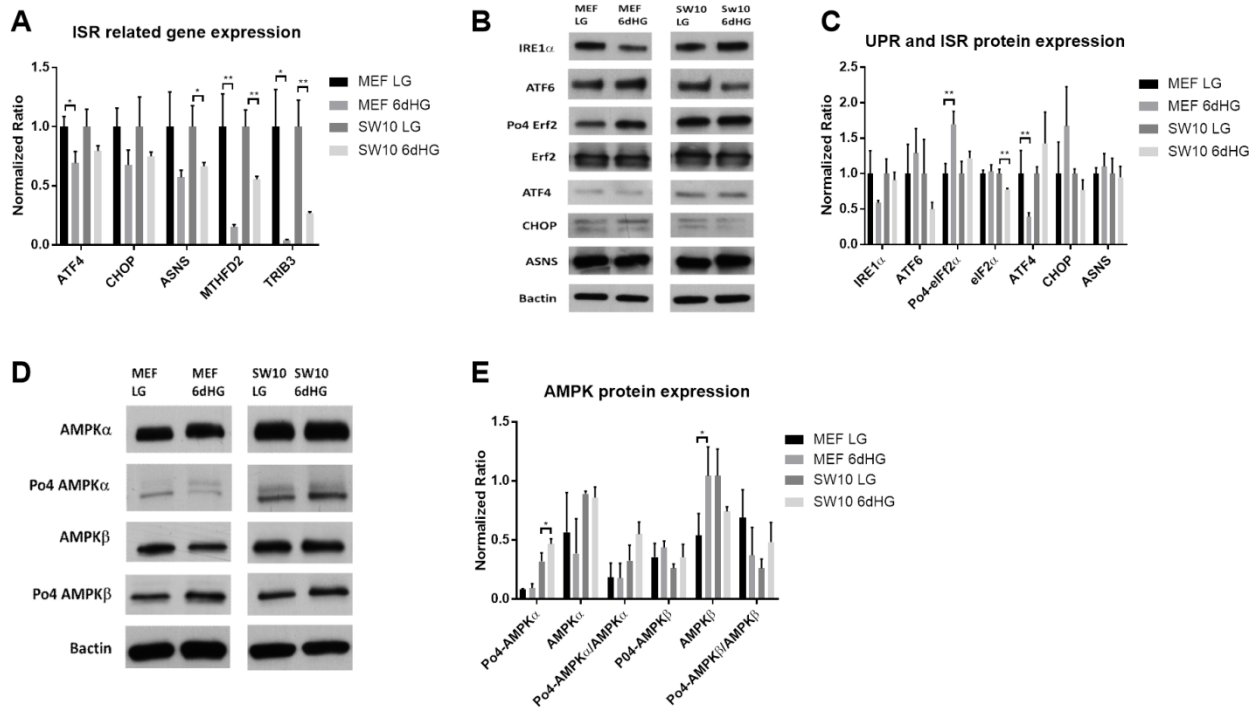


**Figure 15. The ISR, UPR and AMPK pathway.**

The effect of high glucose on possible inducers of the metabolic switch towards increased FAO was determined. mRNA expression of genes related to maladaptive integrated stress response (ISR); activating transcription factor 4 (ATF4), DNA-damage inducible factor (CHOP) asparagine synthetase (ASNS), methylenetetrahydrofolate dehydrogenase 2 (MTHFD2), tribble pseudokinase 3 (TRIB3) was determined by RT-qPCR (**A**). Immunoblotting was performed to measure protein expression of genes related to the IRS (ATF4, CHOP, ASNS) and the uncoupled protein response (UPR); inositol-requiring enzyme 1 alpha (IRE1), activating transcription factor 6 (ATF6), eukaryotic initiation factor 2 (eIF2a) and phosphorylated eIF2a (Po4-eIF2a) (**B, C**). Immunoblotting was performed to measure protein expression of 5'-adenosine monophosphate activated protein kinase (AMPKa, AMPKb), phosphorylated AMPK (Po4-AMPKa, Po4-AMPKb) (**D, E**). Data is represented as normalized ratio  $\pm$  SD, n=3. For statistical analysis two sided *t*-test was applied \* $p < 0.05$ , \*\* $p < 0.01$ .

### 4.7 High glucose induces NOS activation in Schwann cells

Since the differences in mitochondrial metabolism are not associated with the activation of the IRS, UPR or the AMPK pathway, there must be another inducer of the metabolic switch.

## Results

Interestingly, it has been shown that in response to nitric oxide inducer DetaNonoate, the maximal mitochondrial respiration is reduced (Dranka et al., 2010), indicating that nitric oxide can suppress mitochondrial oxidative phosphorylation and thereby the capability of the cell to respond to an energetic demand. Moreover, nitric oxide can induce FAO (Doulias et al., 2013, Le Gouill et al., 2007; Stavniichuk et al., 2010). This, together with our previous finding that nitric oxide is upregulated in response to high glucose (Figure 7.B) was an indication to investigate the nitric oxide pathway in our cell culture model of long term hyperglycemia.

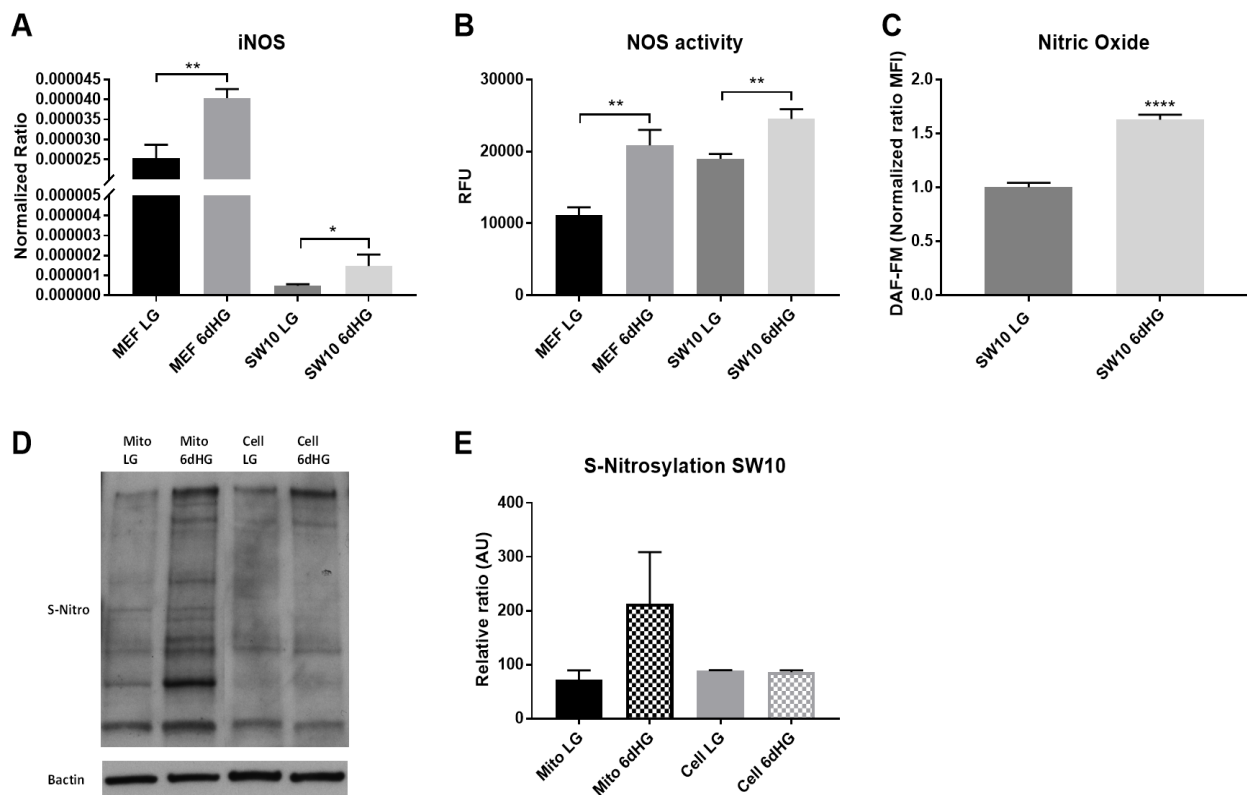


**Figure 16. Effect of high glucose on nitric oxide pathway.**

MEF and SW10 were cultured under high glucose condition for 6 days (6dHG) as compared to low glucose condition (LG). The mRNA expression of inducible nitric oxide synthase (iNOS) was determined by RT-qPCR (A). The NOS activity was measured by colorimetric based assay (B). Nitric oxide production was determined by flow cytometry, using fluorophore DAF-FM (C). Immunoblotting (D) was performed to measure the amount of total S-nitrosylation (S-Nitro) in mitochondrial fraction (Mito) and whole cell lysate (Cell) (E). Data is represented as mean  $\pm$  SD,  $n=3$ , and for S-nitrosylation assay  $n=2$ . For statistical analysis two sided  $t$ -test was applied \* $p<0.05$ , \*\* $p<0.01$ , \*\*\*\* $p<0.0001$ .

## Results

To investigate the role of the nitric oxide synthase pathway, eNOS, iNOS and nNos gene expression were determined by qPCR. Whilst the iNOS mRNA expression was low, the expression was increased by 60% ( $0.00002528 \pm 0.0000034$  vs  $0.00004039 \pm 0.0000022$ ,  $P=0.0030$ ) in MEF and increased by 222% ( $0.00000047 \pm 0.00000008$  vs  $0.00000146 \pm 0.00000058$ ;  $p<0.0425$ ) in SW10, in response to high glucose treatment (Figure 16.A). The other two isoforms, eNOS and nNOS were undetectable (data not shown). The nitric oxide activity, measured by colorimetric assay, was found to be upregulated by 87% in MEF ( $11173.67 \pm 1066.99$  vs  $20852.67 \pm 2147$ ;  $P= 0.022$ ) and upregulated by 29% in SW10 ( $18981.83 \pm 691.06$  vs  $24530.83 \pm 1367.17$ ;  $p=0.0033$ ) when cultured for 6 days under high glucose condition (Figure 16.B). The increase in NO production in SW10 was confirmed by flow cytometry analysis using DAF-FM. The nitric oxide concentration was increased by 63% ( $1 \pm 0.0417$  vs  $1.628 \pm 0.0453$ ;  $P<0.0001$ ) in response to 6 days of high glucose treatment (Figure 16.C). Elevated NOS is associated with increased S-nitrosylation in diabetes (Doulias et al., 2013). Therefore S-nitrosylation of cellular and mitochondrial fractions was detected by immunoblotting. Increased protein S-nitrosylation was observed in the mitochondrial fraction of SW10 and not in cellular fractions, whereas S-nitrosylation was unaffected in mitochondrial and cellular fractions of MEF (Figure 16.D, E). Taken together, these findings indicate that NOS is upregulated in response to high glucose and induces S-nitrosylation of mitochondrial proteins in Schwann cells.

Classic NOS inhibitors were tested to determine whether they are able to reduce NO production. Different concentrations of NOS inhibitor L-NAME in high glucose cultured cells did not reduce NO back to the levels observed low glucose cultured cells (Figure 17.A). The same was observed with the iNOS specific inhibitor 1400W (Figure 17.A). When cells were incubated in high glucose media together with the anti-oxidant N-acetylcysteine (NAC,  $500\mu\text{M}$ ) for 6 days, oxidative stress was reduced ( $3287 \pm 193.2$  vs  $168.8 \pm 107$ ;  $p>0.0001$ ) (Figure 17.C). However, NAC did not reduce the increase of 75% ( $827.1 \pm 43.7$  vs  $1451 \pm 93.5$ ;  $p=0.0005$ ) in NO measured in high glucose cultured SW10 back to control (LG) levels (Figure 17.B), indicating that despite increased expression and activity, the increase NO is not dependent on NOS.

## Results

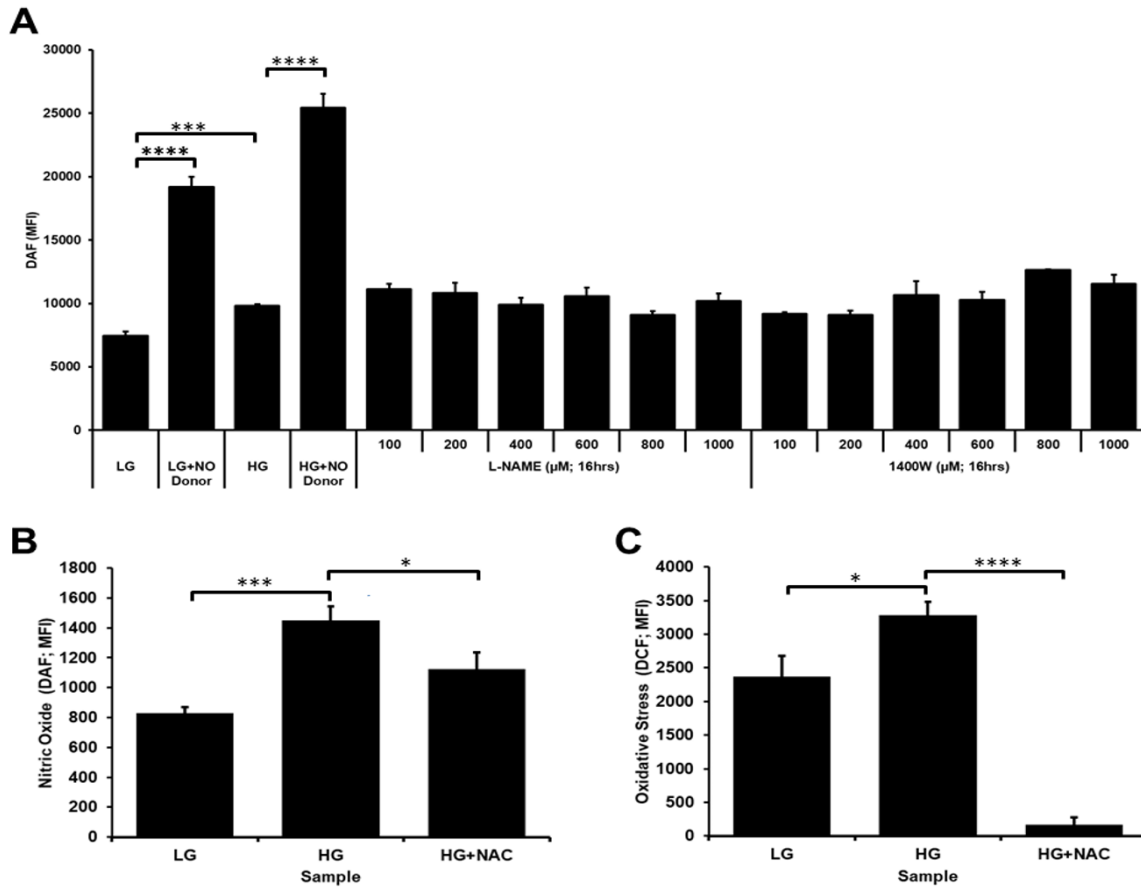


**Figure 17. Effect nitric oxide inhibitor on NO and oxidative stress.**

SW10 cells were cultured for 6 days under high glucose conditions (HG) versus control conditions (LG). The effect of 16hrs stimulation with nitric oxide inhibitors L-NAME and 1500W in SW10 HG on nitric oxide production using DAF fluorescent probe was determined by flow cytometry (**A**). The effect of anti-oxidant N-acetylcysteine NAC on nitric oxide production and oxidative stress production in high glucose cultured cells for 6 days was determined by flow cytometry, using DAF (**B**) and DCF (**C**) fluorescent probe respectively. Data is represented as mean +/- SD, n=3. For statistical analysis two sided t-test was applied \*p<0.05, \*\*\*p<0.001, \*\*\*\*p<0.0001.

### 4.8 Increased glycolytic capacity, mitochondrial respiration and superoxide formation in PBMCs of T2DM

In order to compare mitochondrial bioenergetic changes observed in our in vitro model of long term hyperglycemia in SW10 and MEF to what is happening in diabetic patients, freshly isolated PBMCs of T2DM patients and non-diabetic controls was collected. In collaboration, the glucose uptake was analyzed by flow cytometry in different cell types, distinguished by specific surface

## Results

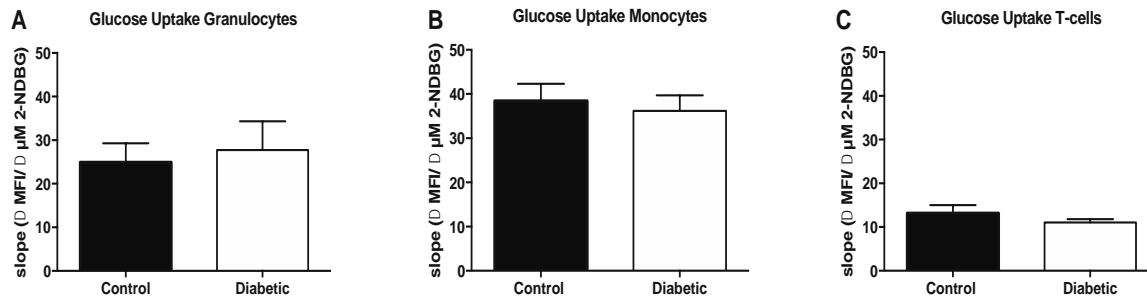


**Figure 18. Glucose uptake in PBMCs.**

Using 2-NDBG, glucose uptake was analyzed in granulocytes (A), monocytes (B) and T-cells (C), which were separated by cell type-specific cell surface markers. Mean fluorescence intensity (MFI) was plotted against the concentration of 2-NDBG used and the slope was calculated. Data is represented as mean  $\pm$  SD. For statistical analysis two sided *t*-test was applied.

markers, of a randomly-chosen subset of seven or eight patients per group. The glucose uptake was not altered in any of the analyzed cell types in diabetic patients as compared to the control patients (Figure 18. A, C). However, the different cell types took up different amounts of glucose with the monocytes taking up the most and the T-cells taking up the least amount of glucose after 30 min of starvation. Despite the unchanged glucose uptake between control and diabetic patients, glucose metabolism was found to be increased (Figure 19.A). No changes in glycolysis itself was observed (Figure 19.C), which supports the findings of the glucose uptake in the different PBMC subtypes. However the glycolytic capacity, which is a measure of the maximum rate of conversion of glucose to pyruvate or lactate, was increased by 34% ( $30.7 \pm 11.31$  vs  $41.04 \pm 10.49$ ;  $p=0.0361$ ) (Figure 19.D) in PBMCs of T2DM as compared to control. In PBMCs of T2DM the glycolytic reserve, which is the difference between the maximum glycolytic capacity and the basal glycolytic rate, was increased by 63% ( $9.6 \pm 5.301$  vs  $15.66 \pm 6.813$ ;  $p=0.0346$ ) (Figure 19.E). The increased glycolytic capacity together with the glycolytic reserve indicates that the capacity of the cells to generate ATP from glycolysis is upregulated in PBMCs of T2DM. Another important source for ATP production is mitochondrial oxidative phosphorylation. It has been shown that the mitochondrial metabolism is elevated in PBMCs of diabetic patients (Chacko et al., 2013). In our study the mitochondrial respiration was increased in PBMCs of T2DM as compared to the control (Figure 19.B). The basal mitochondrial respiration in PBMCs of T2DM was increased by 45% ( $15.49 \pm 3.852$  vs  $22.52 \pm 7.184$ ;  $p=0.0139$ ) (Figure 19.F), the OCR related to ATP production, after the injection of oligomycin, was increased by 44% ( $15.3 \pm 5.109$

## Results

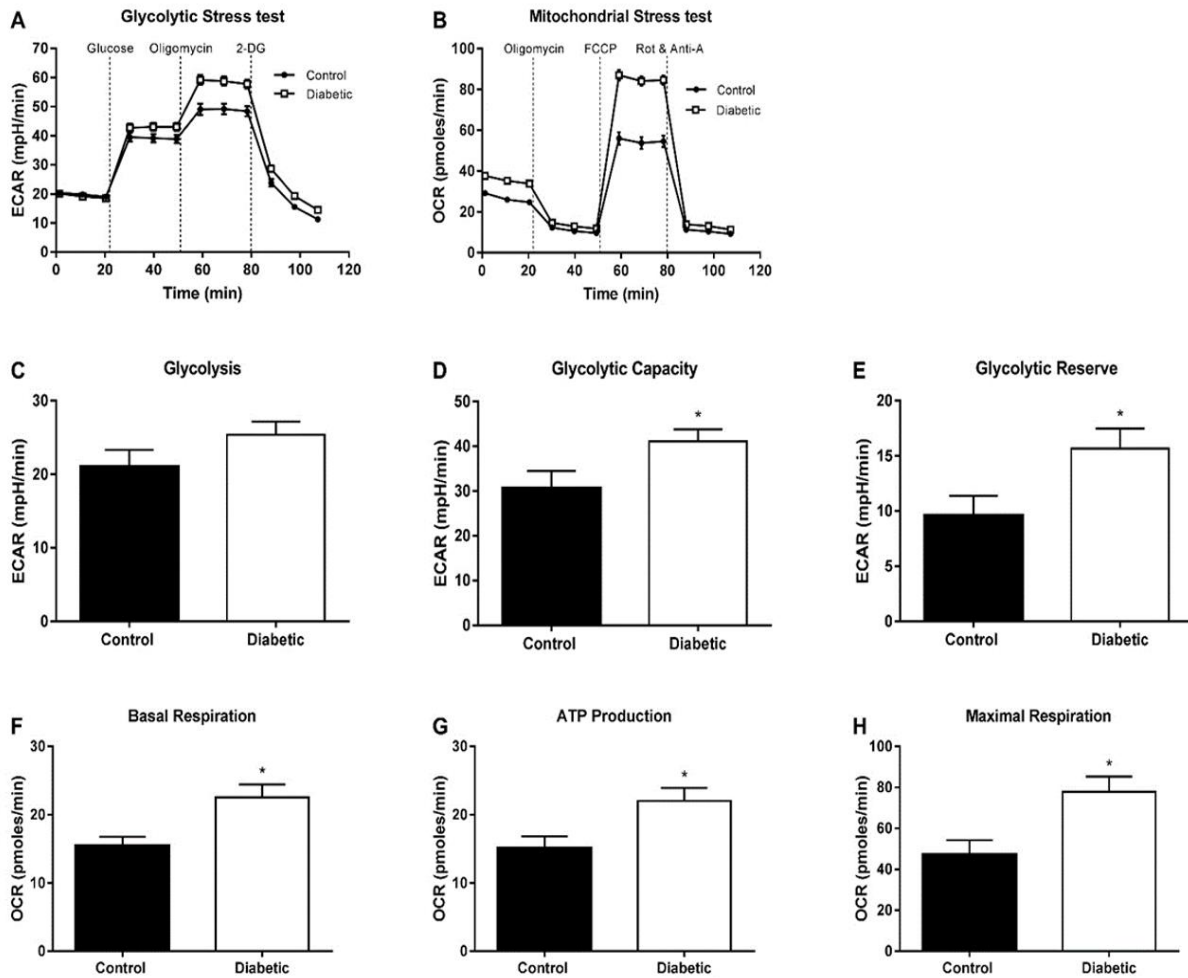


**Figure 19. Bioenergetic profiles of PBMCs.**

Glycolysis (**A**) and Mitochondrial respiratory function (**B**) of isolated PBMCs of T2DM patients and age-matched controls were analyzed using a XF96 Bioanalyzer. Glycolytic stress was determined by basal measurement of extra acidification rates (ECAR) following injection of 10 mM glucose, 1 mM oligomycin and 100 mM 2-deoxy-D-glucose (2-DG) to measure glycolysis (**C**), glycolytic capacity (**D**), glycolytic reserve (**E**) and non-glycolytic acidification. The basal measurement (**F**) of oxygen consumption rates (OCR) of mitochondrial respiration were followed by sequential injections of 1 mM oligomycin, 0.25 mM FCCP and a combination 1 mM rotenone and 1 mM antimycin A (Rot & Anti-A) to measure ATP production (**G**), maximal respiration (**H**) and non-mitochondrial respiration. Data is represented as mean  $\pm$  S.E.M.,  $n=14$  for T2DM patients and  $n=9$  for control patients. For statistical analysis two sided t-test was applied \*  $p<0.05$ .

vs  $22.01 \pm 7.105$ ;  $p=0.0205$ ) (Figure 19.G) and the FCCP induced mitochondrial maximal respiration was increased by 65% ( $47.31 \pm 21.6$ ;  $77.86 \pm 28.78$ ;  $p=0.0101$ ) (Figure 17.H). Elevated mitochondrial bioenergetics is associated with increased ROS formation in PBMCs of T2DM (Hartman et al., 2014). In collaboration, the  $O_2^{\bullet-}$  production of PBMCs of T2DM ( $n=8$ ) and age-matched controls ( $n=7$ ) was determined by flow cytometry using MitoSOXred™. The  $O_2^{\bullet-}$



## Results

production was increased in all analyzed PBMCs; about 10-fold in the granulocytes ( $282 \pm 101$  vs  $2931 \pm 646$  MFI;  $p=0.0026$ ) (Figure 20.D), about 6-fold in the monocytes ( $1930 \pm 839$  vs  $11710 \pm 2583$  MFI;  $p=0.0012$ ) (Figure 20.E) and about 6.5-fold in the T-cells ( $1036 \pm 545$  vs  $6760 \pm 1470$  MFI;  $p=0.0048$ ) (Figure 20.F). No alterations in mitochondrial mass of the different types of PBMCs was observed. The enhanced glycolytic reserve, together with mitochondrial respiratory capacity, reflects a higher metabolic capacity to maintain intracellular ATP levels. Moreover, the increased mitochondrial respiration together with elevated  $O_2\bullet^-$  production in PBMCs of T2DM support the theory that hyperglycemia induced increase in electron transfer donors (NADH and FADH<sub>2</sub>) leads to hyperpolarization of the mitochondrial membrane and increased ATP/ADP ratio. The high electron chemical gradient can induce partial inhibition of ETC complex III and subsequently activate of coenzyme Q, driving the reduction of oxygen to generate free  $O_2\bullet^-$ .

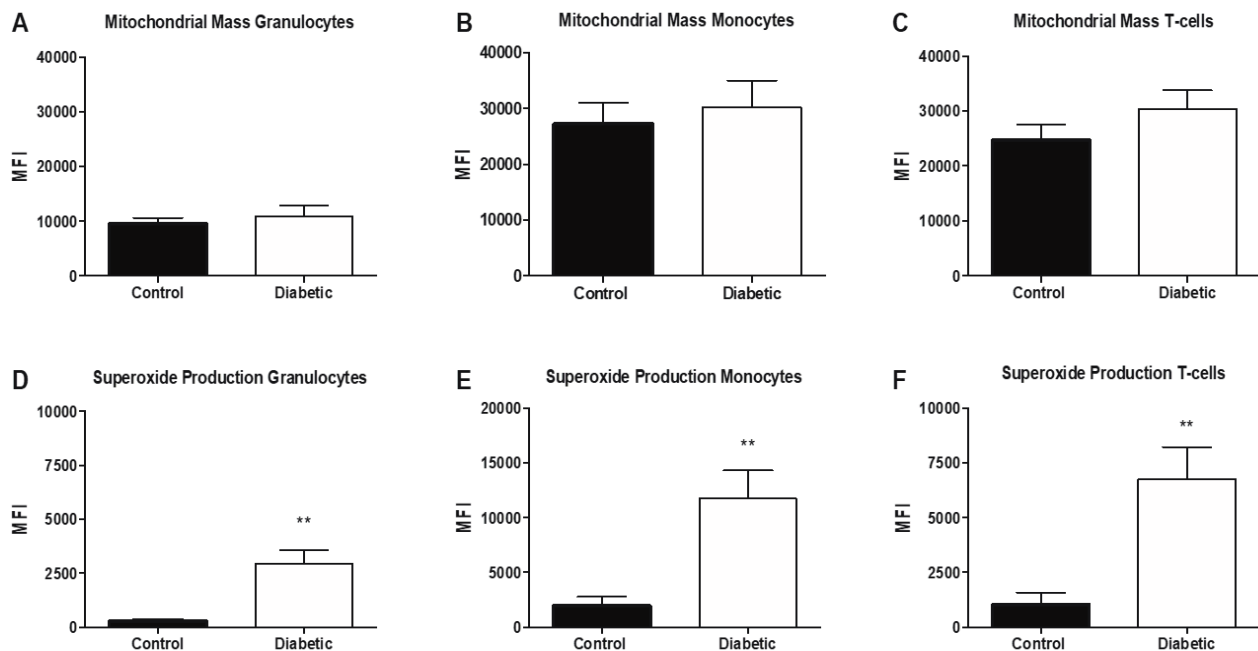


**Figure 20. Mitochondrial mass and superoxide production.**

Using MitoTracker® Green FM, mitochondrial mass was analyzed in granulocytes (A), monocytes (B), and T-cells (C), which were separated by cell type-specific cell surface markers. Mitochondrial superoxide oxidation was determined in granulocytes (D), monocytes (E) and T-cells (F) using MitoSOX™. Mean fluorescence intensity (MFI) was detected by flow cytometry. Data is represented as mean  $\pm$  SD,  $n=14$  for T2DM patients and  $n=9$  for control patients. For statistical analysis two sided  $t$ -test was applied  $**p<0.01$ .

## Discussion

### 5 Discussion

#### 5.1 Hyperglycemia induced alterations are cell type specific.

In this study a long-term hyperglycemia cell culture model was used to investigate the downstream effects of glucose in vitro. It was shown that the alterations in glucose uptake, and glucose transporter expression, mitochondrial reactive metabolites in response to 6 days of high glucose were cell type specific. For instance, elevated glucose uptake in fibroblasts was associated with increased GLUT 1 expression, whereas this was associated with increased GLUT 3 expression in Schwann cells. These findings are in agreement with previous studies showing tissue specific expression of glucose transporters; GLUT 1 is expressed in membranes of erythrocytes, muscles, adipose tissue and brain; GLUT 2 is mainly expressed in hepatocytes and pancreatic  $\beta$ -cells; GLUT 3 is expressed in the brain and nerve cells and GLUT 4 is only expressed in adipocytes and muscles (Gould and Holman et al., 1993). The cell specific effect on hyperglycemia is in agreement with the observation of tissue specific differences in development of insulin resistance in animal models of diabetes and in diabetic patients (Jelenick et al., 2014; Nakae et al., 2001; Rask-Madsen and Kahn 2013). In addition to glucose transporters, tissue specific expression of lipoprotein lipase and insulin receptor may also provide an explanation for the tissue specific effects observed in diabetes (Kim et al. 2001; Thirone et al., 2006). Meta-analysis has indicated that both tissue specific and non-specific genes and pathways are associated with diabetes pathogenesis and common pathway affecting diabetes development is activated through different genes at different tissues (Mei et al., 2017). The cell specific effects on hyperglycemia and/or insulin resistance may also explain to some extent the differential responsiveness of diabetic patients to the same treatment; if one mechanism was to explain all diabetic complications, one specific treatment targeting this pathway would prevent all diabetic complications, which is not the case. It is therefore important to determine not only the effects of hyperglycemia on specific tissues but also on the specific cell types which constitute the tissue.

## Discussion

### 5.2 Unifying theory not applicable in Schwann cells and fibroblast cell culture model of hyperglycemia

Under high glucose condition for 6 days, the cell types studied showed increased glucose uptake and increased generation of reactive metabolites including  $O_2^{\bullet-}$  and NO. This is in agreement with the unifying theory suggesting that increased glucose uptake leads to increased ROS formation. However, these increased were not reflected by an increase in either glycolysis or ATP-related oxygen consumption.

The first pathway which is activated in the unifying theory is the polyol pathway. In this study increased sorbitol levels were observed in fibroblasts in response to high glucose, whereas it was unchanged in the Schwann cells, indicating that high glucose does not affect the polyol pathway. Increased polyol flux is known to be regulated by aldose reductase. The inhibition of aldose reductase has been reported to improve neuronal function in diabetic mice (Obrosova et al., 2003). This has been confirmed in another study which showed that aldose reductase deficient mice are protected against neuropathy, mediated by preservation of glutathione and NADPH pools (Ho et al., 2006). Although these studies indicate a role of aldose reductase in diabetic neuropathy, clinical study of aldose reductase inhibitors showed that the polyol pathway cannot completely account for the development of neuropathy (Goto et al., 1995). It has subsequently been shown that under severe hyperglycemia aldose reductase deficient diabetic mice still develop neuronal dysfunction (Yagihashi et al., 2001; Yagihashi et al., 2011). Despite many preclinical studies, the exact mechanism of how the polyol pathway is involved in DN remains inconclusive. Earlier studies proposed the osmotic theory which describes that increased flux through the polyol pathway induces intracellular hyperosmolarity due to the accumulation of impermeable sorbitol in the cytoplasm, lead to cell expansion and lysis (Gabbay et al., 1975; Kinoshita et al., 1990). Although this mechanism might be involved in some diabetic complications, there is no consistent evidence of nerve edema or swollen cells within the diabetic nerve (Jakobson et al., 1985).

With respect to the triosephosphate-depending pathways, it was shown in this study that PKC activity remained unchanged in both Schwann cells and fibroblasts. Moreover, methylglyoxal

## Discussion

levels were not increased in either short or long term hyperglycemia cell culture model, suggesting that the AGE pathway is not active. This is in contrast to the unifying theory which states that ROS are required for the inactivation of GAPDH and the activation of triosephosphate-dependent pathways (PKC and AGE). This inconsistency with the unifying theory would explain why most clinical trials using antioxidants or inhibitors of the pathways of the unifying theory have not prevented or reduce the pathogenesis of DN.

This study in Schwann cells and fibroblasts showed no activation of the AGE pathway. Glycation has been implicated in the pathogenesis of diabetic neuropathy (Thornally, 2002; Sugimoto et al., 2008; Quattrini et al., 2007). Accumulation of AGEs has been shown in several components of peripheral nerve tissues, including endoneurial vessels, nerve fibers and Schwann cells, in human and animal diabetic nerves and associated with decreased myelinated nerve fiber density (Sugimoto et al., 1997; Sugimoto et al., 2008; Quattrini et al., 2007). In vitro, when exposed to high concentration of AGEs, Schwann cells underwent apoptosis with release of tumor necrosis factor (TNF)- $\alpha$  and other inflammatory cytokines. AGE receptor (RAGE) overexpression in mice showed delayed nerve conduction velocity (NCV) and neuronal changes which were more severe in diabetic condition (Wada et al., 2007), whereas RAGE-deficient mice are protected against the induction of neuropathy (Toth et al., 2008). Indirect evidence of the role of AGEs in neuropathy is the treatment with aminoguanidine in experimental neuropathy, which inhibits AGE production and improved neuronal blood flow, nerve conduction velocity and myelinated fiber structure (Kihara et al., 1991). However, it should be noted that aminoguanidine also acts as an anti-oxidative function and is an inhibitor for iNOS (Cameron et al., 2005). Moreover, due to the secondary side effects, it has been withdrawn as a drug for the treatment of diabetes. Clinical trials of the anti-glycation agent, benfotiamine, has shown some protection against diabetic retinopathy and neuronal dysfunction (Hammes et al., 2003; Haupt et al., 2005), while others have shown that long term treatment with benfotiamine in T1DM patients had no significant effect upon neuronal function (Fraser et al., 2012). These data implies that there is still no effective compound that can suppress the AGE formation *in vivo* and improve diabetic neuropathy in humans and would also suggest that the AGE pathway is not the most important pathway involved in the pathogenesis of diabetic neuropathy. Taken together,

## Discussion

the data in this study would suggest that the pathways described in unifying theory are not activated in Schwann cells and cannot explain the increase in  $O_2^{\bullet-}$  and NO production.

Whilst this study showed no differences in the pathways of the unifying theory, this might be explained by the changes in observed in mitochondrial metabolism in Schwann cells and Fibroblasts which are the opposite to what was expected. This study revealed that culturing Schwann cells and fibroblasts under high glucose condition leads to impaired spare respiratory capacity and glycolytic capacity, whilst the non-glycolytic extracellular acidification and fatty acid oxidation was increased in Schwann cells. This would suggest that the decrease in oxygen consumption in response to an energetic demand is associated with an adaptation to fatty acids as a substrate for oxidation. As such, the absence of glucose through glycolysis as an energy fuel rather than its accumulation and a shift towards increased lipid oxidation might be the driving force in Schwann cell metabolic adaptation to hyperglycemia and subsequently to neuronal changes in diabetes.

### 5.3 High glucose induces a metabolic switch towards fatty acid oxidation in Schwann cells

This study showed a metabolic switch from glycolysis towards fatty acid oxidation in Schwann cells under high glucose condition. Diabetes is associated with altered lipid levels in the circulation and neurons. Especially the altered fatty acid metabolism in Schwann cells is linked to neuropathy (Freeman et al., 2016, Viader et al., 2013). This can be explained by the fact that Schwann cells have a very active lipid metabolism and share many molecular features with adipocytes (Verheijen et al., 2003). As observed in adipocytes, Schwann cells transport long fatty acid via carnitine palmitoyl-transferase 1 (CPT1) from extra cellular space into the cytoplasm. Increased CPT1 expression been shown in cultured Schwann cells in response to long chain fatty acid treatment (Hinder et al., 2014). In rodents, high fat diet activates lipogenesis and induces accumulation of oxidized lipids in peripheral nerves, indicating a prediabetic condition (Obrosova et al., 2007). Disrupted lipid metabolism is also observed in peripheral nerves of streptozotocin induced (STZ) diabetic mice, including reduced short-chain triglycerols (Freeman et al., 2016). A study in a mouse model of Schwann cell mitochondrial defects to peripheral neuropathy also linked mitochondrial dysfunction with altered lipid cell metabolism

## Discussion

leading to neuron degeneration and subsequently neuropathy (Viader et al., 2013). In this study mitochondrial dysfunction in Schwann cells induced a metabolic switch away from lipid synthesis towards lipid oxidation. Viader et al., showed that increased lipid oxidation in Schwann cells leads to the depletion of myelin lipids and increased  $\beta$ -oxidation and a subsequent substrate overload of Acetyl-CoA which are then converted in to acyl carnitines. Once released, the acetyl carnitines are detrimental to the nearby neurons, leading to neurodegeneration (Viader et al., 2013). Interestingly, increased lipid peroxidation and DNA oxidation was already observed in sciatic nerves of 1-2 weeks old STZ diabetic rats prior the development of many functional and structural defects and remained constant over many months (Cunha et al., 2008). Exposure of human Schwann cells to high glucose condition reduced the production of phospholipids that was restored by aldose reductase inhibitor, suggesting that hyperglycemia dysregulates Schwann cell lipid metabolism via the polyol pathway (Kuruvilla and Eichberg, 1998). These findings suggest that Schwann cells play an active role in DN rather than passive insulators for axons. Schwann cells are critical sensors of axonal activity, and play an important role in the axon energy supply. The disruption of this important crosstalk between Schwann cell and neuron due to increased  $\beta$ -oxidation in Schwann cells in response to hyperglycemia might underlie DN.

The limitation of this study concerning  $\beta$ -oxidation is that only indirect evidence of increased  $\beta$ -oxidation in Schwann cells in response to long term high glucose levels was observed. This study showed increased protein phosphorylation of acetyl citrate lyase and acetyl-CoA carboxylase, together with increased gene expression of carnitine palmitoyltransferase 1, indicating an increased flux towards  $\beta$ -oxidation when Schwann cells are cultured under high glucose condition. Metabolome analysis using LC-MS/MS has to be performed to determine which metabolites of the FAO pathway is affected by high glucose. Moreover, Schwann cells have long been known to provide trophic support for axons (Varon and Bunge, 1978), and study in mutant mice that lack Schwann cells showed a developmental loss of PNS neurons/axons (Birchmeier et al., 2009). Furthermore, the interaction between Schwann cells and neurons needs to be considered, as such cross-talk may play an important role in potential diabetes induced changes. As such it cannot be excluded that the changes are observed in this study are not truly reflecting

## Discussion

the *in vivo* situation. Therefore, the results obtained in current study should be verified in Schwann cell and neuron co-culture system as described (Hyung et al., 2015; Wiese et al., 2010). To determine the effect of Schwann cell dependent acyl carnitine accumulation, medium of Schwann cells isolated from Sciatic nerves of 3 month and 6 months STZ diabetic mice (model T1DM) and ob/ob mice (model T2DM) cultured for 48 hrs in appropriated medium should be analyzed for acetyl carnitine concentrations (described by Viader et al., 2013). Preliminary data showed a trend towards increased acetyl carnitine release, especially C18, release in media of 3 months STZ diabetic mice (Table 6), which was not observed in 6 months STZ diabetic mice (n=3) (Table 7), suggesting that increased acyl carnitine release upon aberrant lipid metabolism in Schwann cells might play an important role in the early onset of experimental DN. In addition, acyl carnitine concentrations and the metabolic intermediates of the glycolysis pathway and the fatty acid oxidation pathway in the sciatic nerves of experimental diabetes models should be determined to verify whether the metabolic effect observed *in vitro* are reflected *in vivo*.

Dyslipidemia is a significant contributor to the development of DN. Although lipid lowering drugs are effective in reducing morbidity and mortality from diabetic cardiovascular events, the extent of their effect in relation to neuropathy is not fully understood. The Fremantle Diabetes study in patients with T2DM using statins and fibrates as a means of lipid lowering, showed that treatment with fenofibrate reduced the appearance of neuropathy determined by the Michigan Neuropathy Scoring Instrument (Davis et al., 2008). The Field Study Fenofibrate and Event-Lowering in Diabetes in patients reported lower rate of non-traumatic amputations in patients with T2DM treated with fenofibrate as compared to placebo (Rajamani et al., 2009). The possible explanation of the positive effect of fenofibrate was found in obese db/db mice, where fenofibrate activates the PPAR-AMPK-PGC1 pathway, which is part of the cellular antioxidant system, in the sciatic nerve, thereby improving the neuronal function in these animals (Cho et al., 2014). However, other studies have reported no effect of lipid lowering treatment on DN (Emad et al., 2018), or in contrast, showed that lipid lowering drugs, such as fibrates and statins, negatively affects DN (Corrao et al., 2004; Phan et al., 1995; Vilholm et al., 2014; Weimer, 2003). West et al showed that the prevalence of peripheral neuropathy following drug consumptions was 4–14 times higher among patients using statins (West, 2011). In the current

## Discussion

study, fatty acid synthesis was shown to be decreased, whilst  $\beta$ -oxidation was increased in Schwann cells upon high glucose treatment. Reducing fatty acid concentrations further by lipid lowering drugs may therefore disturb this balance even further, leading to Schwann cells metabolic dysfunction and subsequently to axon demyelination and neuropathy. For example, it has been shown that statin reduced remyelination in the CNS (Miron et al., 2009).

**Table 6. Acyl carnitines measurement in 3 months STZ diabetic mice**

Type Acylcarnitine	3mWT		3mSTZ		Fold Change (%)	p-value
	Mean ( $\mu\text{mol/l}$ )	SD	Mean ( $\mu\text{mol/l}$ )	SD		
C0	2,029	0,224	2,982	0,679	47	0,082
C2	7,042	0,385	8,755	0,749	24	0,024 *
C4	0,139	0,059	0,173	0,048	25	0,482
C5	1,905	0,165	4,429	1,732	133	0,066
C6	0,041	0,007	0,041	0,020	0	0,999
C8	0,030	0,007	0,004	0,007	-86	0,013*
C10	0,015	0,010	0,013	0,006	-14	0,768
C12	0,032	0,022	0,041	0,013	27	0,575
C14	0,017	0,016	0,011	0,010	-38	0,588
C16	0,053	0,032	0,047	0,033	36	0,818
C18	0,011	0,005	0,079	0,048	640	0,072

\*p=0.05

**Table 7. Acyl carnitines measurement in 6 months STZ diabetic mice**

Type Acylcarnitine	6mWT		6mSTZ		Fold Change (%)	p-value
	Mean ( $\mu\text{mol/l}$ )	SD	Mean ( $\mu\text{mol/l}$ )	SD		
C0	3,116	0,697	2,606	0,573	-16	0,242
C2	3,608	0,563	3,268	0,364	-9	0,290
C4	0,096	0,045	0,117	0,028	22	0,399
C5	0,078	0,033	0,083	0,033	6	0,825
C6	0,040	0,024	0,026	0,026	-35	0,400
C8	0,025	0,029	0,007	0,006	-73	0,204
C10	0,052	0,005	0,059	0,032	13	0,651
C12	0,038	0,024	0,032	0,010	-17	0,603
C14	0,025	0,016	0,018	0,013	-26	0,511
C16	0,040	0,027	0,030	0,015	-23	0,527
C18	0,067	0,019	0,045	0,014	-32	0,077



## Discussion

### 5.4 The metabolic switch depends on the nitric oxide pathway

In this study, it was shown that after 6 days of high glucose treatment, there was increased iNOS activity and NO protein expression together with and reduced maximal respiration. Moreover, using the soluble nitric oxide donor, DetaNONOate, had little impacted on basal mitochondrial function but reduced mitochondrial respiratory capacity and spare respiratory capacity in Schwann cells cultured under normal glucose conditions, confirming the link that nitric oxide reduces mitochondrial maximal respiration. This is consistent with the findings of Dranka et al., which showed that treatment with DetaNONOate reduced maximal respiration in bovine aortic endothelial cells in dose-dependent manner, which was reversed upon NO donor removal (Dranka et al., 2010).

NO or other derived RNS can affect mitochondrial function under physiological and pathological conditions. NO reacts with heme moieties and thus can reversibly reduce activity of iron-containing enzymes such as cytochrome c oxidase (complex IV of the ETC), thereby inhibiting mitochondrial maximal respiration and spare respiratory capacity (Lacza et al., 2009). Primary cultures of astrocytes activated to express iNOS by interferon- $\gamma$  and endotoxin revealed NO production up to 1  $\mu$ M, and this endogenous NO reduced mitochondrial respiration by the inhibition of cytochrome c oxidase, which was reversed upon inhibition of NOS or removing NO by oxyhemoglobin (Brown et al., 1995). This is supported by another study where the addition of NO donors to neuroblastoma rapidly reduced mitochondrial respiration, whereas NOS inhibitors had the opposite effect, suggesting a constitutive inhibition of cytochrome c oxidase by NO within the cells (Sarti et al., 2003).

NO also interacts strongly with superoxide anion, which is generated and released from the ETC complex I and III, to form peroxynitrite. iNOS is a key regulator in peroxynitrite induced injury to peripheral nerve, and functional and structural changes of diabetic neuropathy. It has been reported that nitrosative stress in Schwann cells and axons, rather than in dorsal ganglion root ganglion, underlies the development and progression of DN (Vareniuk et al., 2008). Peroxynitrite can have diverse effects on mitochondrial function, including protein S-nitrosylation. Nitrosylation of critical thiols by NO has been described as important in the

## Discussion

control of the activity of certain enzymes such as glyceraldehyde-3-phosphate dehydrogenase, caspases, and transglutaminase (Melino et al., 1997; Mohr et al., 1996), or proteins involved in intracellular signal transduction, such as the ryanodine receptor. In the current study, increased S-nitrosylation of mitochondrial protein was found to occur under high glucose conditions. Further studies, involving proteomic are required to identify which mitochondrial proteins are modified by S-nitrosylation and in turn how the modified protein(s) are affecting mitochondrial function.

This study showed in Schwann cells that both nitric oxide pathway and fatty acid oxidation is upregulated in response to high glucose. It is therefore postulated that NO is involved in the metabolic switch towards FAO in Schwann cells. There is accumulating evidence to suggest that NO affects lipid metabolism in diabetes. Binding of  $Ca^{2+}$  to the pore of Cav1.1., as well as the activation of CAMKK11 and NOS, is required for normal mitochondrial  $\beta$ -oxidation (Georgiou et al., 2015). Doulias et al. showed that NO regulates mitochondrial fatty acid metabolism through reversible protein S-nitrosylation across 6 different mouse tissues (Doulias et al., 2013). iNOS, in particular, has been implicated in S-nitrosylation in peripheral nerve and not in ganglion root, and STZ-induced diabetic iNOS<sup>-/-</sup> mice are partially protected against nerve damage as compared to the wild type mice (Vareniuk et al., 2008). It has been shown that iNOS expression is increased in human Schwann cell cultured for 24 hrs in high glucose medium (30mM) versus control (5mM), whereas inhibition of 4-hydroxyl-nonanal, a product of lipid peroxidation, reversed iNOS expression back to the concentration observed in the control (Obrosova et al., 2005). A study on nitrosative stress and DN showed elevated 12/15 lipogenase expression and activation in the sciatic nerve of STZ diabetic and high fat diet-fed mice, as well as in human Schwann cells cultured under high glucose condition. Inhibition of 12/15 lipogenase in the sciatic nerve reduced nitrated protein and and large and small fiber dysfunction, indication a role of 12/15 lipoxygenase in nitrosative stress (Stavniichuk et al., 2010). The association between nitric oxide and lipid metabolism was confirmed by the observation of defective mitochondrial  $\beta$ -oxidation by elevated intracellular lipid levels in cardiomyocytes of eNOS<sup>-/-</sup> mice (Le Gouill et al., 2007). Moreover, it was shown that NO regulates  $\beta$ -oxidation via reversible protein S-nitrosylation. Proteins of glucose metabolism and TCA cycle as well as very

## Discussion

long acyl-CoA dehydrogenase (VLCAD), which catalysis the first step of  $\beta$ -oxidation have been found to be S-nitrosylated in wild type mouse livers and absent in the livers of eNOS<sup>-/-</sup> mice (Doulias et al., 2013). Another study has reported that nitrate enhanced mice skeletal muscle  $\beta$ -oxidation and reduced long chain fatty acids levels in a dose-respond manner (Ashmore et al., 2015), supporting the theory that NO affects mitochondrial  $\beta$ -oxidation.

The findings in the current study of increased NOS together increased nitrosylation of mitochondrial proteins indicates that either NO or peroxynitrite is transferred into to the mitochondria or NO is produced within the mitochondria. Since classical iNOS inhibitors L-NAME and 1400W did not reverse the increase in NO, it can be concluded that upregulation of NO might be due mitochondrial NOS (mtNOS). This was supported by the finding that the antioxidant *N*-acetylcysteine (NAC), which can directly scavenge free radicals, did reduce O<sub>2</sub>•<sup>-</sup> levels in high glucose culture Schwann cells back to normal levels, whereas the NO levels remained unaffected. This study is in agreement with other studies that showed NO production and NOS activity in the mitochondria, which was not attenuated by classical NOS inhibitors, such as W1400 and L-NAME, and were unable identify mtNOS as one of the three classic NOS isoforms (Tatoyan et al., 1998; Lacza et al., 2003). Mitochondrial NO is produced via the mitochondrial nitric oxide synthase (mtNOS), which is located in the inner membrane or mitochondrial matrix (Ghafourifar and Cadenas, 2005; Tatoyan et al., 1998). mtNOS is a Ca<sup>2+</sup> dependent voltage-dependent enzyme whose generation of NO is regulated by mitochondrial membrane potential and which in turn regulates the activity of the ETC. Although the mitochondrial NOS levels are low, mitochondrial NO production might be underestimated due to the fast elimination of NO by cytochrome oxidase (Pearce et al., 2002). Several studies have reported that mtNOS generates peroxynitrite which leads to a reduction in the activity of cytochrome c oxidase (complex IV) and a reduced maximal mitochondrial respiration of the cells and eventually apoptosis (Cadenas et al., 2001; Ghafourifar et al., 1999). In contrast, S-nitrosylation of caspase-3, which inhibits the apoptotic effect of the protein, indicates an anti-apoptotic role for mtNOS in protecting cells from unwanted apoptosis and organelles from proteolytic activity of the caspase. These findings indicate a crucial role of mitochondria derived NO in the regulation of cell signaling. It has been shown that eNOS is attached to the outer

## Discussion

mitochondrial membrane in sensory neurons and endothelial cells (Gao et al., 2004; Henrich et al., 2002), indicating that mtNOS might be a cellular NOS enzyme and that mitochondria might regulate NOS activity and, conversely, that eNOS might regulate mitochondrial function (Lacza et al., 2009). Although the existence of a genuine mtNOS seems to be ambiguous, mitochondrial derived NO and RNS could play an important role on cellular function and the pathophysiology of diabetes and its complications.

### 5.5. Increased mitochondrial bioenergetics in PBMCs of T2DM

In this study the effect of diabetes on mitochondrial metabolism in PBMCs of patients with T2DM was also determined. A trend towards increased glycolysis and increased glycolytic capacity and mitochondrial respiration together with increased ROS production in PBMCs of T2DM was observed, as compared to non-diabetic controls. This is in accordance with previous findings in PBMCs of patients with T2DM. It has been shown in PBMCs of patient with T2DM that the mitochondrial oxygen consumption was increased, consistent with higher production of ROS (Hartman et al., 2014). Widlansky et al. reported decreased mitochondrial mass, increased mitochondrial hyperpolarization, as well as increased H<sub>2</sub>O<sub>2</sub> and O<sub>2</sub>•<sup>-</sup> in PBMCs of patients with T2DM (Widlansky et al., 2010). Increased levels of ROS have also been reported in lymphocytes of diabetic patients with severe nephropathy, however the type of diabetes was not specified (Nam et al., 2008). These findings support the unifying theory, where an increase in glycolytic flux leads to increased mitochondrial respiration and ROS formation.

Several studies reported that reduced glycolytic capacity is associated with apoptosis, whereas increased glycolytic capacity is associated with cellular reprogramming and differentiation (Chung et al., 2011, Folmes et al., 2010). Therefore, the increased glycolytic capacity observed in PBMCs of T2DM observed in this study might indicate cellular reprogramming of the immune cells in order to cope with hyperglycemic conditions. However, the direct effect of diabetes on glycolysis in PBMCs has not been extensively studied. Increased levels of fructose 2,6-bisphosphate, as a measurement for glycolysis, has been shown in monocytes of diabetic patients and was associated with immune dysfunction in T2DM (Atsumi et al., 2007; Shaheena et al., 2012), indicating that glycolysis is upregulated in PBMCs of T2DM patients. Interestingly,

## Discussion

differential mitochondrial bioenergetics has been shown in monocytes, lymphocytes, neutrophils and platelets (Kramer et al., 2013; Pelletier et al., 2014).

The find of such studies, to some extent, provide the clinical evidence that diabetes can be characterized by increased oxidative stress. However, this phenotype is not necessary associated with alterations in mitochondrial function; a positive association between mitochondrial function and ROS production would have been expected as the major source of ROS. Furthermore, whilst the blood provides the easiest and most readily accessible source of patient material, it is often overlooked that it is an organ in itself and that alterations detected within the blood may not necessary reflect the biochemical and/or molecular situation which is occurring within the tissue. This is particularly relevant in diabetes, as it is a disease which can affect multiple organs and the complications relevant for mortality and morbidity affect parenchymal organs. Future studies would therefore involve the functional analysis of mitochondria in the blood versus the tissue(s).

### 5.6 Conclusion and future directions

This study revealed a cell specific response towards high glucose, showing the importance of tissue-specific changes in cellular energy metabolism in diabetic complications-prone tissues. Interestingly, high glucose induced a metabolic switch from glycolysis towards lipid oxidation in Schwann cells, implying an important role of mitochondrial lipid metabolism in Schwann cells in response to hyperglycemia. In addition, increased NO levels together with proteins S-nitrosylation might be an important inducer of this metabolic switch. Metabolomic analysis should clarify which proteins are S-nitrosylated in Schwann cells under high glucose conditions and how these alterations are associated with the metabolic switch. Future study would focus on the effect of enhanced Schwann cell lipid oxidation in vivo. Furthermore, in vitro, the interaction between Schwann cells and neurons would be studied. These lines of inquiry would increase our knowledge about cell specific alterations in mitochondrial metabolism in diabetes and its effect interactions between different cell types. Within the context of DN, understanding such interactions would lead to a better understanding of the pathophysiology of the disease and in doing so allow for the development of new therapeutic targets.

## Summary

### 6 Summary

Diabetic neuropathy (DN) is a prevalent, complex and debilitating chronic complication of diabetes mellitus. The main clinical treatment is the tight control of blood glucose levels. However, there is accumulating evidence that this does not reduce the incidence and the progression of DN, suggesting that other pathways are involved. Aberrant Schwann cells metabolism, characterized by a shift from fatty acid synthesis towards fatty acid oxidation, may play an important role in neuronal dysfunction and subsequently neuropathy.

In this study the effect of high glucose condition on the downstream mitochondrial metabolism in different cell types was investigated. This study revealed a cell type specific increase in glucose uptake, mitochondrial properties and reactive metabolites in response to high glucose. Collectively, this data supports the emerging idea of tissue-specific alterations in energy metabolism in diabetic complications-prone tissues, such as the peripheral nerves. Hence, this data shows the importance to investigate the tissue- and cell-specific effect and interactions in response to hyperglycemia in diabetes.

Focusing on the effect of hyperglycemia in diabetic neuropathy, the research was continued in Schwann cells and fibroblasts. Markers of the unifying theory including sorbitol, PCK activity and methylglyoxal were mainly unaffected in both fibroblast and Schwann cells in response to high glucose, as compared to low glucose cultured cells. Moreover according to unifying theory, hyperglycemia induces an increased glucose flux through glycolysis leading to increased mitochondrial bioenergetics and subsequently to increased ROS formation causing cellular damage and the development of diabetic complications. However, under long term hyperglycemia the glycolytic capacity and the mitochondrial spare respiratory capacity was reduced in both cell lines, indicating that the capacity of the cells to respond to an energetic demand was diminished when cultured for 6 days under high glucose condition. The reduced glycolytic and respiratory capacity was not reflected in the ATP production and reactive metabolite production. Interestingly, the non-glycolytic acidification was increased in Schwann cells indicating an alternative energy source for the mitochondria to produce ATP and/or reactive metabolites.

## Summary

Another important energy source for mitochondria is the oxidation of fatty acids. This study showed a metabolic switch from glycolysis towards increased fatty acid oxidation in Schwann cells in response to high glucose. In addition, increased dependency on the medium chain fatty acid octanoate in high glucose cultured Schwann cells was observed, confirming the importance of fatty acid metabolism in Schwann cells. Moreover, an increase in nitric oxide synthesis, nitric oxide production, and protein S-nitrosylation was observed in the Schwann cells cultured under chronic high glucose conditions. Upon stimulation with the nitric oxide inducer DetaNONOate the mitochondrial maximal respiration and spare respiratory capacity of Schwann cells was reduced as observed upon hyperglycemia. Previous studies have shown that nitric oxide and S-nitrosylation can induce a shift from fatty acids towards lipid oxidation, leading to an accumulation of fatty  $\beta$ -oxidation intermediates, such as acetyl carnitines. Once released it leads to neuron degeneration and neuron demyelination and subsequently to neuropathy. Future experiments are required to confirm this hyperglycemia induced nitric oxide synthesis and lipid oxidation alterations and interaction in Schwann cells.

This study indirectly confirms the importance of lipid metabolism in Schwann cell in response to hyperglycemia and that nitric oxide synthesis and protein S-nitrosylation may play an important role in the mitochondrial metabolic switch from glycolysis toward fatty acid oxidation. Future study should concentrate on 1) which proteins are S-nitrosylated in response to hyperglycemia in Schwann cells and how this is associated with altered mitochondrial Schwann cell metabolism, including decreased glycolysis and increased lipid oxidation, 2) the effect of increased lipid oxidation in Schwann cells on neuronal function and 3) how these metabolic changes in Schwann cell upon diabetes affect the nearby neurons. Increasing our knowledge about cell specific alterations in mitochondrial metabolism in diabetes will lead to a better understanding of the pathophysiology of diabetic neuropathy and the development of new therapeutic targets.

## Zusammenfassung

### 7. Zusammenfassung

Die diabetische Neuropathie (DN) ist eine weit verbreitete, komplexe und schwächende chronische Komplikation des Diabetes mellitus. Die wichtigste klinische Behandlung ist die strenge Kontrolle des Blutzuckerspiegels. Es gibt jedoch zunehmend Hinweise, dass dies die Ausbildung und das Fortschreiten von DN nicht verringern, und andere Mechanismen beteiligt sein müssen. Veränderungen im Stoffwechsel von Schwann Zellen, gekennzeichnet durch eine Verschiebung von der Fettsäure-Synthese zur Fettsäureoxidation, könnten eine wichtige Rolle bei neuronaler Dysfunktion und Neuropathie spielen.

In dieser Studie wurde der Einfluss von Hyperglykämie auf den mitochondrialen Metabolismus in verschiedenen Zelltypen untersucht. Als Reaktion auf hohe Glukosewerte zeigten sich ein zelltypspezifischen Anstieg der Glukoseaufnahme, veränderte mitochondriale Eigenschaften und Akkumulation von reaktiven Metaboliten. Diese Daten unterstützen die Idee von spezifischen Veränderungen des Energiestoffwechsels in diabetischen, komplikationsanfälligen Geweben, wie den peripheren Nerven. Daher zeigen diese Daten, wie wichtig es ist, den gewebs- und zellspezifischen Effekt und die Interaktionen bei Hyperglykämie in Diabetes zu untersuchen.

Mit dem Fokus auf der Auswirkung von Hyperglykämie auf diabetische Neuropathie wurde die Forschung in Schwann-Zellen und Fibroblasten fortgesetzt. Marker der „Unifying Theory“, wie Sorbitol, PCK-Aktivität und Methylglyoxal, waren sowohl in Fibroblasten- als auch in Schwann-Zellen als Reaktion auf hohe Glucose unverändert. Darüber hinaus postuliert die „Unifying Theory“ bei Hyperglykämie einen erhöhten Glukosefluss durch Glykolyse, was zu einer erhöhten mitochondrialen Bioenergetik und zu einer erhöhten ROS-Bildung führt. Diese verursachen Zellschäden und die Entwicklung diabetischer Komplikationen. Unter Langzeit-Hyperglykämie, bei 6-tägiger Kultivierung mit hoher Glukose, waren jedoch die glykolytische Kapazität und die mitochondriale Reserve-Atemkapazität in beiden Zelllinien reduziert. Dies weist auf eine verringerte Reaktionsfähigkeit der Zellen, auf einen erhöhten Energiebedarf, hin. Die reduzierte glykolytische und respiratorische Kapazität spiegelte sich nicht in der ATP-Produktion und der Produktion reaktiven Metabolite wider. Interessanterweise war die nicht-glykolytische



## Zusammenfassung

Ansäuerung in Schwann-Zellen erhöht, was auf eine alternative Energiequelle für die Produktion von ATP und / oder reaktive Metaboliten durch die Mitochondrien hinweist.

Eine weitere wichtige Energiequelle für Mitochondrien ist die Oxidation von Fettsäuren. Diese Studie zeigte einen metabolischen Wechsel von der Glykolyse zu einer erhöhten Fettsäureoxidation in Schwann-Zellen als Reaktion auf hohe Glukose. Zusätzlich wurde eine erhöhte Abhängigkeit von Octanoate, einer Fettsäuren mittlerer Kettenlänge, in Hoch-Glucose-kultivierten Schwann-Zellen beobachtet, was die Wichtigkeit des Fettsäuremetabolismus in Schwann-Zellen bestätigt. Darüber hinaus wurde eine Zunahme der Stickstoffoxid-Synthese und -Produktion und der Protein-S-Nitrosylierung in diesen Schwann-Zellen beobachtet. Stimulierung mit dem Stickoxidinduktor DetaNONOate reduzierte die maximale Atmung und die Reserve-Atemkapazität der Mitochondrien in Schwann-Zellen, wie bei Hyperglykämie beobachtet. Frühere Studien haben gezeigt, dass Stickoxid und S-Nitrosylierung eine Verschiebung von der Fettsäure- zur Lipidoxidation induzieren können, was zu einer Anhäufung von fettigen  $\beta$ -Oxidation in Zwischenprodukten, wie Acetylkartinin, führt. Bei Freisetzung führt es zu neuronaler Degeneration und Demyelinisierung und anschließend zu Neuropathie. Weitere Experimente sind erforderlich, um diese Änderungen bei der Stickoxidsynthese und Lipidoxidation und ihre Wechselwirkungen in Schwann-Zellen zu bestätigen.

Diese Studie bestätigt indirekt die Bedeutung des Lipidstoffwechsels in hyperglykämischen Schwann-Zelle und die mögliche Rolle von Stickstoffoxidsynthese und die Protein-S-Nitrosylierung beim metabolischen Wechsel von der Glykolyse zur Fettsäureoxidation, in Mitochondrien. Zukünftige Studien sollten sich auf folgende Fragen konzentrieren: 1) Welche Proteine werden in hyperglykämischen Schwann-Zellen S-nitrosyliert und wie korreliert dies mit dem veränderten mitochondrialen Metabolismus, einschließlich verminderter Glykolyse und erhöhter Lipidoxidation? 2) Wie wirkt sich die erhöhte Lipidoxidation in Schwann Zellen auf ihre neuronale Funktion aus? 3) Wie beeinflussen die metabolischen Veränderungen in der Schwann-Zelle die benachbarten Neuronen? Die Erweiterung unseres Wissens über zellspezifische Veränderungen des mitochondrialen Metabolismus bei Diabetes wird zu einem besseren Verständnis der Pathophysiologie der diabetischen Neuropathie und der Entwicklung neuer therapeutischer Ziele führen.

## References

### 8. References

- Adela, R., Nethi, S.K., Bagul, P.K, Mattapally, S., Kuncha, M., Patra, C.R., Reddy, P.N., Banerjee, S.K. (2015). Hyperglycemia enhances nitric oxide production in diabetes: a study from South Indian parents. *Plos One*. *10*, e0115270.
- Ahmed, N. (2005). Advanced glycation endproducts-role in pathology of diabetic complications. *Diabetes Res Clin Prac*. *67*, 3–21.
- Albers, J., Herman, W., Pop-Busui, R., Feldman, E., Martin, C., Cleary, P., Waberski, B.H., Lachin, J.M. (2010). Effect of prior intensive insulin treatment during the Diabetes Control and Complications Trial (DCCT) on peripheral neuropathy in type 1 diabetes during the Epidemiology of Diabetes Interventions and Complications (EDIC) Study. *Diabetes Care*. *33*, 1090–1096.
- Alberti, K.G., and Zimmet, P.Z. (1998). Definition, diagnosis and classification of diabetes mellitus and its complications. Part 1: diagnosis and classification of diabetes mellitus provisional report of a WHO consultation. *Diabet Med J Br Diabet Assoc*. *15*, 539–553.
- Ashmore, T., Roberts, LD., Morash, A.J., Kotwica, A.O., Finnerty, J., West, J.A., Murfitt, S.A., Fernandez, B.O., Branco C., Cowburn A.S., Clarke, K., Johnson, R.S., Feelisch, M., Griffin, J.L., Murray, A.J. (2015). Nitrate enhances skeletal muscle fatty acid oxidation via nitric oxide-cGMP-PPAR-mediated mechanism. *BMC Biology*. *138* (110), doi: 10.1186/s12915-015-0221-6.
- Askwith, T., Zeng, W., Eggo, M.C., Stevens, M.J. (2012). Taurine reduces nitrosative stress and nitric oxide synthase expression in high glucose-exposed human schwann cells. *Exp Neurol*. *233*, 154-162.
- Assmann, T.S., Brondani A., Bouças A.P., Rheinheimer J., de Souza B. M., Canani L.H., Bauer A.C., Crispim D. (2016). Nitric oxide levels in patients with diabetes melitus: A systematic review and meta-analysis. *Nitric Oxide*. *61*, 1-9.
- Atorino, L., Di Meglio, S., Farina, B., Jones, R., and Quesada, P. (2001). Rat germinal cells require PARP for repair of DNA damage induced by gamma-irradiation and H<sub>2</sub>O<sub>2</sub> treatment. *Eur. J. Cell Biol*. *80*, 222–229.
- Atsumi T., Chiba H., Yoshioka N., Bucala R., Koike T. Increased Fructose 2,6-biphosphate in peripheral blood mononuclear cell of patients with diabetes (2007) *Endocrine Journal* *54*,517–520.
- Balaban, R.S. (1990). Regulation of oxidative phosphorylation in the mammalian cell. *Am J Physiol*. *258*, C377–C389.
- Bates, T.E., Loesch, A., Burnstock, G., Clark J.B. (1995). Immunocytochemical evidence for a mitochondrially located nitric oxide synthase in brain and liver. *Biochem Biophys Res Commun*. *213*, 896–900.
- Bierhaus, A., Humpert, P.M., Morcos, M., Wendt, T., Chavakis, T., Arnold, B., Stern, D.M., and Nawroth, P.P. (2005). Understanding RAGE, the receptor for advanced glycation end products. *J Mol Med Berl Ger*. *83*, 876–886.
- Bierhaus A., Fleming, T., Stoyanov, S., Leffler, A., Babes, A., Neacsu, C., Sauer, S.K., Eberhardt, M., Schnözer, M., Lasitschka, F., Neuhuber, W.L., Kicho, T.O., Konrade, Elvert, R., Mier, W. Pirags, V., Lukic, I.K., Morcos, M., Dehner, T., Rabbani N., Thornalley, P.J., Edelstein, D., Nau, C., Forbes, J., Humpert, P.M. Schwaninger, M., Ziegler, D., Stern, D.M., Cooper, M.E., Haberkorn, U., Brownlee, M., Reeh, P.W., Nawroth, P.P. (2012). Methylglyoxal modification of Nav1.8 facilitates nociceptive neuron firing and causes hyperalgesia in diabetic neuropathy. *Nat Med*. *18*, 926-33.
- Birchmeier, C. 2009. ErbB receptors and the development of the nervous system. *Exp Cell Res* *315*, 611–618.
- Birben, E., Sahiner, U.M., Sackesen, C., Erzurum, S., and Kalayci, O. (2012). Oxidative Stress and Antioxidant Defense: *World Allergy Organ. J*. *5*, 9–19.
- Blackmore, R.S., Greenwood, C., Gibson, Q.H. (1991). Studies of primary oxygen intermediate in the reaction of fully reduced cytochrome oxidase. *J Bio Chem.*, *266*, 19245-19249.

## References

- Bleier, L., Dröse, S. (2013). Superoxide generation by complex III: From mechanistic rationales to functional consequences. *Biochim Biophys Acta*. 1827, 1320-1331.
- Boelens, R., Rademaker, H., Wever, R., van Gelder, B.F. (1984). The cytochrome c oxidase-azide-nitric oxide complex as a model for oxygen-binding site. *Biochim Biophys Acta*. 765, 196-209.
- Bongaerts, B.W, Rathmann, W., Kowall, B., Herder, C., Stöckl, D., Meisinger, C., Ziegler, D. (2012) . Postchallenge hyperglycemia is positively associated with diabetic polyneuropathy: The KORA F4 study. *Diabetes Care*. 35, 1891-1893.
- Boudina, S., Sena, S., Theobald, H., Sheng, X., Wright, J.J., Hu, X.X., Aziz, S., Johnson, J.I., Bugger, H., Zaha, V.G., Abel, E.D. (2007). Mitochondrial energetics in the heart in obesity-related diabetes: direct evidence for increased uncoupled respiration and activation of uncoupling proteins. *Diabetes*. 56, 2457–2466.
- Boussageon, R., Bejan-Angoulvant, T., Saadatian-Elahi, M., Lafont, S., Bergeonneau C., Kassai B., Erpeldinger, S., Wringht, J.M., Gueyffier, F., Cornu, C. (2011). Effect of intensive glucose lowering treatment on all cause mortality, cardiovascular death, and microvascular events in type 2 diabetes: meta-analysis of randomised controlled trials. *BMJ*. 343: d4169.
- Bradford, M.M. (1976). A rapid and sensitive method for the quantitation of microgram quantities of protein utilizing the principle of protein-dye binding. *Anal. Biochem*. 72, 248–254.
- Brand, M.D., Affourtit, C., Esteves, T.C., Green, K., Lambert, A.J., Miwa, S., Pakay, J.L., and Parker, N. (2004). Mitochondrial superoxide: production, biological effects, and activation of uncoupling proteins. *Free Radic. Biol. Med*. 37, 755–767.
- Brown, G.C. (1995). Nitric oxide regulates mitochondrial respiration and cell functions by inhibiting cytochrome oxidase. *FEBS Lett*. 369, 136-139.
- Brown, G.C. (2001). Regulation of mitochondrial respiration by nitric oxide inhibition of cytochrome c oxidase. *Biochim Biophys Acta*. 1504, 46-57.
- Brown, G.C., Bortutaite, V., (2002). Nitric oxide inhibition of mitochondrial respiration and its role in cell death. *Free Radic Biol Med*. 33, 1440-1450.
- Brownlee, M. (2001). Biochemistry and molecular cell biology of diabetic complications. *Nature*. 414, 813–820.
- Brownlee, M. (2005). The pathobiology of diabetic complications: a unifying mechanism. *Diabetes*. 54, 1615–1625.
- Brunori, M, Giuffrè A., Forte, E., Mastronicola, D., Barone, M.C., Sarti P. (2004). Control of cytochrome c oxidase activity by nitric oxide. *Biochim Biophys Acta*. 1655, 365-371.
- Bugger, H., Boudina, S., Hu, X.X., Tuinei, J., Zaha, V.G., Theobald, H.A., Yun, U.J., McQueen, A.P., Wayment, B., Litwin, S.E., et al. (2008). Type 1 diabetic akita mouse hearts are insulin sensitive but manifest structurally abnormal mitochondria that remain coupled despite increased uncoupling protein 3. *Diabetes*. 57, 2924–2932.
- Bugger, H., Chen, D., Riehle, C., Soto, J., Theobald, H.A., Hu, X.X., Ganesan, B., Weimer, B.C., and Abel, E.D. (2009). Tissue-specific remodeling of mitochondrial proteome in type 1 diabetic akita mice. *Diabetes*. 58, 1986–1997.
- Cai, D., Yuan, M., Frantz, D.F., Melendez, P.A., Hansen, L., Lee, J., and Shoelson, S.E. (2005). Local and systemic insulin resistance resulting from hepatic activation of IKK- $\beta$  and NF- $\kappa$ B. *Nat Med*. 11, 183–190.
- Cadenas, E., Poderoso, J.J., Antunes, F., Boveris A. (2001). Analysis of the Pathways of Nitric Oxide Utilization in Mitochondria. *Free Radic. Res*. 33, 747-756.
- Callaghan, B., Cheng, H., Stables, C., Smith, A., Feldman, E. (2012a). Diabetic neuropathy: clinical manifestations and current treatments. *Lancet Neurol*. 11: 521–534.

## References

- Callaghan, B., Little, A., Feldman, E., Hughes, R. (2012b). Enhanced glucose control for preventing and treating diabetic neuropathy. *Cochrane Database Syst Rev.* 6: CD007543.
- Cameron, N.E., Gibson T.M., Nangle, M.R., Cotter, M.A. (2005). Inhibitors of advanced glycation end product formation and neurovascular dysfunction in experimental diabetes. *Ann. N. Y. Acad. Sci.* 1043, 784–792.
- Cester, N., Rabini, R.A., Salvolini, E. Staffolani, R., Curatola, A., Pugnaloni, A., Brunelli, M.A., Biagini, G., Mazzanti, L. (1996). Activation of endothelial cells during insulin-dependent diabetes mellitus: a biochemical and morphological study. *Eur J Clin Invest.* 26, 569–573.
- Chacko, B.K., Kramer, P.A., Ravi, S., Johnson, M.S., Hardy, R.W., Ballinger, S.W., and Darley-USmar, V.M. (2013). Methods for defining distinct bioenergetic profiles in platelets, lymphocytes, monocytes, and neutrophils, and the oxidative burst from human blood. *Lab Invest.* 93, 690–700.
- Chacko, B.K., Kramer, P.A., Ravi, S., Benavides, G.A., Mitchell, T., Dranka, B.P., Ferrick, D., Singal, A.K., Ballinger, S.W., Bailey, S.M. Hardy, R.W., Zhang, J., Zhi, D., Darley-USmar, V.M. (2014). The bioenergetics health index: a new concept in mitochondrial translational research. *Clin Sci. (Londen)*, 127, 367-373.
- Chen, J., Chernatynskaya, A.V., Li, J.W. Kimbrell, M.R., Cassidy, R.J., Perry, D.J., Muir, A.B., Atkinson, M.A., Brusko, T.M., Mathews, C.E. (2017). T cells display mitochondria hyperpolarization in human type 1 diabetes. *Sci Rep.* 7: 10835, doi: 10.1038/s41598-017-11056-9.
- Chen, Y.R., Zweier, J.L. (2014). Cardiac mitochondria and reactive oxygen species generation. *Cir Res.* 114, 524-537.
- Cho, Y.R., Lim, J.H., Kim, M.Y., Kim, T.W., Hong, B.Y., Kim, Y.-S., Chang, Y.S., Kim, H.W., Park, C.W. (2014). Therapeutic effects of fenofibrate in diabetic peripheral neuropathy by improving endothelial and neuronal survival in db/db mice. *PLoSOne.* 9, e83204.
- Corrao, G., Zambon, A., Bertù, L., Botteri, E., Leoni, O., Contiero, P. (2004). Lipid lowering drugs prescription and the risk of peripheral neuropathy: an exploratory case-control study using automated databases. *J Epidemiol Community Health.* 58, 1047-1051.
- Cox, B., Emili, A. (2006). Tissue subcellular fractionation and protein extraction for use in mass-spectrometry-based proteomics. *Nat Protoc.* 1, 1872-1878.
- Chung S., Arrell D.K., Faustino R.S., Terzic A., Dzeja P.P.(2010). Glycolytic network restructuring integral to the energetic of embryonic stem cell cardiac differentiation. *J. Mol. Cell Cardiol.* 48, 725-734.
- Cunha, J.M., Jolival, C.G., Ramos, K.M., Gregory, Y.A., Calcutt, N.A., Mizisin, A.P. (2008). Elevated lipid peroxidation and DNA oxidation in nerve from diabetic rats: effects of aldose reductase inhibition, insulin and neurotrophic factors. *Metabolism* 57, 873-881.
- Davies, J.L., Kawaguchi, Y., Bennett, S.T., Copeman, J.B., Cordell, H.J., Pritchard, L.E., Reed, P.W., Gaugh, S.C., Jenkins, S.C., Palmer, S.M., Balfour, K.M., Rowe, B.R., Farrall, M., Barnett A.H., Bain S.C., Todd J.A. (1994). A genome-wide research for human type 1 diabetes susceptibility genes. *Nature.* 8, 130-136.
- Davis, T.M.E., Yeap, B.B., Davis, W.A., BruceDavis, D.G. (2008). Lipid-lowering therapy and peripheral sensory neuropathy in type 2 diabetes: the fremantle diabetes Study. *Diabetologia*, 51, 562-566.
- De Cavanagh, E.M., Ferder, L., Toblli, J.E., Piotrkowski, B., Stella, I., Fraga, C.G., and Inserra, F. (2008). Renal mitochondrial impairment is attenuated by AT1 blockade in experimental Type I diabetes. *Am J Physiol Heart Circ Physiol.* 294, H456–H465.
- Dobler, D., Ahmed, N., Song, L., Eboigbodin, K.E., and Thornalley, P.J. (2006). Increased Dicarbonyl Metabolism in Endothelial Cells in Hyperglycemia Induces Anoikis and Impairs Angiogenesis by RGD and GFOGER Motif Modification. *Diabetes* 55, 1961–1969.

## References

- Doulias, P.T., Tenopoulou, M., Greene, J.L., Raju, K., Ischiropoulos, H. (2013). Nitric oxide regulates mitochondrial fatty acid metabolism through reversible protein S-nitrosylation. *Sci Signal*. 6 doi: 10.1126/scisignal.2003252.
- Dranka B.P., Hill, B.G., Darley-Usmar, V.M. (2010). Mitochondrial reserve capacity in endothelial cells: The impact of nitric oxide and reactive oxygen species. *Free Radic Biol Med*. 48, 905-914.
- Drel, V.R., Mashtalir, N., Ilnytska, O., Shin, J., Li, F., Lyzogubov, V.V., Obrosova, I.G. (2006). The leptin-deficient (ob/ob) mouse: a new animal model of peripheral neuropathy of type 2 diabetes and obesity. *Diabetes*. 55, 3335–3343.
- Drel, V.R., Pacher, P., Varenjuk, I., Pavlov, I.A., Ilnytska, O., Lyzogubov, V.V., Tibrewala, J., Groves, J.T., Obrosova, I.G. (2007). A Peroxynitrite decomposition catalyst counteracts sensory neuropathy in streptozotocin-diabetic mice. *Eur J Pharmacol*. 569, 48–58.
- Du, X., Matsumura, T., Edelstein, D., Rossetti, L., Zsengellér, Z., Szabó, C., and Brownlee, M. (2003). Inhibition of GAPDH activity by poly(ADP-ribose) polymerase activates three major pathways of hyperglycemic damage in endothelial cells. *J. Clin. Invest*. 112, 1049–1057.
- Du, X.L., Edelstein, D., Rossetti, L., Fantus, I.G., Goldberg, H., Ziyadeh, F., Wu, J., Brownlee, M. (2000). Hyperglycemia-induced mitochondrial superoxide overproduction activates the hexosamine pathway and induces plasminogen activator inhibitor-1 expression by increasing Sp1 glycosylation. *Proceedings of the National Academy of Sciences of the United States of America*. 97, 12222–12226.
- Dugan, L.L., You, Y.-H., Ali, S.S., Diamond-Stanic, M., Miyamoto, S., DeClevés, A.-E., Andreyev, A., Quach, T., Ly, S., Shekhtman, G., et al. (2013). AMPK dysregulation promotes diabetes-related reduction of superoxide and mitochondrial function. *J. Clin. Invest*. 123, 4888–4899.
- Dyck, P.J., Overland, C.J., Low, P.A., et al., (2010). Signs and symptoms versus nerve conduction studies to diagnose diabetic sensorimotor polyneuropathy: CI vs. NPhys trial. *Muscle Nerve*. 42, 157–64.
- Ebenezer, G.J., McArthur, J.C., Thomas, D., Murinson, B., Hauer, P., Polydefkis, M., Griffin, J.W. (2007). Denervation of skin in neuropathies: the sequence of axonal and Schwann cell changes in skin biopsies. *Brain*. 130, 2703–2714.
- Eberhardt, M.J., Fiopovic, M.R., Leffler, A., de la Roche, J., Kistner, K., Fischer, M.J., Fleming, T., Zimmermann, K., Ivanovic-Burmzovic, I., Nawroth, P.P., Bierhau, A.A., Reeh, P.W., Sauer, S.K. (2012). Methylglyoxal activate nociceptors through transient receptor potential channel A1 (TRPA1): A possible mechanism of metabolic neuropathies. *J Biol Chem*. 287, 28291-28306
- Edwards, L., Quanttrini A., Lentz, S.I., Figueroa-Romero, C., Cerri, A. , Backus, C., Hong, Y., Feldman E.L. (2010). Diabetes regulates mitochondrial biogenesis and fission in axons and animal models of diabetic neuropathy. *Diabetologia*. 53, 160-169.
- Emad, M., Arjmand, H., Farpour, H.R., Kardeh, B. (2018). Lipid lowering drugs (statins) and peripheral neuropathy. *Electron Physican*. 10, 6527-6533.
- Engelstad, J.K., Davies, J.L., Giannini, C., O'Brien, P.C., Dyck, P.J. (1997). No evidence for axonal atrophy in human diabetic polyneuropathy. *J Neuropathol Exp Neuropathol Exp Neurol*. 56, 255-262.
- Faraci, F.M., Didion, S.P. (2004). Vascular protection: superoxide dismutase isoforms in the vessel wall. *Arterioscler Thromb Vasc Biol*. 24, 1367-1373.
- Fernyhough, P., Roy Chowdhury S.K., Schmidt, R.E. (2010). Mitochondrial stress and the pathogenesis of diabetic neuropathy. *Expert Rev Endocrinol Metab*. 5, 39–49.

## References

- Finocchietto, P.V., Franco, M.C., Holod, S., Gonzalez A.S., Converso, D.P., Arciuch, V.G.A., Serra, M.P., Poderoso J.J., Carreras M.C. (2014). Mitochondrial nitric oxide synthase: a master piece of metabolic adaptation, cell growth, transformation and death. *Exp Biol Med.* 234, 1020-1028.
- Folmes C.D., Nelson T.J., Martinez\_fernandez A., Arrell D.K., LindorJ.Z., Dzeja P.P., Ikeda Y., Perz-Terzic C., Terzic A. (2011). Somatic oxidative bioenergetics transition to pluripotency-dependent glycolysis to facilitate nuclear reprogramming. *Cell Metab.* 14, 264-271.
- Fraser, D.A., Diep, L.M., Hovden, I.A., Nilson, K.B., Sveen, K.A., Seljeflot, I., Hanssen, K.F. (2012). The effects of long-term oral benfotamine supplementation on peripheral nerve function and inflammatory markers in patients with type 1 diabetes; a 24-month, double-blind, randomized, placebo-controlled trial. *Diabetes Care.* 35, 1095-1097.
- Freeman, O.J., Unwin R.D., Dowsey A.W., Begley P., Ali S., Hollywood, K.A., Rustogi N., Petersen R.S., Dunn W.B., Cooper, G.J.S., Gardiner N.J. (2016). Metabolic dysfunction is restricted to the sciatic nerve in experimental diabetic neuropathy. *Diabetes.* 65, 228-238.
- Gabbay, K.H. Hyperglycemia, polyol metabolism, and complications of diabetes mellitus. (1975). *Annu. Rev. Med.* 26, 521-536.
- Gadau, S.D. (2012). Nitrosative stress induces proliferation and viability changes in high glucose-exposed rat Schwannoma cells. *Neuro Endocrinol Lett.* 33, 279-84.
- Gaede, P., Vedel, P., Parving, H.H., Pederson, O. (1999). Intensified multifactorial intervention in patients with type 1 diabetes mellitus and microalbuminuria. The Steno type 2 randomized study. *Lancet.* 353, 617-622.
- Gao, S., Chen, J., Brodsky, S.V., Huang, H., Adler, S., Lee, J.H., Dhadwal, N., Cohen-Gould, L., Gross, S.S., Golorski, M.S. (2004). Docking of endothelial nitric oxide synthase (eNOS) to the mitochondrial outer membrane: a pentabasic amino acid sequence in the autoinhibitory domain of eNOS targets a proteinase K-cleavable peptide on the cytoplasmic face of mitochondria. *J Bio Chem.* 279, 15968-1597.
- Georgiou, D.K., Gagnino-Acosta, A., Lee, C.S., Griffin, D.M., Wang H., Jagor W.R., Pautler R.G., Dirksen R.T., Hamilton S.L. (2015). Ca<sup>2+</sup> binding/permeation via calcium channel, CaV1.1. regulates the intercellular Distribution of fatty acid transport protein, CD36 and fatty acid metabolism. *J Bio Chem.* 290, 23751-237-65.
- Ghafourifar, P. and Richter C. (1997). Nitric oxide synthase activity in mitochondria. *FEBS Lett.* 418, 291-296.
- Ghafourifar, P., Schenk, U., Klein, S.D., Richter, C., (1999). Mitochondrial nitric-oxide synthase stimulation causes cytochrome c release from isolated mitochondria. Evidence for intramitochondrial peroxynitrite formation. *J Biol Chem.* 274, 31185-31188.
- Ghafourifar, P. and Cadenas E. (2005). Mitochondrial nitric oxide synthase. *Trends Pharmacol Sci.* 26, 190-195.
- Giulivi, C., Poderose, J.J., Boveris A. (1998). Production of nitric oxide by mitochondria. *J Biol Chem.* 273, 11038-11043.
- Goligorski, M.S. (2004). Docking of endothelial nitric oxide synthase (eNOS) to mitochondrial outer membrane: a pentabasic amino acid sequence in the autoinhibitory domain of eNOS target a protein K-cleavable peptide in the cytoplasmic face of mitochondria. *J Biol Chem.* 279, 15968-15974.
- Gonçalves, N., Vægter, C.B., Andersen, H., Østergaard, L., Calcutt, N.A., Jensen, T.S. (2017). Schwann cell interactions with axons and microvessels in diabetic neuropathy. *Nat Rev Neurol.* 13, 135-147.
- Goto, Y., Hotta, N., Shigeta, Y., Sakamoto, N. Kikkawa R. (1995). Effects of an aldose reductase inhibitor, epalrestat, on diabetic neuropathy. Clinical benefit and indication for the drug assessed from the results of a placebo-controlled double-blind study. *Biomed Pharmacother.* 49, 269-277.

## References

- Gould, G.W. and Holman G.D. (1993). The glucose transporter family: structure, function and tissue specific expression. *Bio Chem J.* *295*, 329-341.
- Hammes, H.P., Du, X., Edelstein, D., Taguchi, T., Matsumura, T., Ju, Q., Lin, J., Bierhaus, A., Nawroth, P., Hannak, D., et al. (2003). Benfotiamine blocks three major pathways of hyperglycemic damage and prevents experimental diabetic retinopathy. *Nat. Med.* *9*, 294–299.
- Han, J., Tan, P., Li, Z., Wu, Y., Li, C., Wang, Y., Wang, B., Zhao, S., (2014). Fuzi attenuates diabetic neuropathy in rats and protects Schwann cells from apoptosis induced by high glucose. *PlosOne.* *9* e86539.
- Hartman, M.L., Shirihaï O.S., Holbrook, M., Xu, G., Kocherla, M., Shah, A., Fetterman, J.L., Kluge, M.A., Frame, A.A., Hamburg, N.M., Vita, J.A. (2014). Relation of mitochondrial oxygen consumption in peripheral blood mononuclear cells to vascular function in type 2 diabetes mellitus. *Vasc Med.* *19*, 67-74.
- Haupt, E., Ledermann, H., Köpcke, W.(2005). Benfotiamine in the treatment of diabetic polyneuropathy – a three-week randomized, controlled pilot study (BEDIP study). *Int. J.Clin. Pharmacol. Ther.* *43*, 71-77.
- Henrich, M., Hoffman K., König P., Gruss M., Fischbach T., Gödecke A.M., Hempelmann G., Kummer W. (2002). Sensory neurons respond to hypoxia with NO production associated with mitochondria. *Mol Cell Neurosci.* *20*, 307-322.
- Herlein, J.A., Fink, B.D., O'Malley, Y., Sivitz, W.I. (2009). Superoxide and respiratory coupling in mitochondria of insulin-deficient diabetic rats. *Endocrinology.* *150*, 46-55.
- Hinder, L.M., Figueroa-Romero, C., Pacut, C., Hong, Y., Vivekanandan-Giri, A., Pennathur, S., Feldman, E.L. (2014). Long-chain acyl coenzyme A synthetase 1 overexpression in primary cultured Schwann cells prevents long chain long chain fatty acid-induced oxidative stress and mitochondrial dysfunction. *Antioxid Redox Signal.* *21*, 588-600.
- Ho, E.C., Lam, K.S., Chen, Y.S., Yip, J.C., Arvindashan M., Yamagishi, S., Yagihashi, S., Oates, P.J., Ellery, C.A., Chung, S.K. (2006). Aldose reductase-deficient mice are protected from delayed motor nerve conduction velocity, increased c-Jun NH2-terminal kinase activation, depletion of reduced glutathione, increased superoxide accumulation, and DNA damage. *Diabetes.* *55*, 1946-1953.
- Horvat, S., Beyer, C., Arnold, S. (2006). Effect of hypoxia on the transcription pattern of subunit isoforms and the kinetics of cytochrome c oxidase in cortical astrocytes and cerebellar neurons. *J Neurochem.* *99*, 937-51.
- Hruz, T., Wyss, M., Docquier, M., Pfaffl, M.W., Masanetz, S., Borghi, L., Verbrugghe, P., Kalaydjieva, L., Bleuler, S., Laule, O., et al. (2011). RefGenes: identification of reliable and condition specific reference genes for RT-qPCR data normalization. *BMC Genomics* *12*, 156.
- Hyung, S., Lee, B.Y., Park, J.C., Kim, J., Hur, E.M. Suf, J.K.F. (2015). Coculture of primary motor neurons and Schwann cells as a model for in vitro myelination. *Sci Rep.* *15122*. doi: 10.1038/srep15122.
- Jaffrey, S.R., Erdjument-Bromage, H., Ferris, C.D., Tempst, P., Snyder, S.H. (2003). Protein s-nitrosylation: a physiological signal for neuronal nitric oxide. *Nat Cell Biol.* *3*, 193-197.
- Jakobsen, J., Sidenius, P. (1985). Nerve morphology in experimental diabetes. *Clin. Physiol.* *5*, 9–13.
- Javed, S., Alam, U., Malik, R.A. (2015). Burning through the pain: treatments for diabetic neuropathy. *Diabetes Obes Metab.* *17*, 1115-11125.
- Jelenik, T., Séquaris, G., Kaul, K., Ouwens, D.M., Phielix, E., Kotzka, J., Knebel, B., Wieß J., Reinbeck, A.L., Janke, L., Nowotney P., Partke H.J., Zhang D., Shulman, G.I., Szendroei J., Roden, M. (2014). Tissue-specific differences in the development of insulin resistance in a mouse model for type 1 diabetes. *Diabetes.* *63*, 3856-3867.
- Jena, N.R. (2012). DNA damage by reactive species: Mechanisms, mutation and repair. *J. Biosci.* *37*, 503–517.

## References

- Johansen, J.S., Harris, A.K., Rychly, D.J., Ergul, A. (2005). Oxidative stress and the use of antioxidants in diabetes: linking basic science to clinical practice. *Cardiovasc Diabetol.* 4: 5, doi: 10.1186/1475-2840-4-5.
- Kanwar, M., and Kowluru, R.A. (2009). Role of Glyceraldehyde 3-Phosphate Dehydrogenase in the Development and Progression of Diabetic Retinopathy. *Diabetes* 58, 227–234.
- Kanwar, Y.S., Wada, J., Sun, L., Xie, P., Wallner, E.I., Chen, S., Chugh, S., Danesh, F.R. (2008). Diabetic nephropathy: mechanisms of renal disease progression. *Exp Biol Med.* 233, 4–11.
- Kalichman, M.W., Powell, H.C., Mizisin, A.P. (1998). Reactive, degenerative, and proliferative Schwann cell responses in experimental galactose and human diabetic neuropathy. *Acta Neuropathol.* 95, 47–56.
- Kelley, D.E., He, J., Menshikova, E.V., Ritov, V.B. (2002). Dysfunction of mitochondria in human skeletal muscle in type 2 diabetes. *Diabetes.* 51, 2944–2950.
- Kihara, M., Schmelzer, J.D., Poduslo, J.F., Nickander, K.K., Low, P.A. (1991) Aminoguanidine effects on nerve blood flow, vascular permeability, electrophysiology, and oxygen free radicals. *Proc. Natl. Acad. Sci. USA* 88, 6107–6111.
- Kim J.K., Fillmore, J.J., Chen, Y., Yu C., Moore I.K., Pypaert M, Lutz E.P., Kako, Y., Velez-Carrasco, W., Goldberg, I.J., Breslow J.L, Gerald I. Shulman, G.I. (2001) Tissue-specific overexpression of lipoprotein lipase causes tissue-specific insulin resistance. *PNAS* 98, 7522-7527.
- Kinoshita, J.H. (1990). A thirty year journey in the polyol pathway. *Exp Eye Res.* 50, 567–573.
- Kowaltowski, A.J., de Souza-Pinto, N.C., Castilho, R.F., Vercesi, A.E. (2009). Mitochondria and reactive oxygen species. *Free Radic. Biol. Med.* 47, 333-343.
- Kozlov, A.V., Staniek, K., H. Noh, H. (1999). Nitrite reductase activity is a novel function of mammalian mitochondria. *FEBS Lett.* 454, 127-130.
- Kramer, P.A., Chacko B.K, Ravi, S., Johnson, M.S., Mitchell T., Darley-Usmar, V.M. (2014). Bioenergetics and oxidative burst: protocols for the isolation and evaluation of Human leukocytes and platelets. *J. Vis. Exp.* 85, doi: 10.3791/51301.
- Kuruville, R., Eichberg J. (1998). Depletion of phospholipid arachidonyl-containing molecular species in a human Schwann cell line grown in elevated glucose and their restoration by an aldose reductase inhibitor. *J Neurochem.* 71, 775-783.
- Kushnareva Y., Murpy A.N., Andreyev A. (2002). Complex I-mediated reactive oxygen species generation: modulation by cytochrome c and NAD(P)<sup>+</sup> oxidation-reduction state. *Biochem J.* 363, 545-553.
- Kusmaul L. and Hirst J. (2006). the mechanisms of Superoxide production by NADH:ubiquinone oxidoreductase (complex 1) from bovine heart mitochondria. *Proc Natl Acad Sci.* 103, 7607-7612.
- Kowluru, R.A., Kanwar, M., Kennedy, A. (2007). Metabolic memory phenomenon and accumulation of peroxynitrite in retinal capillaries. *Exp Diabetes Res.* 2007:21976.
- Lacza, Z., Snipes, J.A., Horváth, E.M, Figueroa, J.P., Szabó, C., Busija, D.W. (2003). Mitochondrial nitric oxide synthase is not eNOS nNOS or iNOS. *Free Rad Biol Med.* 10, 1217-1228.
- Lacza, Z., Pankotai, E., Csordás A., Gero D., Kiss L., Horváth, Kollai M., Busija D.W., Szabó C. (2006) Mitochondrial NO and reactive nitrogen species production: Does mtNOS exist? *Nitric Oxide.* 14, 162-168.
- Lacza, Z., Pankotai, E., Busija, D.W. (2009). Mitochondrial nitric oxide synthase: current concepts and controversies. *Front Biosci.* 14, 4436-4443.



## References

- Laemmli, U.K. (1970). Cleavage of structural proteins during the assembly of the head of bacteriophage T4. *Nature* 227, 680–685.
- Lee, H.J., Park, H.G., Lee, J.K., Park H.J. (2011). Changes in the arginine methylation of organ proteins during the development of diabetes mellitus. *Diabetes Res Clin Pract.* 94, 111-118.
- Le Gouill E., Jimenez M., Binnert C., Jayet P.Y., Thalmann S., Nicod P., Scherrer U, Vollenwieder P. (2007). Endothelial nitric oxide synthase (eNOS) knockout mice have defective mitochondrial beta-oxidation. *Diabetes* 56, 2690-2696.
- Lehmann, H.C., Köhne, A., Meyer zu Hörste, G., Dehmel, T., Kiehl, O., Hartung, H.P. Kastenbauer, S., Kieseier, B.C. (2007). Role of nitric oxide as a mediator of nerve injury in inflammatory neuropathies. *J Neuropathol Exp Neurol.* 66, 305-212.
- Like, A.A., and Rossini, A.A. (1976). Streptozotocin-induced pancreatic insulinitis: new model of diabetes mellitus. *Science.* 193, 415–417.
- Malik, R.A., Tesfaye, S., Newrick, P.G., Walker, D., Rajbhandari S.M., Siddique, I., Sharma, A.K., Boulton A.J., King R.H., Thomas P.K., War J.D. (2005). Sural nerve pathology in diabetic patients with minimal but progressive neuropathy. *Diabetologia.* 48, 578-585.
- Mei, H., Lianna, L., Lui, S., Jiang, F., Grisword, M. Mosley, T. Tissue non-specific genes and pathways associated with diabetes: an expression Meta-analysis. *Genes.* 8 (1) doi: 10.3390/genes8010044.
- Melino G, Bernassola F, Knight R A, Corasaniti M T, Nisticò G, Finazzi-Agrò A. (1997). S-nitrosylation regulates apoptosis. *Nature (London).* 388, 432–433.
- Miron, V.E., Zehntner, S.P., Kuhlman, T, Ludwin S.K., Owens, T., Kennedy, T.E., Bedell, B.J., Antell, J.P. (2009). Statin therapy inhibits remyelination in the central nervous system. *Am J Pathol.* 174, 1880-1890.
- Mitchell, P. (1975). The protonmotive Q cycle: a general formulation. *FEBS Lett.* 59, 137–139.
- Mizisin, A. P. (2014). Mechanisms of diabetic neuropathy: Schwann cells. *Handb. Clin. Neurol.* 126, 401–428.
- Mohr S, Stamler J S, Brüne B. (1996). Posttranslational modification of glyceraldehyde-3-phosphate dehydrogenase by S-nitrosylation and subsequent NADH attachment. *J Biol Chem.* 271, 4209–4214.
- Muijsers, B.R., Folkerts, G., Henricks, P.A., Sadeghi-Hashjin, G., Nijkamp, F.P. (1997). Peroxynitrite: a two-faced metabolite of nitric oxide. *Life Sci.* 1833-1845.
- Murphy, M.P. (2009). How mitochondria produce reactive oxygen species. *Biochem. J.* 417, 1–13.
- Nakae, J., Kido, Y., Accili, D. (2014). Tissue specific insulin resistance in type 2 diabetes: lessons from gene-targeted mice. *Ann Med.* 33, 22-27.
- Nam, J.S., Cho, M.H., Lee, G.T., Park, J.S., Ahn, C.W., Cha, B.S., Lim, S.K., Kim, K.R., Ha, H.J., and Lee, H.C. (2008). The activation of NF- $\kappa$ B and AP-1 in peripheral blood mononuclear cells isolated from patients with diabetic nephropathy. *Diabetes Res Clin Pract.* 81, 25–32.
- Nathan, D.M., Genuth, S., Lachin, J., Cleary, P., Crofford, O., Davis, M., Rand, L., Siebert, C. Diabetes Control and Complications Trial Research Group. (1993). The effect of intensive treatment of diabetes on the development and progression of long-term complications in insulin dependent diabetes mellitus. *N. Eng.* 329, 977-986.
- Navarro, X., Sutherland, D.E., Kennedy, W.R. (1997). Long-term effects of pancreatic transplantation on diabetic neuropathy. *Ann Neurol.* 42, 727–736.

## References

- Nawroth, P.P., Rudofsky, G., and Humpert, P. (2010). Have We Understood Diabetes? New Tasks for Diagnosis and Therapy. *Exp Clin Endocrinol Diabetes*. *118*, 1–3.
- Nishikawa, T., Edelstein, D., Du, X.L., Yamagishi, S., Matsumura, T., Kaneda, Y., Yorek, M.A., Beebe, D., Oates, P.J., Hammes, H.P., Giardino, I., Brownlee, M. 2000. Normalizing mitochondrial superoxide production blocks three pathways of hyperglycaemic damage. *Nature*. *404*, 787–790.
- Obrosova, I.G., Mabley, J.G., Zsengeller, Z., Charniauskaia, T., Abatan, O.I., Groves, J.T., Szabo, C. (2005). Role for nitrosative stress in diabetic neuropathy: evidence from studies with a peroxynitrite decomposition catalyst. *FASEB J*. *19*, 401–403.
- Obrosova I.G., Ilnytska O., Lyzogubov V.V., Pavlov, I.A., Mashtalir N., Nadler, Drel V.R. (2007). High-fat diet induced neuropathy of pre-diabetes and obesity: Effects of “healthy” diet and aldose reductase inhibition. *Diabetes*. *56*, 2598-2608.
- Ogurtsova, K., da Rocha Fernandes, J.D., Huang, Y., Linnenkamp, U., Guarigueta, L., Cho, N.H., Cavan, D., Shaw J.E., Markaroff, L.E. (2017). IDF Diabetes Atlas: Global estimates for the prevalence of diabetes for 2015 and 2040. *Diabetes Res Clin Pract*. *128*, 40-50.
- Okado-Matsumoto, A., Fridovich, I. (2001). Subcellular distribution of superoxide dismutases (SOD) in rat liver. Cu,Zn-SOD in mitochondria. *J Biol Chem*. *276*, 38388-38393.
- O’Neill, H.M., Holloway, G.P., Steinberg G.R. (2013). AMPK regulation of fatty acid metabolism and mitochondrial biogenesis: implications for obesity. *Mol Cell Endocrinol*. *366*, 135-151.
- Pacher, P., Obrosova, I.G., Mabley, J.G., Szabo, C. (2005). Role of nitrosative stress and peroxynitrite in the pathogenesis of diabetic complications. Emerging new therapeutical strategies. *Curr Med Chem*. *12*, 267–275
- Pacher, P., Beckman J.S., Liaudet L. (2007). Nitric oxide and peroxynitrate in health and disease. *Physiol Rev*. *87*, 315-424.
- Pelletier, M., Billingham, L.K., Ramaswamy, M., Siegel, R.M. Extracellular flux analysis to monitor glycolytic rates and mitochondrial oxygen consumption. *Methods Emzymol*. *542*, 125-149.
- Phan, T., Mcleod, J.G., Pollard, J.D, Peiris, O., Rohan, A., Halpern, J.P. (1995). Peripheral neuropathy associated with simvastatin. *J Neurol Neurosurg Psychiatry*. *58*, 625-628.
- Quattrini, C., Tavakoli, M., Jeziorska, M., Kallinikos, P., Tesfaye, S., Finnigan, J., Marshall, A., Boulton, A.J., Efron, N., Malik, R.A., (2007). Surrogate markers of small fiber damage in human diabetic neuropathy. *Diabetes* *56*, 2148-2154.
- Rabbani, N., and Thornalley, P.J. (2014). Measurement of methylglyoxal by stable isotopic dilution analysis LC-MS/MS with corroborative prediction in physiological samples. *Nat. Protoc*. *9*, 1969–1979.
- Rajamani, K., Colman, P.G., Li, L.P., Voysey, M., D’Emden, M.C., Laakso, M., Baker, J.R., Keech, A.C. (2009). Effect of fenofibrate on amputation events in people with type 2 diabetes mellitus (FIELD study): a prespecified analysis of randomized controlled trial. *Lancet*. *373*, 1780-1788.
- Rask-Madson, C. and Kahn, R.C. (2012). Tissue specific insulin signaling, metabolic syndrome and cardiovascular disease. *Atheroscler Thromb Vasc Biol*. *32*, 2052-2059.
- Ray, P.D., Huang, B.-W., and Tsuji, Y. (2012). Reactive oxygen species (ROS) homeostasis and redox regulation in cellular signaling. *Cell Signal*. *24*, 981–990.
- Ristow, M., and Schmeisser, K. (2014). Mitohormesis: Promoting Health and Lifespan by Increased Levels of Reactive Oxygen Species (ROS). *Dose-Response*. *12*, 288–341.

## References

- Said, G. (2007). Diabetic neuropathy-a review. *Nat Clin Pract Neurol.* 3, 331-340
- Salabei J.K., Gibb, A.A., Hill B.G. (2014). Comprehensive measurement of respiratory activity in permeabilized cell using extracellular flux analysis. *Nat. Protoc.* 9, 421-438
- Sarti, P., Arese, M., Bacchi, A., Barone, M.C., Forte, E., Mastronicola, D., Brunori, M., Giuffrè, A. (2003). Nitric oxide and mitochondrial complex IV. *IUBMB Life.* 55, 605-611.
- Sayeski, P.P., Kudlow, J.E. (1996). Glucose metabolism to glucosamine is necessary for glucose stimulation of transforming growth factor- $\alpha$  gene transcription. *J Biol Chem.* 271, 15237–15243.
- Schroder, J.M. (1993) Neuropathy associated with mitochondrial disorders. *Brain Pathol.* 3, 177–190.
- Shaheena A.W.S., Ghafoor, S., Saleem, A.. (2012). Correlation of fasting blood sugar and glycated hemoglobin levels with Fructose 2,6 Bisphosphate Levels in Immune Cells of Diabetic patients. *Pak J Med Health Sci.* 6: 9-12.
- Shtein, R.M., Callaghan, B.C. (2013). Corneal confocal microscopy as a measure of diabetic neuropathy. *Diabetes.* 62, 25-6.
- Sivitz, W.I., Yorek, M.A. (2010). Mitochondrial dysfunction in diabetes: from molecular mechanisms to functional significance and therapeutic opportunities. *Antioxid Redox Signal.* 12, 537-77.
- Skyler, J.S. (1993). DCCT: The study that forever changed the nature of the treatment of type 1 diabetes. *New Engl J Med.* 329, 977-986.
- Smith, A.G., Russell, J., Feldman, E.L., Goldstein, J., Peltier, A., Smith, S., Hamawi, J., Pollari, D., Bixby, B., Howard, J., Singleton, J.R. (2006). Lifestyle intervention for pre-diabetic neuropathy. *Diabetes Care.* 29,1294–1299.
- Spranger, J., Kroke, A., Mohlig, M., Hoffmann, K., Bergmann, M.M., Ristow, M., Boeing, H., and Pfeiffer, A.F.H. (2003). Inflammatory Cytokines and the Risk to Develop Type 2 Diabetes: Results of the Prospective Population-Based European Prospective Investigation into Cancer and Nutrition (EPIC)-Potsdam Study. *Diabetes.* 52, 812–817.
- Stavniichuk, R., Drel V.R., Shevalye H., Varenjuk I, Stevens M.J., Nadler J.L., Obrosova I.G. (2010). Role of 12/15-lipoxygenase in nitrosative stress and peripheral prediabetic and diabetic neuropathies. *Free Radic Biol Med.* 49, 1036-1015.
- Stewart, J.D., McKelvey, R., Durcan L., Carpenter, S., Karpati, G., (1996). Chronic inflammatory demyelinating polyneuropathy (CIPD) in diabetics. *J Neurol Sci.* 142, 59–64
- Sugimoto, K., Nishizawa, Y., Horiuchi, S., Yagihashi, S. (1997). Localization in human diabetic peripheral nerve of N(epsilon)-carboxymethyllysine-protein adducts, an advanced glycation endproduct. *Diabetologia* 40, 1380–1387.
- Sugimoto, K., Yasujima, M., Yagihashi, S. (2008). Role of advanced glycation end products in diabetic neuropathy. *Curr. Pharm. Des.* 14, 953–961.
- Svingen, T., Letting, H., Hadrup, N., Hass, U., and Vinggaard, A.M. (2015). Selection of reference genes for quantitative RT-PCR (RT-qPCR) analysis of rat tissues under physiological and toxicological conditions. *PeerJ* 3, e855.
- Szabo, C., Ischiropoulos, H., Radi, R. (2007). Peroxynitrite: biochemistry, pathophysiology and development of therapeutics. *Nat Rev Drug Discov.* 6, 662–680.
- Tarnow, L., Hovind, P., Teerlink, T., Stehouwer, C.D., Parving, H.H. (2004). Elevated plasma asymmetric dimethylarginine as a marker of cardiovascular morbidity in early diabetic nephropathy in type 1 diabetes. *Diabetes Care.* 27, 765-769.
- Tatoyan, A., Giulivi, C. (1998). Purification and characterization of a nitric-oxide synthase from rat liver mitochondria. *J Biol Chem.* 273, 11044-11048.

## References

- Tay, Y.M., Lim, K.S., Sheu, F.S., Jenner, A., Whiteman, M., Wong, K.P., Halliwell, B. (2004). Do mitochondria make nitric oxide? No? *Free Radic Research*. *38*, 591-599.
- Tesfaye, S., Boulton, A.J., Dyck, P.J., Freeman, R., Horowitz, M., Kempner, P., Lauria G, Malik, R.A., Spallone, V., Vinik, A., Bernardi, L., Valensi, P. (2010). Diabetic neuropathies: update on definitions, diagnostic criteria, estimation of severity, and treatments. *Diabetes Care*. *33*, 2285-2293.
- TeSlaa, T., Teitell, M.A. (2014). Techniques to monitor glycolysis. *Methods enzymol*.*542*, 91-114.
- Thirone, A.C., Huang, C., Klip, A. (2006) Tissue-specific roles if IRS proteins in insulin signaling and glucose transport. *Trends Endocrinol Metab*. *17*, 72-78.
- Thornalley, P.J. (2002). Glycation in diabetic neuropathy: characteristics, consequences, causes, and therapeutic options. *Int. Rev. Neurobiol*. *50*, 37-57.
- Thornalley, P.J., and Rabbani, N. (2014). Assay of methylglyoxal and glyoxal and control of peroxidase interference. *Biochem. Soc. Trans*. *42*, 504–510.
- Timar, B., Popescu, S., Timar, R., Baderca, F., Duica, B., Vlad, M., Levai, C., Balinisteanu, B., Simu, M. (2010). The usefulness of quantifying intraepidermal nerve fibers density in the diagnostic of diabetic pipheral neuropathy: a cross-sectional study. (2016). *Diabetol Metab Syndr*. *8*:31, 1-7.
- Toth, C., Rong, L.L., Yang, C., Martinez, J., Song, F., Ramji, N., Brussee, V., Liu, W., Durand, J., Nguyen, M.D., Schmidt, A.M., Zochodene D.W. (2008). Receptor for advanced glycation end products (RAGEs) and experimental diabetic neuropathy. *Diabetes* *57*, 1002–1017.
- Tukey, J.W. (1977). *Exploratory data analysis* (Reading, Mass: Addison-Wesley Pub. Co).
- VanderJagt, D.J., Harrison, J.M., Ratliff, D.M., Hunsaker, L.A., and Vander Jagt, D.L. (2001). Oxidative stress indices in IDDM subjects with and without long-term diabetic complications. *Clin Biochem*. *34*, 265–270.
- Vareniuk, I., Pavlov, I.A., Dre,l V.R., Lyzogubov, V.V., Ilnytska, O., Bell S.R., Tibrewala J., Groves J.T., Obrosova, I.G. (2007). Nitrosative stress and peripheral diabetic neuropathy in leptin-deficient (ob/ob) mice. *Exp Neurol*. *5*, 425–436.
- Vareniuk, I., Pavlov I.A., Obrosova I.G. (2008). Inducible nitric oxide synthase gene deficiency counteracts multiple manifestations of peripheral neuropathy in a streptozotocin-induced mouse model of diabetes. *Diabetologia*. *51*, 2126-2133.
- Vareniuk I., Pacher P., Pavlov I.A., Drel V.R., Obrosova I.G. (2009). Peripheral neuropathy in mice with neuronal nitric oxide synthase gene deficiency. *Int J Mol Med*. *23*, 571-580.
- Varon, S.S., Bunge, R.P. 1978. Trophic mechanisms in the peripheral nervous system. *Annu Rev Neurosci*. *1*, 327–361.
- Venkatakrisnan P., Nakayasu E.S., Almeida I.C., Miller R.T. (2009). Absence of nitric-oxide synthase in sequentially purified liver mitochondria. *J Biol Chem*. *284*, 19843-19855.
- Verheijen, M.H., Chrast, R., Burrola, P., Lemke, G. (2003). Local regulation of fat metabolism in peripheral nerves. *Genes Dev*. *17*, 2450-2464.
- Viader, A., Golden, J.P., Baloh, R.H., Schmidt, R.E., Hunter, D.A., Milbrandt, J. (2011). Schwann cell mitochondrial metabolism supports long term axonal survival and peripheral nerve function. *J. Neurosci*. *31*, 10128-10140
- Viader, A., Sasaki, Y., Kim, S., Stickland, A., Workman, C.S., Yang, K., Gross, R.W., Milbrandt, J. (2013). Abberant Schwann cell lipid metabolism linked to mitochondrial deficits leads to axon degeneration and neuropathy. *Neuron*. *77*, 886-98.

## References

- Vilholm, O.J., Christensen, A.A., Zedan, A.H., Itani, M. (2014). Drug-Induced Peripheral Neuropathy. *Basic Clin Pharmacol Toxicol.* *115*, 185-92.
- Vincent, A.M., Feldman, E.L. (2004). New insights into the mechanisms of diabetic neuropathy. *Reviews in endocrine & metabolic disorders.* *5*, 227-236
- Vincent, A.M., Edwards, J.L., Mclean, L.L., Hong, Y., Cerri, F., Lopez, I., Quattrini, A., Feldman, E.L. (2010). Mitochondrial biogenesis and fission in axons in cell culture and animal models of diabetic neuropathy. *Acta Neuropathol.* *120*, 477-489.
- Vinik, A.I., Kong, X., Megerian, J.T., Gozani, S.N. (2006). Diabetic nerve conduction abnormalities in the primary care setting. *Diabetes Technol Ther.* *8*, 654–662.
- Vinogradov A.D. and Grinnikova V.G. (2005). Generation of superoxide-radical by NADH: ubiquinone oxidoreductase of heart mitochondria. *Biochemistry.* *70*, 120-127.
- Wada, R., Yagihashi, S. (2005). Role of advanced glycation end products and their receptors in development of diabetic neuropathy. *Ann. N.Y. Acad. Sci.* *1043*, 598–604.
- Widlansky, M.E., Wang, J., Shenouda, S.M., Hagen, T.M., Smith, A.R., Kizhakekuttu, T.J., Kluge, M.A., Weihrauch, D., Gutterman, D.D., and Vita, J.A. (2010). Altered mitochondrial membrane potential, mass, and morphology in the mononuclear cells of humans with type 2 diabetes. *Transl Res J Lab Clin Med.* *156*, 15–25.
- Weimer, L.H. (2003). Medication-induced peripheral neuropathy. *Curr Neurol Neurosci Rep.* *3*, 86-92.
- Weiss, H., Friedrich, T., Hofhaus, G., Pries, D. (1991). The respiratory-NADH dehydrogenase (complex I) of mitochondria. *Eur J of Biochem.* *197*, 563-576.
- Wiese, S., Herrmann, T., Drepper, C., Jablonka, S., Funk, N., Klausmeyer, A., Rogers, M.L., Rush, R., Sendtner, M. (2010). Isolation and enrichment of embryonic mouse motoneurons from the lumbar spinal cord of individual mouse embryos. *Nat Protoc.* *5*, 31–38.
- Wiggin, T.D., Sullivan, K.A., Pop-Busui, R., Amato, A., Sima, A.A., Feldman, E.L. (2009). Elevated triglycerides correlate with progression of diabetic neuropathy. *Diabetes.* *58*, 1634–1640.
- West B. (2011). The implications of statin induced peripheral neuropathy. *J Foot Ankle Res.* *4*, 57. doi: 10.1186/1757-1146-4-S1-P57.
- Wu, M., Neilson, A., Swift, A.L., Moran, R., Tamagnine, J., Parslow, D., Armistead S., Lemire, K., Orrell, J., Teich, J., Chomicz, S., Ferrick, D.A., 2007. Multiparameter metabolic analysis reveals a close link between attenuated mitochondrial bioenergetic function and enhanced glycolysis dependency in human tumor cells. *Am J Physiol Cell Physiol.* *292*, C125–C136.
- Xia, P., Inoguchi, T., Kern, T.S., Engerman, R.L., Oates, P.J., and King, G.L. (1994). Characterization of the mechanism for the chronic activation of diacylglycerol-protein kinase C pathway in diabetes and hypergalactosemia. *Diabetes.* *43*, 1122–1129.
- Yagihashi, S., Matsunaga, M. (1979). Ultrastructural pathology of peripheral nerves in patients with diabetic neuropathy. *J Exp Med.* *129*, 357–366.
- Yagihashi, S., Yamagishi, S.I., Wada, R.R., Baba, M., Hohman, T.C., Yabe-Nishimura, C., Kokai Y.(2001). Neuropathy in diabetic mice overexpressing human aldose reductase and effects of aldose reductase inhibitor. *Brain.* *124*, 2448-2458.
- Yagihashi, S., Mizukami, H., Sugimoto, K. (2011). Mechanism of diabetic neuropathy: Where are we now and where to go? *J. Diabetes Investig.* *2*, 18-32.

## References

Zhang, L., Yu, L., Yu, C.A. (1998). Generation of superoxide anion by succinate-cytochrome c reductase from bovine heart mitochondria. *J. Biol. Chem.* 273, 33972–33976.

Zhang, L., Yu, C., Vasquez, F.E., Galeva, N., Onyango, I., Swerdlow, R.H., Dobrowsky, R.T. (2010). Hyperglycemia alters the schwann cell mitochondrial proteome and decreases coupled respiration in the absence of superoxide production. *J Proteome Res.* 9, 458-471.

Zhao, Y., Wieman, H.L., Jacobs S.R., Rathmell J.C. (2008). Mechanisms and methods in glucose metabolism and cell death. *Methods Enzymol.* 442, 439-457.

Zimmet, P., Alberti, K.G.M.M., Shaw, J. (2001) Global and social implications of diabetes epidemic. *Nature.* 414, 782-787.

# Appendix

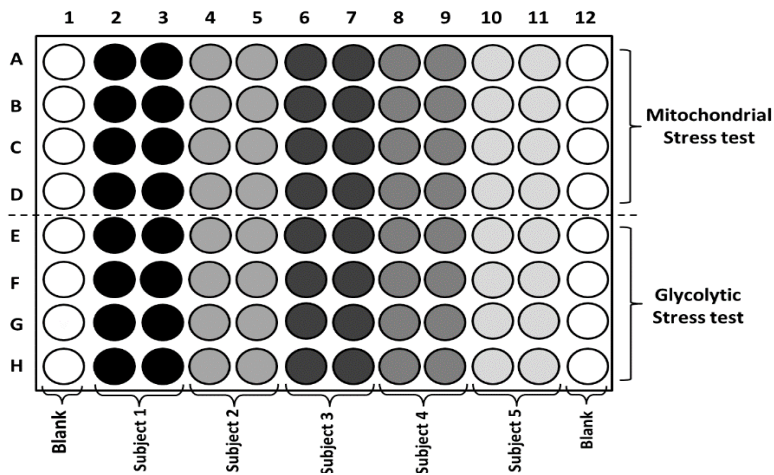
## 9. Appendix

### XF Bioanalyzer protocol:

**Calibration**  
**Equilibrate**  
  
 Mix 4 min }  
 Wait 2 min } Repeat 3x  
 Measure 3 min }  
  
**Inject port A: Oligomycin**  
  
 Mix 4 min }  
 Wait 2 min } Repeat 3x  
 Measure 3 min }  
  
**Inject port B: FCCP**  
  
 Mix 4 min }  
 Wait 2 min } Repeat 3x  
 Measure 3 min }  
  
**Inject port C: Rotenone & Antimycin A**  
  
 Mix 4 min }  
 Wait 2 min } Repeat 3x  
 Measure 3 min }  
  
**End of run**

### Supplemental figure 19. XF96 Bioanalyzer protocol.

The program set-up for XF96 Bioanalyzer for both the Glycolysis assay and the MitoStress test. The time of the “Mix” and “Measure” steps can be adjusted as desired. It is important to keep the “measure” steps 2-3min, since 2 minutes is the minimal time required to generate a rate.



### Supplemental figure 20. XF96 Bioanalyzer plate layout for PBMCs.

Plate layout for simultaneous measurement of Mitochondrial stress test and the glycolytic stress tested. First and last column were filled with only media and used for blank correction. The first four rows (A-D) were used for the mitochondrial stress test. The last four rows (E-F) were used for the glycolytic stress test. Mitochondrial stress test and glycolytic stress test was performed in octuplicate per subject.

## **Publications**

### **10 Publications**

#### **Manuscript in preparation**

Volk, N., **Smit, T.T.A.**, Kliemank, E., Gröner, J.B., Eckstein, V., Fleming, T.H., Nawroth, P.P. (2018). Mitochondrial function in white blood cells: protocol for isolation and measurement of mitochondrial properties, glycolysis and mitochondrial respiration.

#### **Conference proceedings**

**Smit, T.T.A.**, Fleming, T.H., Nawroth P.P. (2017). Metabolic shift from glycolysis towards lipid peroxidation in Schwann cells in response to hyperglycemia. 4<sup>th</sup> Heidelberg International Symposium on Diabetic Complications.

**Smit, T.T.A.**, Fleming, T.H., Nawroth P.P. (2017). Metabolic shift from glycolysis towards lipid peroxidation in Schwann cells in response to hyperglycemia. EASD 53-p980.

**Smit, T.T.A.**, Fleming, T.H., Nawroth P.P. (2016). Metabolic shift from Glycolysis towards lipid peroxidation in Schwann cells in response to hyperglycemia. 3<sup>rd</sup> Heidelberg International Symposium on Diabetic Complications.

**Smit, T.T.A.**, Fleming, T.H., Nawroth P.P. (2015). The Importance of Enzymatic Regulation of Methylglyoxal Metabolism in Diabetic Neuropathy. 2<sup>nd</sup> Heidelberg International Symposium on Diabetic Complications.



# Curriculum Vitae

## 11 Curriculum Vitae

### Personal information

---

Name: Tamara Tjitske Antje Smit  
Address: Blumenthalstraße 7,  
69120 Heidelberg  
Telephone: +49 (0)176 81480736  
E-mail: tta.smit@gmail.com  
Date of birth: 07-05-1988  
Place of birth: Achtkarspelen  
Nationality: Dutch

### Education

---

- 12/2014 - 06/2018 **University of Heidelberg, Germany.**  
SFB 1118, DIAMICOM (associate member)
- **Doctoral degree**  
Internal Medicine and Clinical Chemistry, Prof. Dr. P.P. Nawroth:  
Metabolic switch from glycolysis towards fatty acid oxidation in Schwann cells in response to high glucose.
- 09/2011 - 03/2014 **University of Groningen, the Netherlands.**  
Faculty of Biology, Master Biomedical Sciences, P-variant, degree
- **Master of Science**  
Clinical Pharmacology, Prof. Dr. R.H. Henning and Dr L.E. Deelman. Master essay: Mitochondrial dysfunction in diabetes mellitus: pathophysiology and therapeutic opportunities.  
Medical Biology (CAVAREM), Dr. G. Krenning. Colloquium: Epigenetic disbalance of GLUT4 in diabetic cardiovascular complications.
- 08/2007 - 12/2011 **University of Groningen, the Netherlands.**  
Faculty of Biology, Bachelor Biomedical Sciences, degree

## Curriculum Vitae

- **Bachelor of Science**

Neurobiology, Prof. Dr. H.W.G.M. Boddeke. Bachelor essay: Microglia: the physiology and its role in the aging brain.

08/2000-07/2007

**Dockinga College, the Netherlands.**

VWO, Nature and Health (Natuur en Gezondheid), degree.

- **VWO**

## Work experience

---

09-12/2013

**University Medical Centre Groningen, the Netherlands.**

- Clinical Pharmacology, Prof Dr. R.H. Henning, in collaboration with pharmaceutical company Sulfateq (Groningen).

Student assistant; determining the effect of several potential anti-apoptotic drugs on mitochondrial respiration using mitochondrial respiration assay of Seahorse Bioscience and cell culturing.

04/2011-06/2011

**University Medical Centre Groningen, the Netherlands.**

- UMCG and University of Groningen.

Student assistant for the course Biomedical Sciences.

## Internships

---

03/2012-04/2013

**University of Mannheim, Germany.**

- Endocrinology and diabetology, Prof. Dr. H.P. Hammes. Research project: Signaling transduction pathways involved in progressive diabetic retinopathy.

05/2011-07/2011

**University Medical Centre Groningen, the Netherlands.**

- Clinical pharmacology, Prof Dr. R.H. Henning and Dr H.R. Bouma. Research project: Adenosine receptors play an important role in leukocytedynamics during suspended animation in mice.

## Acknowledgement

### 12 Acknowledgement

I am indebted to all of the people who helped and supported me to accomplish this thesis.

I would like to thank Prof. Dr. Peter P. Nawroth for giving me the opportunity to work in his laboratory and for his valuable comments during preparation of the thesis. I would like to thank my supervisor Dr. Thomas H. Fleming for fruitful discussions, advice and support.

I would like to thank all the collaborators, who helped with this work. Thanks to Dr. J. G. Okun of the Kinderklinik to measure acyl carnitines. Thanks to Dr. Nadine Volk for measuring the reactive metabolites in PBMCs.

A big thank you goes to all the current and former colleagues of the department of AG Nawroth/Fleming, AG Nawroth/Mendler and AG Nawroth/Tyedmers. I would like to thank Ita Hernandez for the organizing lab trips and social activities. Elisabeth Kliemank, Anja Buhl, Serap Kaymak and Katarina Abramovic for their technical support, helping me to learn the German language and Axel Erhardt for his effort in the animal facility.

Thanks also to Brigitte Löser and Mirjam Knöll for their organizational work allowing the scientist to focus on their research.

A big thank you goes to my friends and family for their support and above all the acceptance that I was working and living in another country and sometimes had little time for them. In particular I like to thank my parents and my brother, without whom this work would not have been possible, because they have always believed in me and supported me during my doctoral study with infinite patience and loving care. They sended me sometimes Dutch magazines and Dutch specialities, including cheese and liquorice, so I would not miss home. My nephews for their beautiful drawings and post cards. My grandmother for her loving support, telling me to study hard, but also to have fun and follow my dreams.

The biology buddies; Rianne, Hilda and Thea for their friendship and understanding life as a PhD student. It feels like yesterday when we met 11 years ago during the first year of our Biology study at the University of Groningen. Although we lived in different countries, we tried to meet

## **Acknowledgement**

when possible, having nice weekend trips, lovely dinners, interesting discussions and always understanding each other when research does not go as planned. Sjoerd and Hilda, I will never forget that you guys cycled from Groningen to Heidelberg to visit me.

## Eidesstattliche Versicherung

### 13 Eidesstattliche Versicherung

1. Bei der eingereichten Dissertation zu dem Thema „Metabolic switch from glycolysis towards fatty acid oxidation in Schwann cells in response to high glucose“ handelt es sich um meine eigenständig erbrachte Leistung.
2. Ich habe nur die angegebenen Quellen und Hilfsmittel benutzt und mich keiner unzulässigen Hilfe Dritter bedient. Insbesondere habe ich wörtlich oder sinngemäß aus anderen Werken übernommene Inhalte als solche kenntlich gemacht.
3. Die Arbeit oder Teile davon habe ich bislang nicht an einer Hochschule des In- oder Auslands als Bestandteil einer Prüfungs- oder Qualifikationsleistung vorgelegt.
4. Die Richtigkeit der vorstehenden Erklärung bestätige ich.
5. Die Bedeutung der eidesstattlichen Versicherung und die strafrechtlichen Folgen einer unrichtigen oder unvollständigen eidesstattlichen Versicherung sind mir bekannt. Ich versichere an Eides statt, dass ich nach bestem Wissen die reine Wahrheit erklärt und nichts verschwiegen habe.

-----

Ort und Datum

-----

Unterschrift